Developing a Retrofitting System to Mitigate Floodwall Failures of New Orleans

A Thesis

Presented for the

Master of Science

Degree

The University of Mississippi

James Tyler Kidd

March 2011

ABSTRACT

Hurricane Katrina exposed many areas of weakness in the hurricane protection system in the New Orleans, LA area. In addition, severe damage and catastrophic failures occurred throughout the hurricane protection system. This study focuses on two key aspects of failure: erosion by plunging water and strength reduction of the floodwall due to piping.

Erosion by plunging water was the first failure mode considered in this study. The aim of this research was to mitigate erosion by reinforcing the soil, and also to study the effects the plunging water thickness had on erosion.

The prevention or reduction of erosion using a retrofitting technique or a ground modifier was used for erosion mitigation. The two main ground modifiers that were tested are the Vetiver plant and Polyhedral Oligomeric Silsesquioxanes (POSS). Both modifiers showed improvements in erosion resistance and reduced the total erosion of the samples. The Vetiver plant showed a greater resistance to erosion as compared to POSS. However, the Vetiver plant has limited applicability and also takes a number of years to grow to its full potential. Furthermore, POSS showed less erosion resistance, but is easily applicable to most any soil condition because it is sprayed onto the soil.

To accurately predict the erosion behavior for a real world scenario or a catastrophic event, erosion tests had to be scaled up. One of the most significant factors when dealing with erosion is the thickness of the nap from the plunging water. Consequently, when the thickness of

plunging water increases, the amount of erosion should also increase; the rate of this increase is the one of under researched areas. To evaluate this behavior of erosion, tests were conducted with the thickness of plunging water equal to: .0003, .0065, .013, and .2 m. The velocity of the plunging water was kept at a constant 6 m/sec; because this is the expected velocity of plunging water during Hurricane Katrina. Tests were conducted for three different soil samples at the University of Mississippi Erosion Test Bed (UMETB) and also at the USDA-HERU facility in Stillwater, OK. From these tests, it was concluded that increasing the water thickness also increases the equilibrium erosion depth. However, this increase does not follow a linear pattern.

The second failure mode considered in this study was the loss of strength in the underlying levee material due to piping and also the infiltration of water between the soil and floodwall. This infiltration of water between the soil and floodwall was caused by the development of a gap between the soil and floodwall which is a result from the floodwall leaning. When high water pressure (caused by rising water) is exerted onto the floodwall; the floodwall is deformed or leans outward away from the pressure.

This study aimed at preventing the gap formation by inlaying an expansive bentonite and sand mixture. Bentonite is highly expansive, but has a low permeability; therefore, sand is added to increase the permeability which increases the rate of expansion. The mixture was designed to swell and seal the gap formation. After testing several mixtures it was confirmed that bentonite and sand would adequately swell to seal the gap. The mixture that proved most effective was 30% bentonite and 70% sand by weight. It was concluded this mixture was the most effective

because: it swelled fast enough to seal the gap with only letting a negligible amount of water infiltration, and also this mixture excerpted low lateral swelling pressure onto the floodwall.

The results of these three topics were documented in the form of three journal papers. This thesis, therefore, presents the results in the draft form of journal papers.

DEDICATION

This work is dedicated to my parents: Billy and Melanie Kidd, who have continued to encourage and support me throughout all my endeavors.

ACKNOWLEDGMENTS

It is a joy to convey my sincere gratitude and appreciation to my advisor Dr. Chung Song for his patience, advice, cooperation, and encouragement throughout my entire Masters degree. In addition, I am grateful to my committee members: Dr. Alex Cheng, Dr. Ahmed Al-Ostaz, and Dr. Greg Hanson for their commitment and help throughout the duration of this research. Also, I would like to thank the faculty and staff of The Department of Civil Engineering for the support and encouragement.

This research was supported by funding received from the Department of Homeland Security-sponsored Southeast Region Research Initiative (SERRI) at the Department of Energy's Oak Ridge National Laboratory, USA. I also thank the COE, New Orleans Office, for granting permission to take samples. In addition, I also would like to thank Dr. Gregg Henderson at LSU, and Dr. Bruce Fu at Hybrid Plastics Co. for supplying Vetiver and POSS, respectively. Also, I would like to thank Mr. Jimmy Jackson and Mr. Mathew Hosey for their devoted service to this research. I would like to express my gratitude to Dr. Jinwon Kim and Mr. Sudarshan Adhikari for their assistance in my research.

I would like to express my sincere gratitude to Rooster Kidd, for his loyalty and cooperation throughout this research. In addition, I would like to thank Charity Baptist Church for the continued support and prayers. Also, a special thanks to Don Sullivan for invaluable advice and encouragement over the years.

TABLE OF CONTENTS

LIST OF FIGURES

LIST OF TABLES

CHAPTER I

INTRODUCTION

Hurricane Katrina hit New Orleans, LA August 29, 2005 bringing substantial wind, storm surge, and rainfall. The hurricane protection system was not designed to accommodate such a catastrophic event. As a result, many of the floodwalls failed or were determinately damaged which caused widespread flooding and loss of property as seen in Figure 1.1.

The majority of the New Orleans hurricane protection system was built through a process called land reclamation. This involves pumping marsh material for the construction of earthen levees. The type of floodwalls that were built include: I-walls and T-walls to accommodate for the low lying areas of New Orleans. However, New Orleans experienced the failure of 50 of the floodwalls. This is primarily due to the fact, flood water rose past design expectations which caused the water to overtop the floodwalls (IPET, 2007).

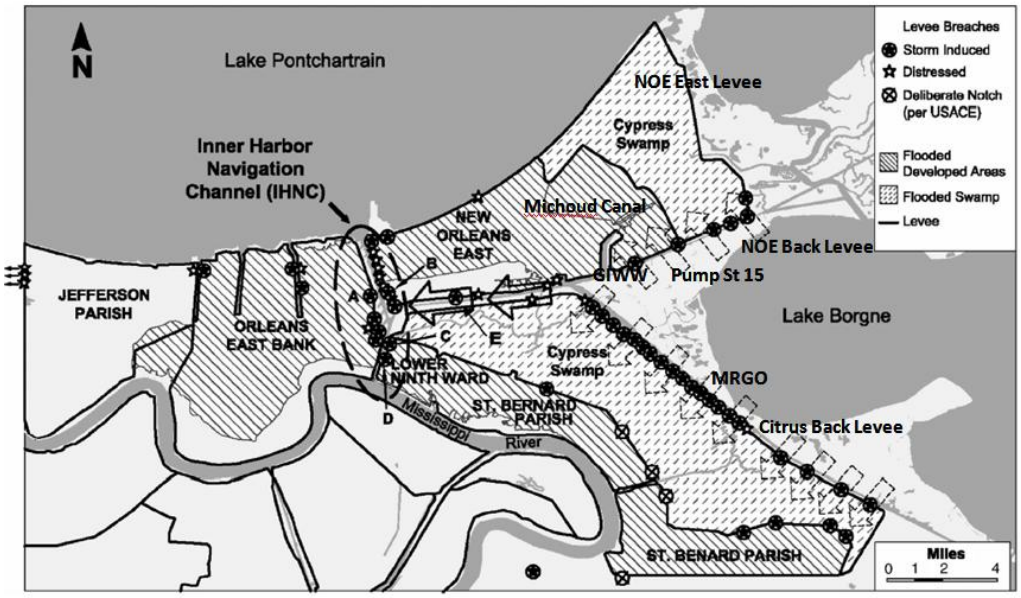

Figure 1.1 Schematic Map Showing Levee Breaches (Seed et al., 2008)

1.1. Motivation

The lack of a new hurricane protection system for New Orleans makes the area vulnerable to another catastrophic flood. This research focuses on studying and understanding the causes of past failures, and implementing a new retrofitting technique. The new hurricane protection system should be more resilient and capable of handling an event such as Hurricane Katrina. In addition, the new hurricane protection system should be cost effective and easily applicable to the current hurricane protection system in New Orleans.

1.2. Erosion Due to Plunging Water

New Orleans experienced widespread erosion due to plunging water. There were 50 major breaches during Hurricane Katrina; of these 50 breaches, 46 were attributed to erosion due to plunging water; therefore, it was a critical part of this research. Erosion due to plunging water is caused by rising water overtopping floodwalls. This type of erosion is deemed impact erosion (Jang et al, 2010).

Several studies have been conducted involving erosion similar to impact erosion. These studies include (Stein et al., 1991, 1993, and 1997; Hanson et al., 2002) which presented an pioneering analytical solution for erosion depth. Their researches focused on the shear strength concept; shear strength is one of the governing parameters effecting erosion (Jang et al, 2010). However, this type of erosion is different from the erosion observed in New Orleans. The erosion in New Orleans was caused by a nap (planar nozzle); and the soil being saturated due to heavy rainfall. Erosion resistance was reduced due to the saturation of the soil from the rainfall.

This research focuses on implementing previously developed equations to determine the erosion depth relationships for New Orleans. Understanding the effects of plunging water and the resulting erosion is crucial for analyzing possible solutions for erosion. In addition, the accurate prediction of erosion depth in the field is important for disaster mitigation and retrofitting solutions.

1.3. Instability of Levee Soils

Instability in the floodwall foundation or levee soils caused 4 known failures in the hurricane protection system. The instability is predominantly caused by a gap forming between

the floodwall and the soil. This gap allows for the infiltration of water to seep or pipe under the floodwall. The seepage additionally weakens the already stressed floodwall causing failure. Furthermore, the piping caused by the gap formation may induce internal erosion of the earthen levee.

This research focuses on developing a system to reduce or prevent the formation of the gap between the floodwall and soil. If the gap can successfully be prevented; the resulting failure of the floodwall will also be mitigated. This is accomplished by the addition of a buried bentonite and sand mixture next to the floodwall. Bentonite is a highly expansive and absorbent mineral and the primary function of bentonite is to expand in the presence of water. The addition of sand is used to allow the water to infiltrate the mixture quickly.

One of the primary goals of the research is to find a sand and bentonite mixture that swells quick enough to seal the gap formed, has high swelling strain, and a low swelling pressure. If the bentonite does not swell quick enough, the water will infiltrate and cause damage before the mixture has the opportunity to swell. The high swelling strain will give the mixture enough deformation to expand to seal the gap. However, if the swelling pressure is too high, it can cause lateral movement of the floodwall and add additional pressure onto the floodwall. Therefore, the swelling pressure should not be high.

1.4. Objectives and Approach

This research is to provide new design principles and retrofitting techniques for the New Orleans Hurricane Protection System. The proposal for the research is titled "*Structural,*

Material, and Geotechnical Solutions to Levee and Floodwall Construction and Retrofitting," which include the following four technical approaches:

1. Geotechnical solutions for a resilient levee and floodwall systems that include improved floodwall section design to prevent overturning; piling and anchoring to increase the resistance to sliding; clay and bentonite apron to reduce the seepage, and levee backside protection to prevent erosion caused by overtopping.
2. Structural solutions to increase the lateral stiffness of the sheet pile system for load transfer to geotechnically reinforced stations, and to increase the bending stiffness of the buried sheet piles by cross-sectional design to prevent the formation of the gap in front of the floodwall.
3. Material solutions that use a new generation of lighter, stronger, and non-corrosive materials, such as: polymer composite sheet pile, polymer concrete, or nano-particle enhanced spray-on polymer coating, to improve the performance of the system in terms of strength, durability, and resistance against sabotage.
4. Testing and validation of the tools, technologies, and systems developed in this research.

The first and second objectives were addressed in this research. The first objective was addressed by evaluating and testing the erosion behavior of New Orleans levee soils; and developing a cost effective retrofitting strategy to reduce erosion. The second objective was addressed by developing a sand and bentonite mixture to mitigate the effects of the gap formation.

1.5. Organization

This thesis is focused on producing three peer reviewed journal articles. Therefore, Chapter 2, Chapter 3 and Chapter 4 have been written as standalone manuscripts for publication. The brief summaries of the three articles are as follows.

Article #1 (Chapter 2)

This chapter presents the methods and results for applying a retrofitting technique to existing soil to reduce erosion caused by plunging water. The soil modifications include: POSS and the Vetiver plant. Results for each ground modifier were compared against an untreated soil specimen to determine effectiveness.

Article #2 (Chapter 3)

This chapter presents theory and test results for forming an analytical solution to erosion behavior and determining a final erosion depth for field conditions. This was accomplished through running a series of laboratory tests and also full scale tests that mimic field conditions in New Orleans. The governing variable in determining field erosion behavior is the effects of water width.

Article #3 (Chapter 4)

In this chapter we demonstrated the development of a buried bentonite and sand mixture to prevent water infiltration through the gap formed between the floodwall and soil. This was accomplished through 2/3 scale floodwall testing, and varying mixtures of sand and bentonite. We also tested the effectiveness of an expansive material using numerical analysis software.

CHAPTER II

EROSION CONTROL USING MODIFIED SOILS

2.1. Abstract

As a result of Hurricane Katrina, many sections of the flood protection systems in New Orleans were eroded due to plunging water, and sections of flood walls were determinately damaged. Therefore, mitigating this type of erosion and failure is necessary for counteracting similar catastrophic events. This study evaluated the method to mitigate erosion due to plunging water by strengthening the soil with ground modification. The Vetiver plant and Polyhedral Oligomeric Silsesquioxanes (POSS) were the two main ground modifiers used in this test. Test results showed that both POSS and the Vetiver were effective in reducing erosion. POSS showed good erosion resistance with good applicability to field soils; Vetiver showed higher resistance to erosion by plunging water, but required time to achieve a well established root/stem system.

2.2. Introduction

Erosion caused by plunging water from the floodwalls during Hurricane Katrina caused extensive damage to the levee systems in New Orleans, Louisiana. Typical runoff erosion is initiated when the flow direction is parallel to the ground surface. Plunging water causes impact erosion which is initiated when the flow is almost vertical to the ground, and erosion behavior of soils may be different.

New Orleans is located on the Gulf Coast of Louisiana and is surrounded almost entirely by water: the Gulf of Mexico, the Mississippi River, Lake Pontchartrain, and numerous canals. Also, a substantial portion of New Orleans is located approximately two meters below sea level as shown in Figure 2.1, and all rainwater must be pumped up to the canals, Mississippi River, or lakes. Due to these conditions, during times of excess rainfall coupled with failure of pumping stations, New Orleans may experience severe flooding; that actually happened during Hurricane Katrina.

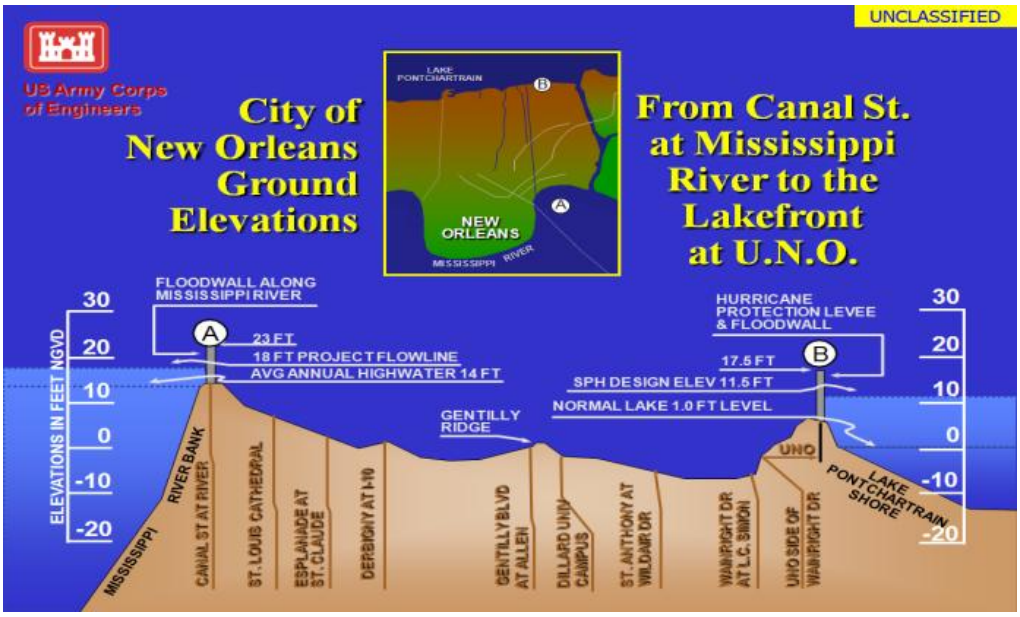

Figure 2.1 Representative Cross Section of New Orleans (*IPET,2007*)

Trying to cope with rising flood waters, New Orleans has implemented several techniques to prevent flood damage including elevated levees and flood walls. One method of prevention is to raise the levee height, but this can be accomplished only by an accompanying

process of widening the levee base. This may interfere with the private land ownership in urban areas. Therefore, most levee systems in urban areas cannot be raised above their current height; concrete flood walls are constructed on the top of the levees instead.

Hurricane Katrina made landfall on August 29, 2005 as a category three hurricane with peak wind speeds sustained at 125 mph, causing roughly two billion dollars' worth of damage to the infrastructure (*IPET, 2007)*. The storm surge that accompanied Hurricane Katrina was roughly 3.5-4.5 meters high. In addition to the storm surge, rainfall was estimated to be at 36 cm over a 24-hour period. However, these are only estimates because most of the instruments used to measure storm surge and rainfall were destroyed (*IPET, 2007*). Eighty percent of the New Orleans metropolitan area was flooded (*IPET, 2007*).

New Orleans hurricane protection systems were not designed to accommodate such high water levels. Water levels in canals exceeded the height of the flood walls by 30 to 60 cm, and overtopping water impacted the levee soil with approximate velocity 6m/sec. Approximately 50 major breaches occurred in the hurricane protection system; 46 of which were the result of overtopping water which caused the soil erosion that eventually led to the failure of many floodwalls (*IPET, 2007*). Soil compositions on overtopping breached areas are not well known, but it is known that the fat clay levee in Orleans Canal was overtopped but did not fail. On the other hand, sandy (SM) levee in IHNC (Inner Harbor Navigation Channel) was overtopped and experienced wide spread failure (*IPET, 2007*).

There are several factors that influence the erosion of soil which include: the applied shear stress, clay content, soil temperature, water temperature, unit weight, water content, and the undrained shear strength (Briaud et al 1999a). Also, the shear strength of soil is increased

when: unit weight is increased, clay content increases, undrained shear strength increases, and void ration decreases (Briaud et al 2001a). However, reliable relationships between the erosion process and soils properties are not reported yet.

This study primarily focuses on preventing or reducing erosion from overtopping water through ground modification. In order to do this, the bare (untreated) soil samples were used as a reference soil. These were bare soils that have no chemicals added or additional enhancements that may increase erosion resistance of the soil. All the soil samples that have been tested are a mixture of fine and course soils taken from a quarry site in New Orleans and mixed in the lab based on material specification of levees (*Vroman,* 2008).

2.3. Test Samples

The fine grained soil was classified as CH or CL with the percentage passing the # 200 sieve about 80%. Course grained soil was classified as SM with 4.5% passing the #200 sieve. For detailed sample mixing and preparation procedures please refer to *Song et al.* (2010). Four different mixtures of fine and course soil are used in testing: 50/50, 57/43, 65/35, and 73/27 (with % of fines being the first number and course materials following respectively). Four different intended degrees of compaction are also tested: 95%, 91%, 87%, and 83%, this is assuming a ± 2 % tolerance. With four mixtures and four degrees of compaction, this gives a total of sixteen different combinations of soil samples as shown in Table 2.1.

Table 2.1. Basic Soil Properties of Soil Samples (*Jang et al*. 2010)

Soil Identification	Degree of Compaction (%)	γ_{sat} $\left(\frac{kN}{m^3}\right)$	γ_d $\left(\frac{kN}{m^3}\right)$	e	Sr (%)
F50S50	83	16.5	14.1	.96	48
Clay 15%	87	17.1	14.6	.88	52
Silt 35 %	92	18.3	15.7	.86	54
Sand 50 %	99	19.5	16.7	.74	62
F57S43	85	16.8	14.2	.9	54
Clay 18%	88	17.4	14.7	.83	58
Silt 40 %	92	18.1	15.4	.76	64
Sand 42 %	97	19.1	16.2	.67	73
F65S35	84	17.9	14.5	.9	57
Clay 20%	87	17.8	14.9	.84	61
Silt 45 %	91	19.1	16.2	.78	65
Sand 35 %	97	20.2	17	.62	82
F73S27	83	16	12.8	1.15	58
Clay 23 %	87	16.6	13.3	1.05	63
Silt 50 %	90	17.4	14	.96	69
Sand 27 %	95	18.2	14.6	.89	74

The ground modifiers chosen for this study were based on environmental impact and applicability. POSS is a silicone based solution which is very similar to natural geo-materials and USDA approved. Vetiver is a green solution, therefore it is environmentally safe. In addition, both can be applied with relative ease. However, there are ground modifiers such as soil-cement and geotextile fibers. These were not chosen for this study due to the fact that they may cause environmental issues for the case of soil-cement and need elaborated mixing process in the field for the case of geotextile fibers.

For a chemical ground modifier, Polyhedral Oligomeric Silsesquioxanes (POSS) is used.

POSS is a liquid chemical poured onto soil samples to reduce erosion. There are two different POSS consolidates used in the erosion testing: SO1455 (3% TriSilonollsooctyl POSS $C_{56}H_{122}O_{12}Si_7$) and SO1458 (3% TriSilonalPhenyl POSS $C_{42}H_{38}O_{12}Si_7$) (*www.hybridplastics.com*).

After completion, the samples treated with POSS were cured and dried at room temperature for two weeks. This process allows the POSS ample time to penetrate into the soil samples and interact with the soil.

For a biological ground modifier, the Vetiver plant (*Chrysopogon zizanioides)*, a native of Southern Indian plant commonly referred to as Vetiver, is used. It is a very tall and dense grass that provides good stability, and is sterile and non-invasive to other plants and animals. Vetiver is a very deeply rooted grass, and for this reason it has been used in Southern India for many years to prevent soil erosion. (*Hengchaovanich*, 1996), as shown in Figure 2.2. The roots of Vetiver are thought to be able to penetrate into soils to a depth of 2-3 meters depending on the ground conditions (*Hengchaovanich*,1996). In addition, the reinforcing effect of this root system provides additional resistance to the shearing force of plunging water (*Hengchaovanich*, 1996). POSS and Vetiver are the primary ground modifiers used in this research. The test results will be discussed further in this paper.

Figure 2.2 Root system of Vetiver (*www.vetiver.org*)

2.4. Test Set Up and Procedure

The University of Mississippi Erosion Test Bed (UMETB) is a combination of two tanks, five pumps, and pipes that were designed to mimic plunging water in New Orleans as shown in Figure 2.3. The UMETB circulates water into and out of an inner tank that in turn circulates water into and out of an outer tank. Water is pumped from the outer tank into the inner tank to fill clean water in the inner tank; then clean water is pumped from the inner tank through a series of pipes directly to the nozzle as seen in Figure 2.3.1. In doing so, the water passes through a planar nozzle that is .003 m thick that simulates water plunging over a flood wall. The velocity of this plunging water was controlled to be 6 m/s; this is approximately the same velocity of plunging water from the top of 1.8 m high flood walls which was the field conditions in New Orleans. The soil sample is placed in a metal holder in the bottom of the outer tank, and then the soil sample is moved directly next to the nozzle as seen in Figure 2.5.

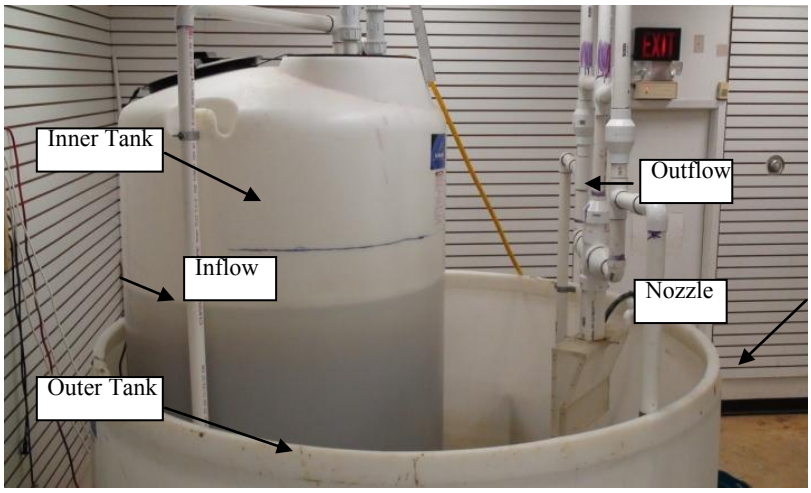

Figure 2.3.1 Depiction of UMETB

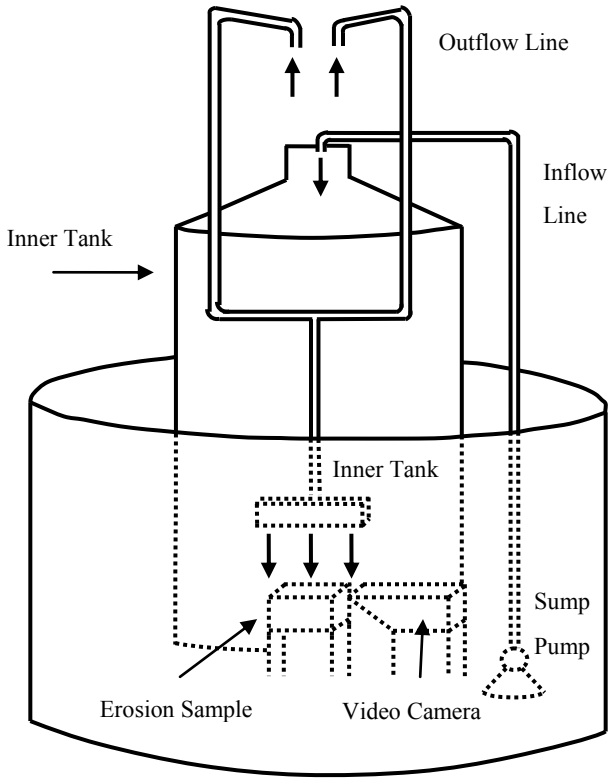

Figure 2.3.2 Schematics of UMETB

Soil samples are prepared as discussed in the Test Samples chapter. Before any soil samples are made, the maximum dry density and optimum water content are measured for each mixture by the Standard Proctor Test (ASTM D698). The basic soil properties of each mixed and tested soil samples are shown in Table 2.1.

An erosion mold is a wooden container built of lumber and clear acrylic plate and designed to hold soil samples for testing (*Jang et al*. 2010). The clear acrylic plate is used to view and record, on video camera, the erosion progress during the tests. The acrylic plate has a network of measured marks (1 cm x 1 cm) in order to accurately quantify erosion behavior on

the video camera. After being built, the erosion molds are measured in order to obtain the volume Length (.253 m) x Width (.20 m) x Height (.20 m) = Volume (.010537323 m^3). The soil samples are compacted to a specific degree of compaction in the erosion molds. Compaction is carried out in eight separate layers in order to obtain uniform compaction. Also, in order to mimic field compaction techniques, a gasoline powered tamper (Dynapac, LF45) was used. A coat of bentonite and water paste are applied to the inside of the erosion mold to decrease the amount of friction between the soil and the erosion mold during compaction (For further details on this technique, please see *Jang et al.* 2010).

During times of excess rainfall, flooding, and hurricanes, the soils surrounding the area may be soaked. To reproduce this condition, soil samples are completely submerged in water for 48 hours before testing, as shown in Figure 2.4. The water level was kept at .05 m above the sample in order not to apply too much water pressure to the samples. The dimensions of soil samples are taken before and after submersion in order to calculate changes in soil parameters such as void ratio and the degree of saturation.

Figure 2.4 Soil Sample after being submerged

2.4.1. Testing Procedure

The following test procedure is followed in this study.

1) Mount the erosion mold under the nozzle.

2) Set the video camera in front of the graduated acrylic plate to record the erosion profile with time.

3) Focus the video camera on the grid of the acrylic plate as shown in Figure 2.5.

4) Turn on the five sump pumps (three of 1/3 Horse Power for out-flow, two of 1/2 Horse Power for in-flow) to circulate water from inner tank to outer tank via the nozzle so that it initiates the erosion on the soil sample surface.

5) Record the erosion process with the video camera.

6) Analyze the recorded video images with PMB (Picture Motion Browser) software and obtain erosion depth and lap time data.

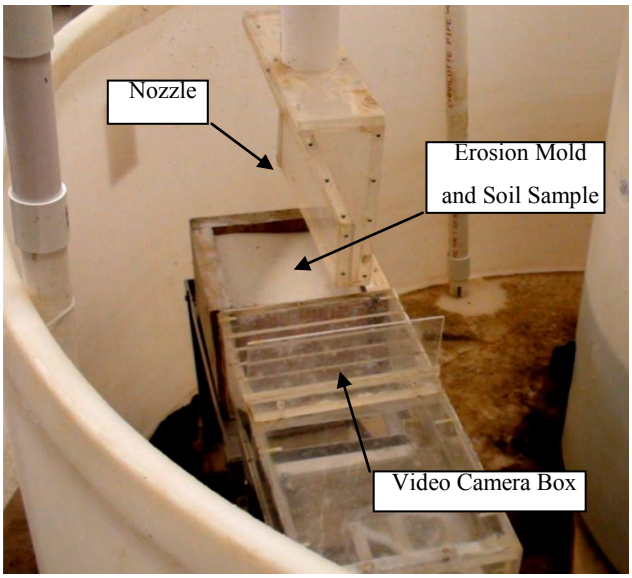

Figure 2.5 Erosion testing mold

2.5. Analytical Equations for Erosion

The excess stress concept (*Hanson et al*. 2002 modified from *Stein et al*. 1993), postulates that erosion of soil takes place if the effective shear stress from the moving fluid is higher than the critical (resisting) shear stress as shown in Equation [3.1]. Note that the erosion rate coefficient (k_d value), the difference between the effective shear stress and the critical shear stress, and the erosion time. This study computed k_d so that erosion resistance of different soils may be compared quantitatively. This study, however, computed k_d at each time step rather than computing a single average k_d throughout the test. $\frac{dD}{dt}$ at a certain time is obtained from the test, τ_o and τ_c are obtained from tests and hydrodynamics. The calculation procedure of k_d at time intervals is shown as follows.

$$\frac{dD}{dt}=k_d(\tau_o-\tau_c)^a \qquad 3.1$$

Where:

D=erosion depth

t=time

k_d= erosion rate coefficient

τ_o= shear stress caused by flowing water

τ_c= critical shear stress

a= constant

Equation [3.1] is solved using dimensionless parameters as follows

When $D^* \leq D_P^*$

$$T^* = D^* \left(\frac{D_p^*}{1 - D_P^*} \right)^a \quad 3.2$$

When $D^* \geq D_P^*$

$$T^* - T_p^* - \left[-D^* - \ln(1 - D^*) \right]_{D_P^*}^{D^*} = 0 \quad 3.3$$

Where:

$$D^* = \text{normalized erosion depth} = \frac{D}{D_e} \quad 3.4$$

D=erosion depth at a given time

D_e=equilibrium erosion depth

$$D_P^* = \text{normalized depth of potential core} = \frac{D_p}{D_e} \quad 3.5$$

D_p=depth of potential core= $C_d^2 y_0$ 3.6

C_d=diffusion constant= $\sqrt{5.5(1+\cos\theta)}$ 3.7

θ= impinging angle

y_o=thickness of plunging water

T^*=normalized time= $\frac{t}{T_r}$ 3.8

T_r=reference time= $\frac{D_e}{k_d \tau_c}$ 3.9

$T_p^* = \frac{\tau_c}{\tau_e} \left(\frac{\tau_c}{\tau_e - \tau_c} \right)^a$ Stein et al 1993 (a=1) 3.10

τ_c=critical shear stress= $\frac{D_p}{D_e} \tau_e$ 3.11

τ_o=effective shear stress= $C_d^2 C_f \rho u_0^2 \frac{y_o}{D}$ 3.12

C_f=coefficient of friction=$\frac{0.0474}{2} R_0^{-\frac{1}{5}}$ 3.13

R_0=Reynolds Number=$\frac{2y_0 u_0}{\nu}$ 3.14

u_o= flow velocity of impinging water

ν=viscosity of water

This research focuses on the research conducted by *Stein et al* (1993, 1997) and *Hanson et al* (2002, 2003). Their research proposed finding a constant k_d value, which is a detachment coefficient. However, the Stein et al and Hanson et al. approach was modified by Jang (2010) by using non constant k_d incorporating the change of erosion coefficient due to the changes in soils strength, confining pressure, density and so on. This study adapted concepts by Jang, and the details of this approach can be found in Jang.

All of the values are known for the Equation [3] through [14], except for k_d, D_e, and τ_c. However, the final erosion depth (D_e) can be found by plotting erosion depth vs. time and finding the ultimate value; then, the value for τ_c can be computed. After these two parameters are found, it is not difficult to use a spreadsheet to find the detachment coefficient k_d.

Sample Calculation

Sample calculation at time=200 seconds for POSS treated (SO1458) soil sample (F50S50 at 83% Degree of Compaction) is conducted here. The correlating erosion depth for this time was found to be 5.5 cm; this can be seen in Figure 2.6.

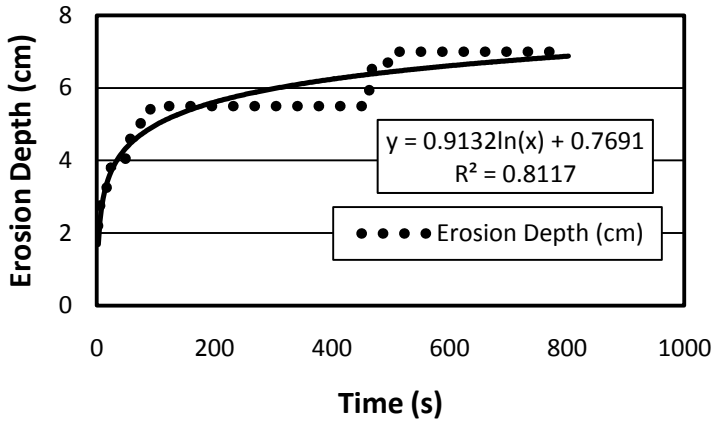

Figure 2.6 Sample graph in order to show k_d calculation

In order to perform these calculations it is assumed that the time to reach equilibrium depth (D_e) is one hundred days; the depths in Figure 2.6 were found using logarithmic curve fitting. Therefore, from Figure 2.6 it is found that D_e =.1535 m

Data known from UMETB:

θ=angle that water strikes soil=90^0

y_o=plunging water width=.003 m

u_o=velocity of water=6 $\frac{m}{s}$

ν=viscosity of water=1.004×10^{-6} $\frac{m^2}{s}$

ρ=density of water=1000 $\frac{kg}{m^3}$

Computed Numbers

$C_d=\sqrt{5.5(1+\cos\theta)}=2.345$

$D_p=C_d^2 y_0=2.345^2*.003=.0165$ m

$\tau_o=C_d^2 C_f \rho u_0^2 \frac{y_o}{D}=$

$=2.345^2(.0029)(1000)\left(6^2\right)\frac{.003}{.055}=31.31$ Pa

$D_e = .1535$ m

$\tau_c=\frac{D_p}{D_e}\tau_e=\frac{.0165}{.1509}*31.31=3.42$ Pa

Using a data point in Figure 2.6 when time is 200 sec, and using t_o, t_c, and k_d is computed as follows.

$$k_d=.000024311\,\frac{m^3}{N*sec}$$

Since most soil parameters such as density, shear strength, and water content vary with depth; the detachment coefficient k_d should also vary with depth. This was accomplished by analyzing the erosion behavior at time intervals of 2 seconds, and calculating a k_d value for each time interval, in doing so it allows for the calculation of a non-constant k_d value

2.6. Results and Analysis

2.6.1. Bare Soil

The representative sample that was chosen for comparison was F50S50, which has 50% fines and 50% sand, and a degree of compaction at 83%. The primary reason for this selection is that this sample shows quite low resistance to erosion in previous studies (*Jang*, 2010). This is

illustrated in Figure 2.7. In principle, if a chemical or a plant can control erosion for this sample, it should be able to decrease erosion in other samples with higher clay percentages and degrees of compaction. The computed final erosion depth, or equilibrium depth (D_e), was found to be .494 m when time is equal to 100 days; this is illustrated in Figure 2.8. The actual equilibrium depth would be slightly higher when time is equal to infinity; however, for analytical calculations the time was assumed to be 100 days for simplicity.

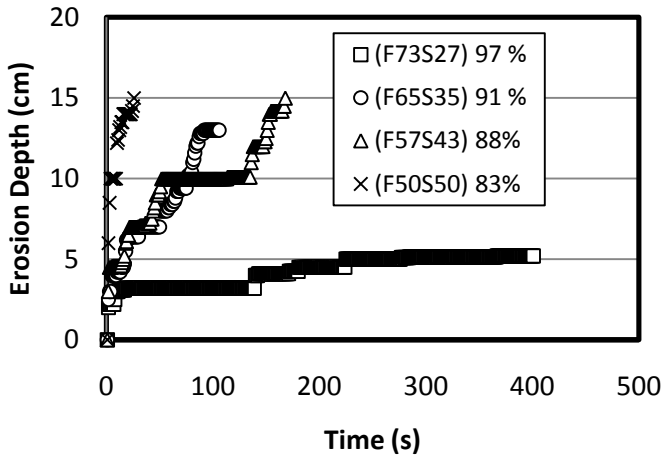

Figure 2.7 Erosion Depth vs. Time relationship for bare soils

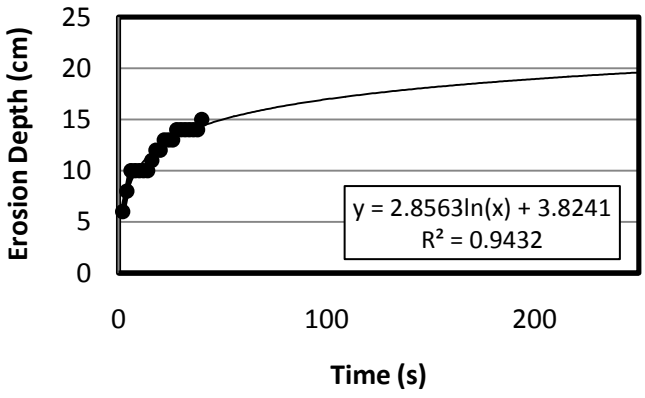

Figure 2.8 Equilibrium Depth Equation

2.6.2. POSS Treated Samples

There were two tests conducted for POSS samples because there were two different types of POSS chemicals (SO1455 and SO1458), and the results along with bare soil can be found in Figure 2.9. The same clay content and degree of compaction were used for the POSS samples (F50S50 and DOC 83%) and bare soil samples. Both treated specimens showed a substantially higher resistance to erosion than the bare soil. However, SO1458 showed higher erosion depth initially, but it showed lower final erosion depth than SO1455. To compare the erosion resistance of samples in a more quantitative manner, the erosion rate coefficient was computed and compared in Figure 2.10, which shows that POSS treated samples have a much lower (k_d of bare soil ≈ 2.0 E-03 m^3/N*sec , k_d of POSS treated soil ≈ 2.0 E-05 m^3/N*sec) erosion rate coefficient when compared to bare soil.

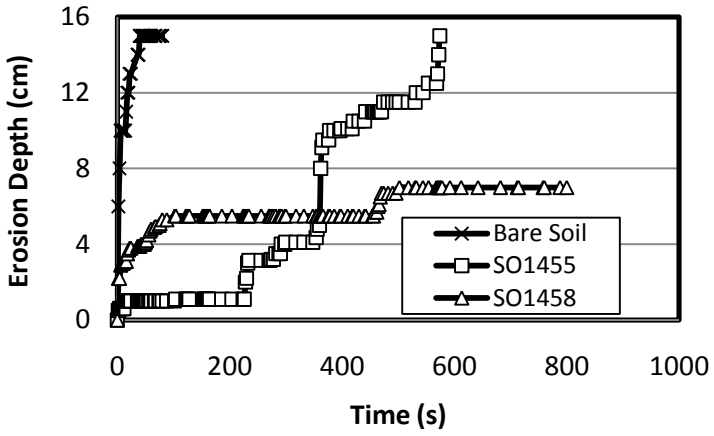

Figure 2.9 Graphical Comparisons of POSS

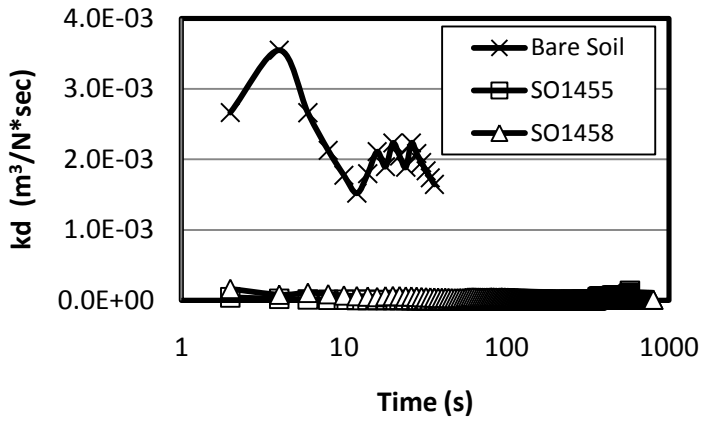

Figure 2.10 Comparison of k_d values for all POSS samples

To investigate engineering reasons for these findings, water content of test samples are compared. Following the submersion, the POSS samples appeared to be less water saturated compared to the bare soils. Figure 2.11 shows that POSS treated samples decreased the water content an average of 25%, meaning that POSS was smeared into the substantial portion of pore spaces and provided additional adhesion that may contribute to the higher erosion resistance. At a deeper depth, however, POSS samples showed about the same or higher water content at the bottom, indicating that POSS might not penetrate to deeper depths and erosion resistance might not be improved. Therefore, the soil might behave more like bare soil than reinforced soil at deeper depths.

Comparing the water contents of SO1455 and SO1458 at shallower depths (less than 10 cm depth), it can be seen that SO1458 has lower water content, indirectly indicating the higher POSS content, and higher erosion resistance. But this water content plot does not explain why SO1458 showed lower erosion resistance initially. Therefore, strength tests were conducted for

test samples.

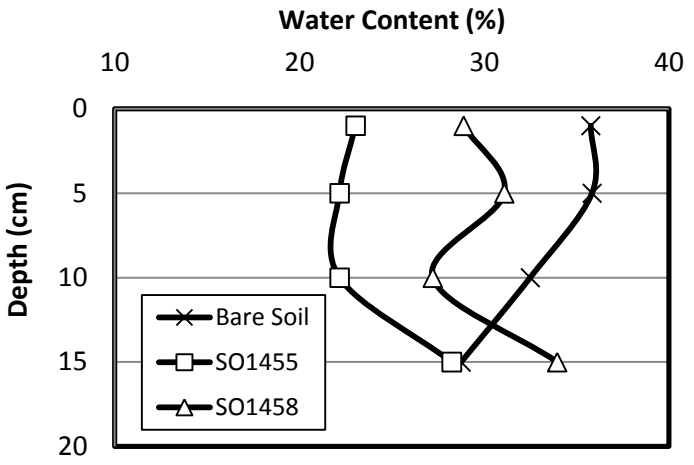

Figure 2.11 Water Content Comparisons for POSS

The shear strength of the POSS samples was measured by the miniature vane shear test apparatus. The results seen in Figure 2.12 show the shear strength of POSS samples. Without POSS, the shear strength at the surface to 2 cm depth is very close to zero; however, POSS increases the shear strength at the surface substantially, which is also the point of impact for plunging water. Following that, the shear strength was reduced to approximately the same level as that of the bare soil at deeper depths. This may explain why POSS treated samples show (particularly SO1455) quite high erosion rate coefficients for prolonged time periods. From Figure 2.12, it shows that the initial lower erosion resistance for SO1458 is mainly due to the lower shear strength of surface layers. As erosion progressed, the water needed to erode higher strength layer, and it showed higher erosion resistance. Therefore, it seems that shear strength provide a better indicator than water content to predict the erosion behavior of soils.

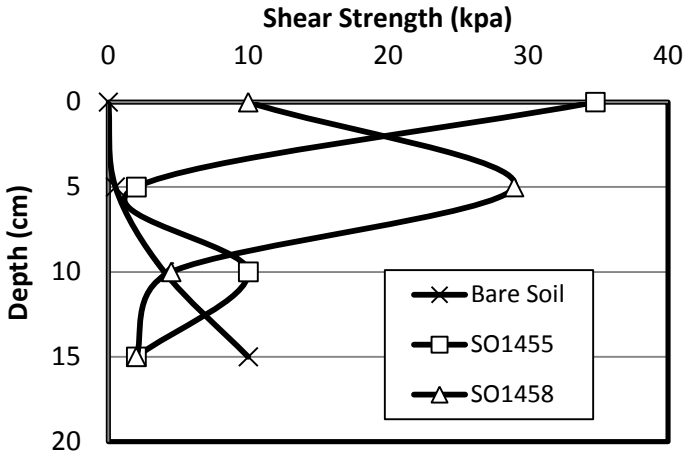

Figure 2.12 Shear Strength of POSS samples

2.6.3. Vetiver Plant: The Vetiver proved to be very effective in reducing the erosion of soil. It was so effective that currently no graphs, tables, or data can be obtained for the Vetiver because no erosion occurred. The Vetiver plant used in the experiment was grown for 12 years; and no quantitative data was available. Two separate tests were conducted. The first test, conducted with 10 cm of stem and root system, showed no recordable erosion.

Test results can be seen in Figure 2.13. The second test was conducted on the root system only with the stems completely removed. No visible erosion was noted. Test results are shown in Figure 2.14. From the figures, it can be seen that no measurable erosion occurred for either the root and stem together or the roots only in Vetiver samples. The plunging water seemed not to reach further than the root system of the Vetiver. The structure of the plant (root system and grass stems) also held up well after being exposed to plunging water. Since the water never reached past the Vetiver stems to the actual soil, no data collection could be made. Therefore, the Vetiver proved effective in enhancing erosion resistance.

Figure 2.13 Vetiver stems after erosion testing

Figure 2.14 Vetiver roots after erosion testing

2.6. Conclusion

Erosion caused by plunging water caused extensive damage, in the New Orleans area during Hurricane Katrina. This research focused on reducing erosion through ground modification: erosion mitigation performance of POSS and Vetiver were assessed. Applying the previously developed excess shear stress concept and laboratory tests, all soil samples were

evaluated by how effective each sample was at reducing erosion. From the results the following conclusions could be made:

1. POSS reduced erosion rate significantly ((k_d of bare soil ≈ 2.0 E-03 m^3/N*sec) , (k_d of POSS treated soil ≈ 2.0 E-05 m^3/N*sec)). Shear strength was increased and water content was decreased due to POSS filling the voids in the soil samples.
2. POSS seemed to be effective only to a depth of about 9-12 cm; after erosion reached this depth; samples exhibited similar erosion characteristics to bare soils. It is thought that this condition is due to POSS only penetrating the soil samples to this depth. However, it should be noted that POSS can easily by applied to field soils by simply spraying the liquid.
3. The Vetiver proved to be quite effective. No recordable amounts of erosion occurred. Due to the dense vegetation and root system, water was unable to penetrate into soil samples.
4. The Vetiver would be cost effective and relatively easy to apply to soil along earthen levee systems. However, it may take substantial time to establish and grow Vetiver.

Suggested future work includes determining the erosion limit of Vetiver; this includes increasing the flow rate and water width thickness to reach maximum capacity of Vetiver. Also, testing different ages of Vetiver, because the density of the plant with increase with age. In addition, field investigation of the applicability of both POSS and Vetiver; full scale testing of the effects of both modifiers to ensure adequate erosion resistance. This includes planting Vetiver on a given levee system and monitoring the growth with respect to time. In addition, application methods for POSS should be tested such as: spraying methods, quantity of POSS, and sprayed coverage area

CHAPTER III

INFLUENCE OF THICKNESS OF PLANAR NOZZLES ON EROSION DEPTH OF LEVEE SOILS

3.1. Abstract

To predict the erosion depth for field conditions from the small scale laboratory erosion tests; the difference of scale should be considered. One of factors to be considered is the thickness of plunging water or nap thickness. This study evaluates the effect of the thickness of planar nozzles on soil erosion. Three different cohesive soils were tested by the UMETB and USDA-HERU facility with approximately the same water velocity of 6 m/s, which is the expected velocity of plunging water falling from I-walls in the New Orleans area. The measured dynamic erosion depth with different nozzle thickness, 0.003 m, 0.065 m, 0.013 m, and 0.2 m, is used to evaluate the effect of nozzle thickness. Experimental results showed that equilibrium depths increased, with respect to the increasing nozzle thickness, but not in a linear fashion.

3.2. Introduction

Hurricane Katrina caused a number of overtopping failures on the floodwall and ensuing erosion of the levee soils. Based on the hydrographs and video images, the thickness of plunging water hitting the ground is estimated to be approximately 0.2 m, with impact velocity close to 6 m/sec (Jang et al., 2010).

The dynamic energy of this plunging water was high enough to cause the erosion of levee soils and subsequent failure and flooding.

To analyze the stability of the levee system, the prediction of erosion depth in the field is critical. However, this prediction of erosion depth is well under-studied as pointed out by Seed et al. (2008). Currently, a possible solution is performing small scale laboratory tests for the field soil, and the use of a series of analytical equations to predict the field erosion depth. In this process, one of the most critical factors is the scale factor. Plunging water thickness for lab tests is usually in the mm range while the field thickness is approximately 0.2 m.

For the case of excess shear stress concept, fundamental equations (Rajaratnam, 1976) are derived for air to air jet (or water to water jet). Rajaratnam's fundamental equations (shown in the next chapter) explicitly assumed several conditions such as: steady state flow (constant flow velocity), no aeration, negligible effect of normal stress and so on. Particularly, the effect of the thickness of the plunging water on the flow pattern was derived by Buckingham's π-theorem using the relationship among four variables that include: nozzle velocity, centerline velocity, thickness of nozzle, and distance from the nozzle along the centerline. π-theorem is a very useful tool to derive a relationship among different parameters. It is also noted that the relationship from the π-theorem is not always a unique one; it may be revised if additional factors (e.g. oscillating stresses and aeration effects) are considered. Based on Rajaratnam's fundamental equations and excess shear stress concept (Stein et al., 1991, 1993, and 1997; Hanson et al., 2002), the erosion depth is linearly proportional to 0.8^{th} power to the thickness of plunging water (Kim et al, 2011). For the case of overtopping water in New Orleans during Hurricane Katrina, the plunging water passed through air, then hit the levee soil. As time passes and erosion depth

becomes deeper, it is clear that aeration cannot be prevented. When aeration occurs, the fluid flow may be quite turbulent, stresses may oscillate substantially and the flow pattern may change substantially from no-aeration condition as pointed out by Bonetto and Lahey Jr. (1993), Cummings and Chanson (1997) and Chanson et al. (2002). Considering this mechanism, it is clear that the erosion mechanism in this case could be different from that assumed in Rajaratnam's fundamental concepts. Therefore, the erosion depth may be different from that predicted by the excess stress concept.

In this study, tests were performed to evaluate the effects of the thickness of the plunging water using laboratory and full scale field tests. The result showed that the erosion depth increased with increased thickness of the plunging water, but in a much slower manner.

3.3. Fundamental Formulations for Erosion Depth

The relationship between the flow induced shear stress and flow velocity is described as follow from fundamental fluid mechanics.

$$\tau = C_f \rho U_m^2 \qquad 3.1$$

Where, τ =shear stress between solid surface and fluid, C_f =friction coefficient , ρ =density of fluid, and U_m= flow velocity along the centerline.

From the π-theorem, the relationship between nozzle velocity, centerline velocity, thickness of nozzle and distance from the nozzle along the centerline is derived as follows.

$$\frac{U_m}{U_0} = C_d\sqrt{\frac{y_0}{J}}\text{, outside the potential core } (J>J_p) \qquad 3.2.1$$

$U_m=U_o$, within the potential core ($J \leq J_p$) 3.2.2

Where, U_o= nozzle velocity, C_d= diffusion coefficient, y_o= one half thickness of the nozzle, J is the centerline distance from the nozzle, J_p is the potential core length. The potential core length is the distance along the major flow direction where the centerline velocity is the same as the nozzle velocity. When equations 3.2.1 and 3.2.2 are substituted into equation 3.1, the following equations are obtained.

$\tau = C_f C_d^2 \rho U_0^2 \frac{y_0}{J}$, outside the potential core ($J > J_p$) 3.3.1

$\tau_0 = C_f \rho U_0^2$, within the potential core ($J \leq J_p$) 3.3.2

When erosion depth reaches the length of the potential core ($J = J_p$), $\tau = \tau_0$. In equation 3.3.1 and 3.3.2, τ within the potential core is denoted as τ_0. Using equation 3.3.1 and 3.3.2 the following expression is obtained.

$J_p = C_d^2 y_0$ 3.4

Using equation 3.4 and 3.3.1 is expressed as follows.

$\tau = C_f \rho U_0^2 \frac{J_p}{J}$ 3.5

The erosion rate equation using the excess shear stress concept is expressed as follows.

$\frac{dJ}{dt} = k(\tau - \tau_c)^a = k(C_f \rho U_0^2 \frac{J_p}{J} - \tau_c)^a$ 3.6

Where, k = erosion rate coefficient (or called detachment coefficient), a = material parameter (typically 1 to 1.5). Equation 3.6 means that the erosion continues until the induced shear stress by fluid flow is the same as the shearing resistance of the solid that is called critical shear stress.

When it reaches this equilibrium condition, $\frac{dJ}{dt}$ becomes zero, J (the same as the erosion depth) at this condition is called J_e (equilibrium erosion depth). Then from Equation 3.6 the following equation is derived.

$$J_e = \frac{C_f \rho U_0^2 J_p}{\tau_c} \tag{3.7}$$

In Equation 3.7, C_d, the diffusion constant, is taken as 2.6 and 2.28 by Stein et al. (1993). C_f, the friction coefficient, is the function of Reynolds number as follows.

$$C_f = \frac{0.0474}{2} R_o^{-0.2} \tag{3.8}$$

And Reynolds number is the function of several parameters as follows.

$$R_o = (2 y_o U_o)/\nu \tag{3.9}$$

With Equations 3.7, 3.8, 3.9 and 3.4, the equilibrium (ultimate) erosion depth J_e is expressed as follows.

$$J_e = \frac{0.027 C_d^2 \rho U_0^{1.8} y_o^{0.8} \nu^{0.2}}{\tau_c} \tag{3.10}$$

Equation 3.10 shows that the equilibrium (ultimate) erosion depth is proportional to 0.8^{th} power of the thickness of the nozzle.

To see the variation of transient erosion depth with the thickness of the nozzle, Equation 3.6 is revisited here. Considering that all other terms are constants except J and t, it can be easily seen that the transient erosion depth J will increase proportionally to $y_0^{\frac{a}{a+1}}$. The constant a is typically 1 for cohesive soils (Stein et al. 1993), so the transient erosion depth J will be approximately proportional to $y_0^{0.5}$, that is different from the case for the equilibrium erosion

depth. From this analytical result, the effect of the nozzle thickness is proportional to $y_0^{0.5}$ during transient condition, but the equilibrium (ultimate) erosion depth is proportional to $y_0^{0.8}$.

3.4. Test Soils

Test soils were taken from a quarry site in New Orleans, and mixed based on the material specification of levees (Vroman, 2008). Two different soil types are mixed to prepare test samples: fine grained and course grained. The fine grained soil is classified as CH or CL with 80% passing #200 sieve. The course grained soil is classified as SM or SP with 4.5% passing #200 sieve. Samples are mixed at air dried conditions and compacted at optimum moisture content. Samples were also submerged under the water for 48 hours to mimic heavy rain conditions in the field. For more detailed soil mixing and sample preparation procedures, Jang et al. (2010) is referred to.

In this study, three different mixtures of fine and course soil are prepared: 50/50, 57/43, and 65/35 (with the % of fines being the first number, and course soils being the second number). These soils are compacted to 83%, 87%, and 91% of maximum dry density. The fundamental properties of these samples are shown in Table 3.1.

Table 3.1. Basic Soil Properties of Soil Samples

Soil Identification	Degree of Compaction (%)	$\gamma_d (kN/m^3)$	$\gamma_w (kN/m^3)$	Void Ratio
F50S50 (Clay15%, Silt35%, Sand 50%)	83	16.5	14.1	.96
F57S43 (Clay 18%, Silt 40%, Sand 42%)	87	17.4	14.7	.83

F65S35 (Clay 20%, Silt 45%, Sand 35%)	91	19.1	16.2	.78

3.5. Experimental Setup

3.5.1. UMETB

Among several erosion testing techniques (RCT by Moore and Masch (1962), EFA by Briaud et al. (1999, 2001), HET by Wan and Fell (2004) and JET by Hanson et al. (2002, 2005, and 2006)), JET utilizes a water jet to erode soils. However, JET has a fixed 13 mm diameter circular nozzle. This study, therefore, utilized UMETB (University of Mississippi Erosion Testing Bed) with several different size nozzles for three different soils. Detailed information of UMETB is shown in Kim et al. (2011) and Jang et al. (2010), but essential information is presented here for completeness.

UMETB is an erosion testing apparatus that jets water through a planar nozzle using a series of pumps and pipes as seen in Figure 3.1. UMETB was designed to mimic over topping water caused by Hurricane Katrina, and therefore the velocity of the water passing through the planar nozzle is kept at a constant 6.00 m/s which is equivalent to the velocity of plunging water from I-walls. The thickness of the water passing through the planar nozzle was controlled by using nozzles of different slit thickness. The nozzle thicknesses used in this study are 0.003,0.0065, and 0.013 m. All other parameters such as flow velocity were kept constant. To measure true dynamic erosion depths, the erosion profile was recorded by a digital video camera, the video images were analyzed later to obtain the erosion depths.

a) UMETB apparatus

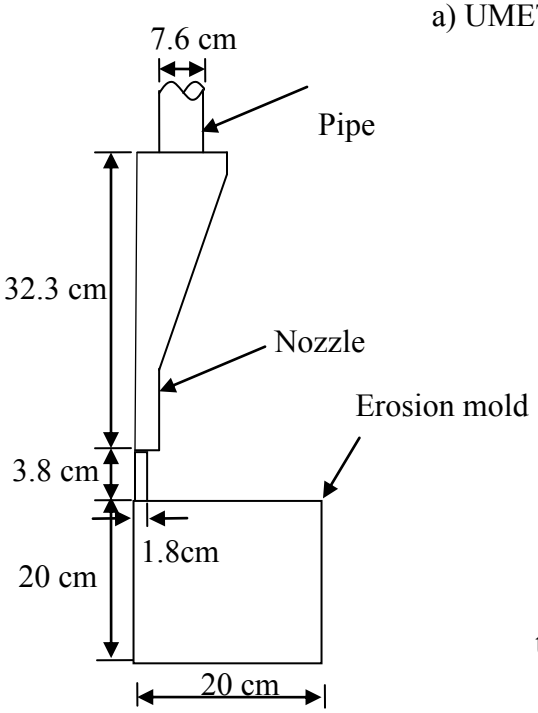

b) Schematics of nozzle and erosion mold

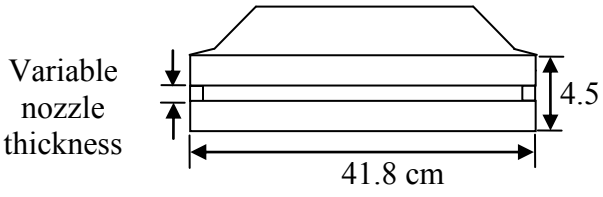

c) Schematics of nozzle outlet

Figure 3.1 Description of UMETB (Kim et al., 2011)

3.5.2. USDA-HERU Test

The highest achievable flow rate with UMETB was approximately 32,600 Gal/hr that provides 6 m/s flow rate for 0.013 m nozzle (including bypass water that flows outside the sample box). This flow rate was obtained by using six 0.75 HP sump pumps (Flotec, FPSC4550A) assisted by two external generators. The thickness of this nozzle was still far narrower than the thickness of the plunging water in the field. Therefore, the full scale erosion tests were conducted in one of the weir's in USDA-HERU facility in Stillwater, OK. The essential specification of the weir is shown in Figure 3.2.

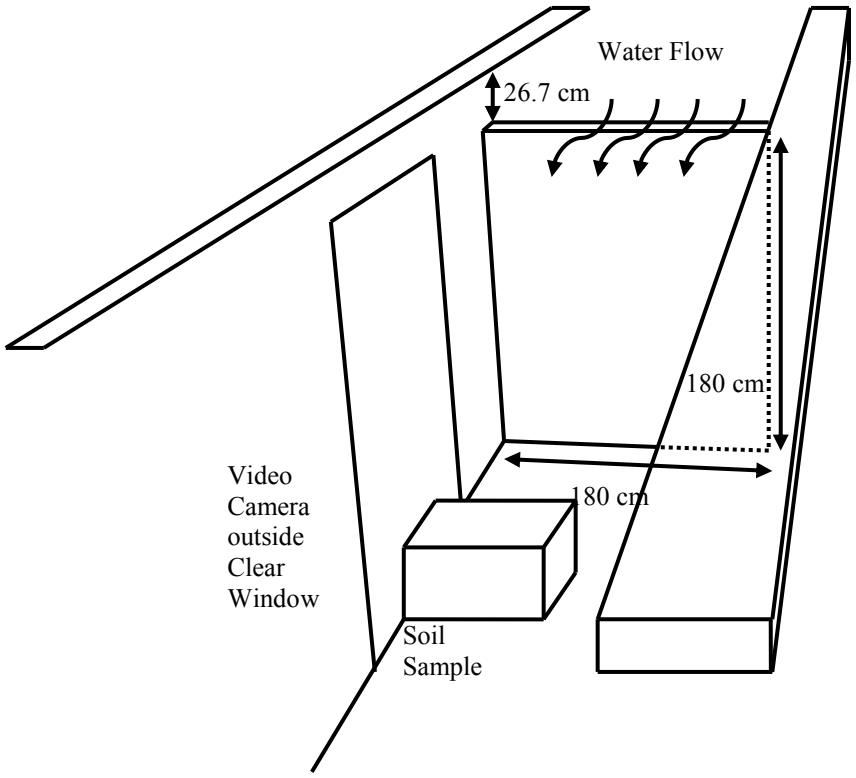

Figure 3.2 Specification of USDA-HERU weir

The water used for these tests was drawn from Lake Carl Blackwell and supplied to the test weir through a series of water ways and gates to control the flow rate. For this study, the flow rate was controlled by trial error so that the elevation of the upstream water is close to 0.3 m above the brink of the weir that is the recorded hydrograph results during Hurricane Katrina in New Orleans. In this study, the upstream water was actually 0.27 m above the brink of the weir elevation. The drop height of the weir was 1.63 m (the maximum obtainable drop height.)

To reduce the flow velocity of water in the water ways, a retention pond was used close to the weir. The intake duct to the weir was also aligned 90° so that the flow velocity to the weir is not further affected by the flow velocity of the intake water. Based on USDA-HERU measurement, the flow velocity in the weir is close to 0.03 m/s. The trajectory of the plunging water from the weir is very similar to that from the floodwall in New Orleans. In addition, the vacuum tube under the weir was left open so that the plunging water was not forced to stick to the wall. Actual pictures of the full scale weir tests are shown in Figure 3.3. The plunging water thickness was measured to be 0.2 m, with the flow rate being 0.51 m^3/ sec.

Figure 3.3 Depiction of Floodwall Testing

3.6. Erosion Mold

An erosion mold is a container made of wood and clear acrylic glass. The purpose of the erosion mold is to retain soil samples in place for erosion testing. The clear acrylic glass is placed on the front of the mold in order to view erosion as it takes place. The glass has a grid (1 cm x 1 cm) etched on the surface. The purpose of this gird is to accurately record the erosion behavior on the video camera. There were two different size erosion molds built and implemented in testing. The volume of the erosion mold used in UMETB was 0.010537323 m^3 while the volume of the erosion mold used in HERU was approximately 0.16990108 m^3 (0.3 tons or 675 lbs).

Compaction of the soil samples were carried out in eight separate layers, this is to ensure that uniform compaction takes place. In addition, a gasoline powered tamper (Dynapac, LF45,Sweden) was used to obtain uniform compaction, and also to mimic field compaction techniques. To reduce the friction between the soil and wood erosion mold, a thin coat of bentonite and water paste is applied to the surface of the erosion mold. (For further details on this procedure, please see Jang et al. 2010). In order to mimic field conditions during Hurricane Katrina (soil was soaked due to intense rainfall), soil samples were submerged for 48 hours as seen in Figure 3.5. The soil samples were submerged with a constant .05 m water height above the samples. This is to ensure that all soil samples were kept at a constant pressure before testing, and also not to apply excess water pressure to the samples. The weight of each sample was measured before and after submersion in order to determine void ratio, and also degree of saturation.

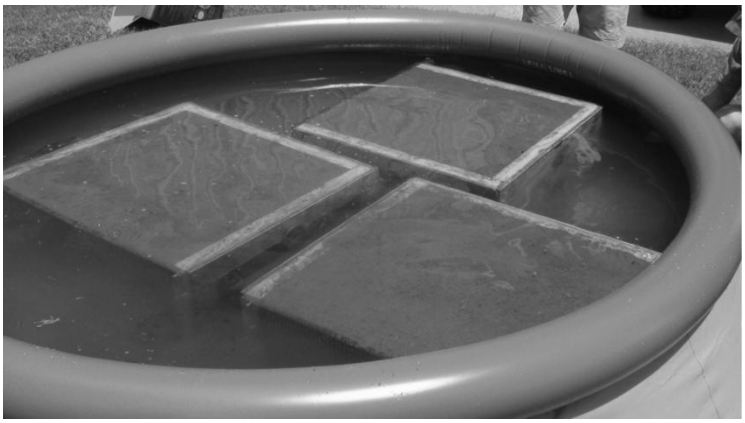

Figure 3.4 Submersion of soil samples at USDA-HERU

3.7. Results and Analysis

The erosion depths are measured by allowing continuous flow conditions and recording the erosion profile by a video camera. Using UMETB, three different nozzle thickness, 0.003 m, 0.0065 m, and 0.0130 m, are used while field tests at HERU are equivalent to 0.2032 m nozzle thickness. As shown in Figure 3.5, the erosion data is collected until the erosion depth reaches 15 cm for 0.003 m, 0.0065 m, 0.0130 m thickness nozzles and 40 cm for USDA HERU tests.

For F50S50 with 83% degree of compaction, as shown in Figure 3.5.1, it takes 38, 24, 15, and 4 sec to reach to the 15 cm with respect to the 0.003 m, 0.0065 m, 0.0130 m, and 0.2032 m nozzle thickness, respectively. For increased fines content, F57S43 with 88% degree of compaction shown in Figure 3.5, it took longer time, 327, 67, 19, 17 sec to reach 15 cm. Meanwhile, for F65S35 with 91% degree of compaction, due to the higher compaction and increasing fines percent, it was quite difficult to analyze the data because it showed discrete

erosion behavior that is typical for cohesive soils (Hanson, personal communication, June, 2010). Thus, the erosion depth is measured until it takes 800 sec for nozzle thickness of 0.003 m, 0.0065 m, and 0.0130 m, while for 0.2032 m nozzle thickness, the test is conducted until the erosion depth reaches 40 cm.

The test results using F65S35 with 91% of degree of compaction are generally analogous to F50S50 and F57S43. With increasing the nozzle thickness from 0.003 m to 0.2032 m, each erosion depth is increased from 13 cm, 14 cm, 15 cm, and 25 cm during 800 sec as shown in Figure 3.6, One of the remarkable trends of this study is that the nozzle thickness is increased almost linearly, however, the erosion depth does not show the linear trends with respect to the nozzle thickness. To clarify the non-linear erosion depth trend with respect to relatively linear nozzle thickness, the relations between erosion rate and nozzle thickness is plotted. The erosion rate is the ratio between the measured erosion depth and the time. In this study, due to the discrete erosion with respect to the time, the constant erosion rate (slope) is not measured as shown in Figures 3.5.(1), 3.5.(3), and 3.5.(4). Therefore, each erosion rate is obtained with five different time periods, and then, averaged to obtain the average erosion rate. As shown in Figure 3.5, all soil conditions show increasing erosion rate with increasing nozzle thickness. The decreasing erosion rate after comparing Figures 3.5.(2), 3.5.(4), and 3.5.(6), could be influenced by the increasing fines (or cohesive) materials and degree of compaction. Similar results, the influence of degree of compaction on the erodibility of cohesive sediments, is also reported by Hanson (1991, 1995) using a submerged JET test device. As shown in Figure 3.6, it should be pointed out that the erosion rate is not linearly proportional to the nozzle thickness.

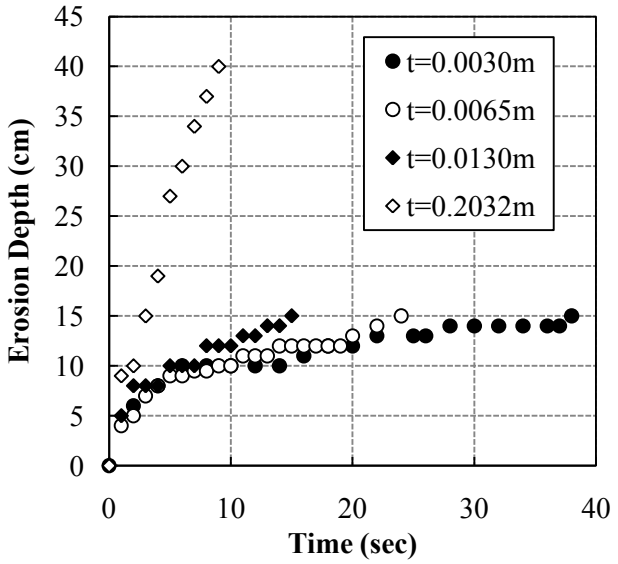

(1) Erosion test results for F50S50

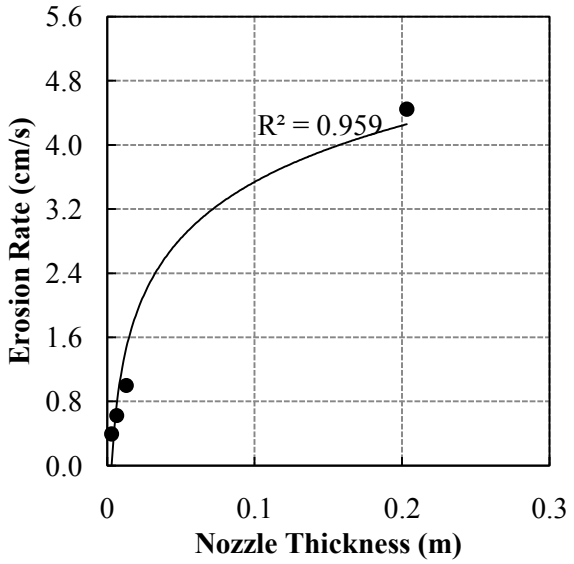

(2) Erosion Rate for F50S50

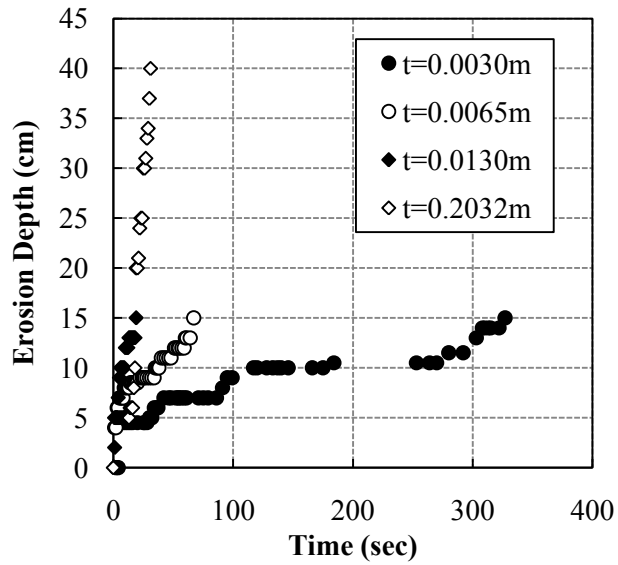

(3) Erosion test results for F57S43

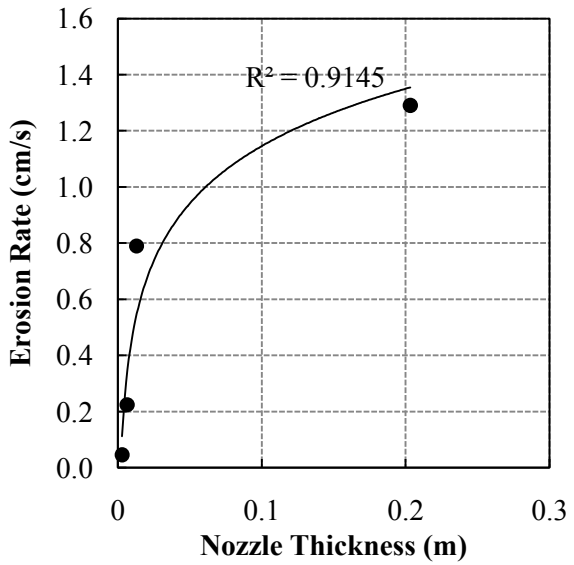

(4) Erosion Rate for F57S43

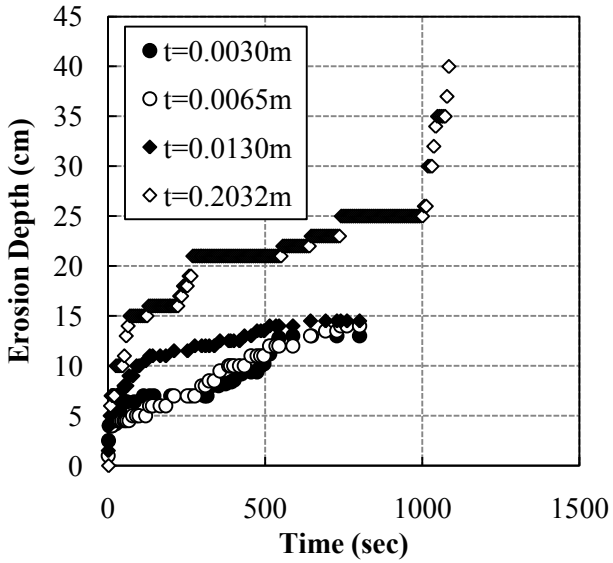

(5) Erosion test results for F65S35

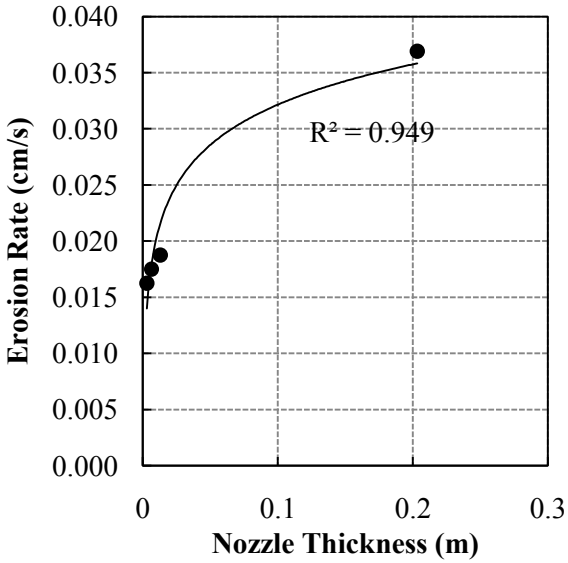

(6) Erosion Rate for F65S35

Figure 3.5 Erosion Test Results and Rate for different soils and nozzle thickness

3.8. Prediction of the Equilibrium Erosion Depth

To predict the equilibrium erosion depth from data in finite erosion time, three different curve fitting techniques – logarithmic, power trend, and hyperbolic fittings are used using EXCEL®. The hyperbolic method is one of the techniques to predict the settlement or consolidation of soils in geotechnical areas (Tan et al., 1991). The hyperbolic method assumes that the rate of the settlement or consolidation decreases as a hyperbolic pattern. One of the advantages of this method is it assumes the trend converge to a certain magnitude as shown in Equation 3.11.

$$D = D_0 + \frac{t}{\alpha + \beta t} \qquad 3.11$$

where, D and D_o is the predicted erosion depth and initial erosion depth, t is the time, α and β are the slope and intercept of the straight line. α and β can be computed when the straight line is shown from plot of $\frac{t}{\Delta D}$ vs. t. When time t is infinity in Equation 3.11, it shows that D converges to D_0 +1/β. The examples of $\frac{t}{\Delta D}$ and t plot is shown in Figure 3.6 from F57S43, 0.0065 nozzle thickness. As shown in Figure 3.7, the measured data may not show the proper straight line enough to compute reliable slope, α, and β intercept. Significantly, the computed slope and intercept with the measured run time are 0.063 and 0.2901. Using Equation 3.11, the predicted equilibrium depth is 15.88cm which is little bit higher than the measured erosion depth, 15 cm, during 67 sec as shown in Figure 3.5. This indicates that the computed slope, α, is under-estimate the overall erosion behavior of soil. It may be due to the reason that step-like erosion behavior of soil caused by the layer by layer compaction (Jang et al., 2010). As shown in Figure 3.5, when the erosion occurs at the each compacted layer, erosion depth is not increased significantly. Instead, the horizontal erosion which mainly caused the shear and oscillating stress rather than normal stress is taken place. After one of the compacted layers is eroded, normal stress from the plunging water governs the overall erosion behavior and resumes the vertical erosion. Therefore, after removing initial data set, several segments are used for computing α and β as shown in Figure 3.6.1 and 3.6.2. Firstly, after removing measured data within 1 to 9 sec, slope, α, and interception β, are computed and used to predict the equilibrium erosion depth using Equation 3.11 as shown in Figure 3.6.1. The expected erosion depth with 8640000 sec shows 28.88 cm Secondly, the measured data during 0-9 and 20-24 sec are removed and regressed it as shown in Figure 3.6.2. With computed α and β, the expected erosion depth turns out to be 25.10 cm with

8640000 sec. Based on the predicted erosion depth with some segments, it may be reasonable to conclude that the hyperbolic methods may be applicable to predict the erosion behavior of soils. However, some aspects have to be taken into considerations such as the step-like erosion behavior and mass erosion. Additionally, the erosion pattern of the sandy soil is generally shown as particle by particle. However, silty and clayey soils have a tendency to be eroded by chunk by chunk. It also may difficult to have linear relationship between $\frac{t}{\Delta D}$ and t plot. Due to the difficulties mentioned above, in this study, to use hyperbolic methods, several segments with different periods are applied to predict averaged equilibrium erosion depth as shown in Figure 3.7. Examples of the predicted erosion depth using averaged logarithmic, power trend, and hyperbolic fittings are used using EXCEL®. are shown in Figure 3.8. After comparing the measured erosion depth, it is observed that power trend lines may over-estimate the overall equilibrium depth. This is due to the fact that the power trend line does not converge to a certain number. Instead, it increases continuously. Thus, the prediction of equilibrium erosion depth using the power trend line may results in over estimation.

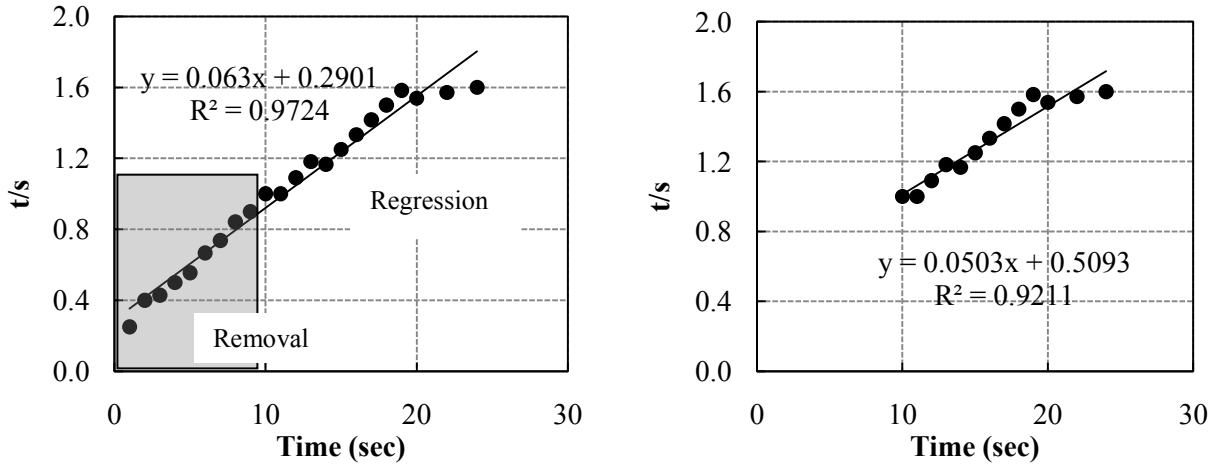

(1) computation of slope and interception with measured data at 10 to 25 sec

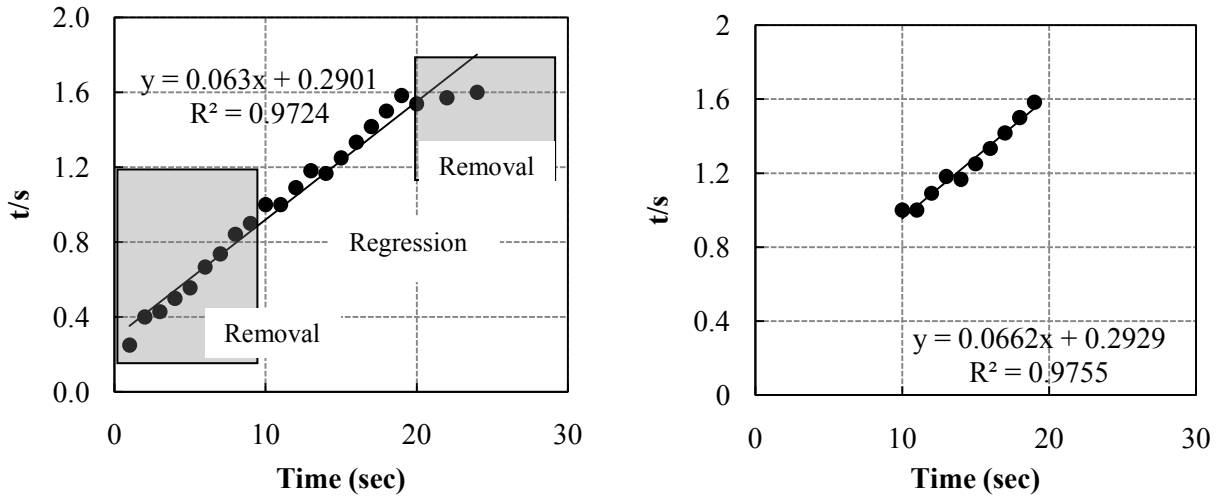

(2) Computation of slope and interception with measured data at 10 to 19 sec

Figure 3.6 Difference of computed slope and interception

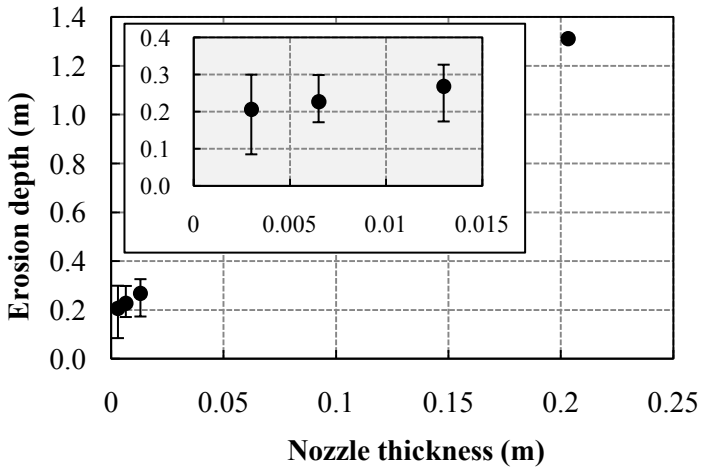

(1) F50S50

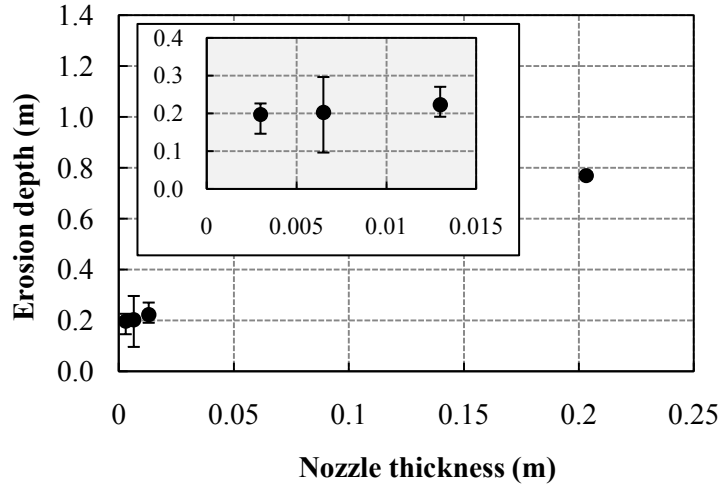

(2) F57S43

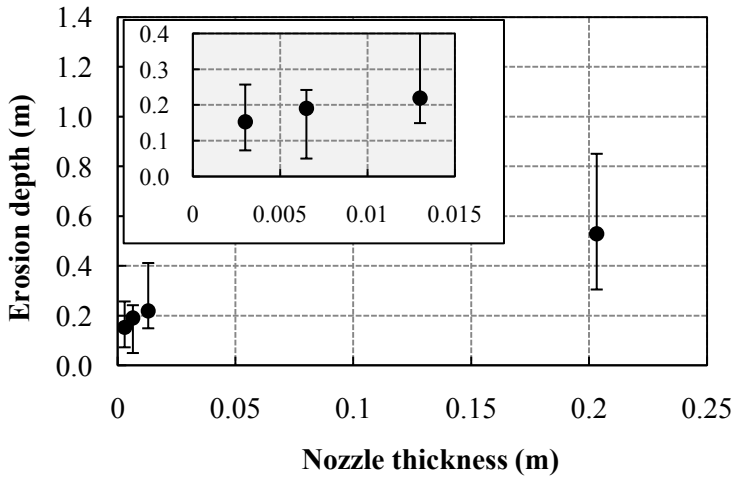

(3) F65S43

Figure 3.7 Predicted equilibrium depth from hyperbolic method

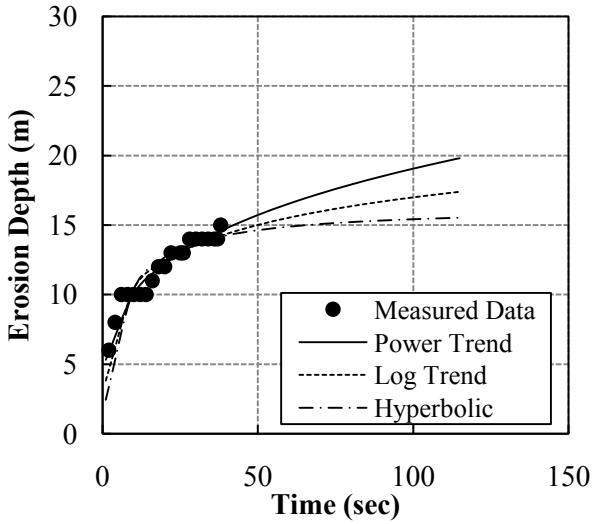

(1) Nozzle thickness = 0.003 m

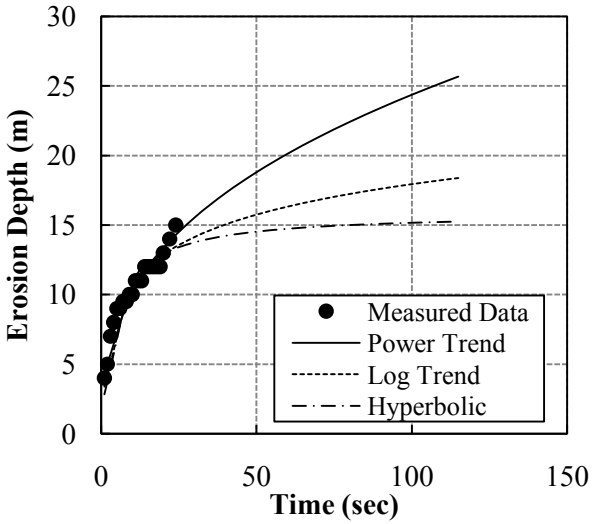

(2) Nozzle thickness = 0.065 m

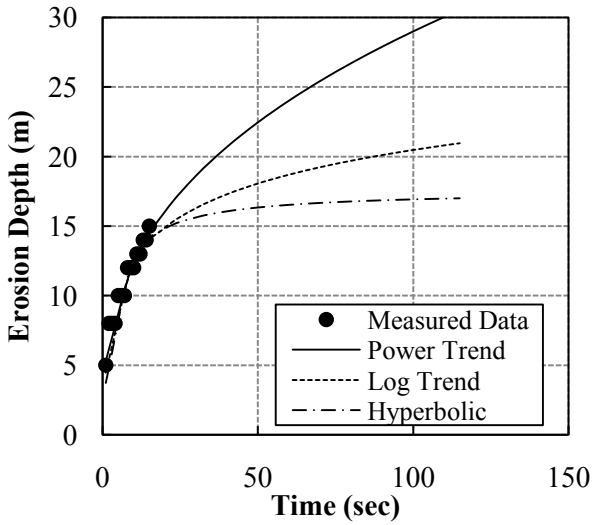

(3) Nozzle thickness = 0.0130 m

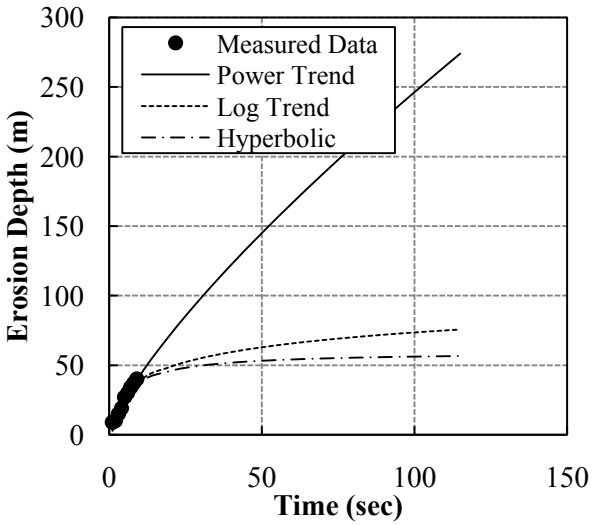

(4) Nozzle thickness = 0.2032 m

Figure 3.8 Equilibrium Depths F50S50 DOC 83%

3.9. Comparison of the Equilibrium Erosion Depth

To compare the predicted equilibrium erosion depth using the hyperbolic method and logarithmic trend lines with theoretical predictions, results are compared with other empirical equations.

Briaud et al. (1999) proposed the equation to predict the critical shear stress as follows:

$$\tau_c(N/m^2) = D_{50}(mm) \qquad 3.12$$

where, τ_c and D_{50} are the critical shear stress and mean diameter. As explained by Briaud et al. (1999), Equation 3.12. seems to fit well for cohesionless soils such as sand and gravel. However, it shows poor correlations to cohesive soils such as silt and clay due to the electromagnetic and electrostatic interparticle forces which increase the scour resistance (Briaud et al. 1999). Determination of the critical shear stress is proposed by Smerdon and Beasley (1961) with respect to the soil properties such as plasticity index, dispersion ratio, mean particle size (m), and percent clay by weight (%) using a flume study on eleven cohesive Missouri soils. Julian and Torres (2006) presented an equation for estimating the critical shear stress as follows:

$$\tau_c = 0.1 + 0.1779(SC) + 0.0028(SC)^2 - 2.34E-5(SC)^3 \qquad 3.13$$

Where, (SC) is the silt-clay percentage defined as the particle size less than 0.063 mm. Clark and Wynn (2007) presented that the estimated critical shear stress SC method proposed by Julian and Torres (2006) is higher than other methods which used Shields's diagram, as plasticity index, dispersion ratio, mean particle size (m), and percent clay by weight (%), however, maximum τ_c is close to the value measured in situ with the jet test device. After substituting Equations. 3.12 and 3.11 into Equation 3.11, the final form used in this study to predict the equilibrium depth can be re-derived as follows:

$$D_e = \frac{(0.139)\rho U_0^{1.8} y_0^{0.8} \nu^{0.2}}{\left[0.1 + 0.1779(SC) + 0.0028(SC)^2 - 2.34E - 5(SC)^3\right]} \quad 3.14$$

Aderibigbe and Rajaratnam (1996) developed semi-empirical equations by submerged circular impinging vertical jets. Dynamic scour depth can be predicted using following equations

$$\varepsilon_{m\infty} = 7.32E_c \left(\frac{d}{h}\right)^{\left(1.53E_c^{0.22}-1\right)} - 1 \quad 3.15$$

where, $\varepsilon_{m\infty}$ is the dynamic scour depth. E_c is an estimate of the ratio of the force exerted by the circular jet on a bed particle located directly under the jet and at the original bed level to its resistive force which can be determined as $E_c=U_0(d/h)/(gD\Delta\rho/\rho)^{1/2}$, $\Delta\rho$ is the difference between density of soil and water, $\Delta\rho=\rho_s-\rho_w$. g is the acceleration due to the gravity. U_0 is the velocity of jet at nozzle. d and h are diameter of nozzle and impinging distance measured from the original bed level. D is the median size of bed material.

The comparisons of the predicted equilibrium erosion depth and theoretical formulas are shown in Figure 3.9. Both the experimental and theoretical erosion predictions are increased with increasing the nozzle thickness. Hence, the increment of soil erosion is not linearly proportional to the nozzle thickness. Moreover, it is observed that as the contents of the finer and compaction ratio are increased, the predicted equilibrium erosion depths are decreased as shown in Figure 3.8. After comparing the theoretical results, the predicted equilibrium depth using the hyperbolic methods shows quite comparable trends with less than 0.013 m nozzle thickness. However, with the 0.2032 m nozzle thickness, the computed equilibrium depths based on both Stein et al. and Aderibigbe and Rajaratnam equations are two or three times higher magnitudes than the prediction from the hyperbolic method. However, the predicted erosion depths resulted in

logarithmic trend line may be equated with the theoretically predicted erosion depth while the predicted erosion depths with less than 0.0065 m nozzle thickness are higher than those predicted based on Stein et al. and Aderibigbe and Rajaratnam equations. From the log *D* (depth) and log *Nozzle thickness* plots, both theoretical predictions show linear trends, while predicted erosion depth by logarithmic trend and hyperbolic methods does not show the linear relations. Therefore, it may be an adequate conclusion, that both curve fitting techniques may not fully represent the correct relations between the equilibrium erosion depth and nozzle thickness.

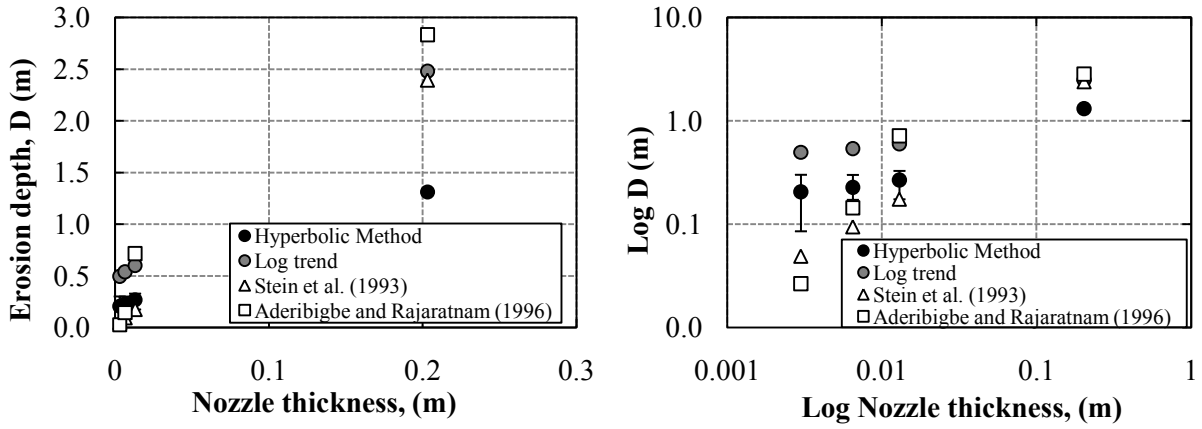

(1) F50S50

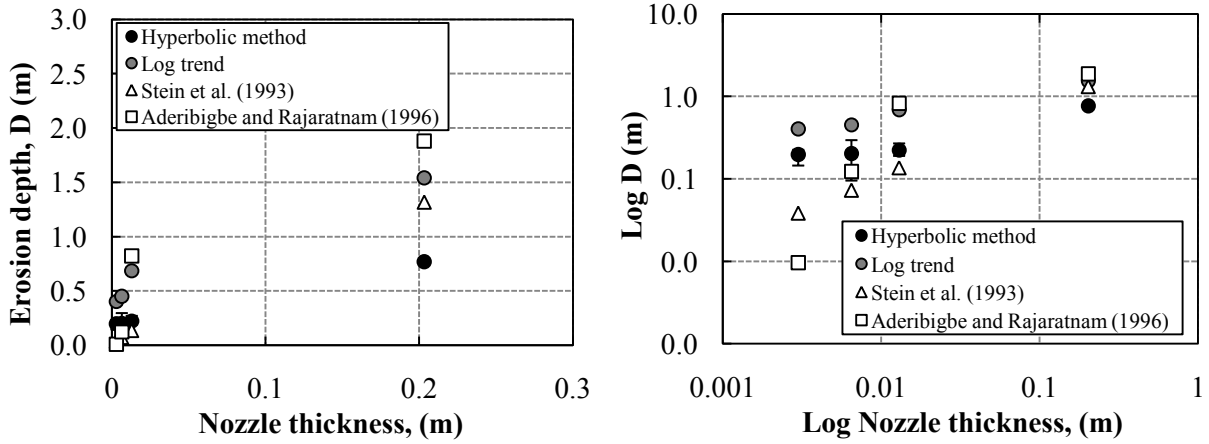

(2) F57S43

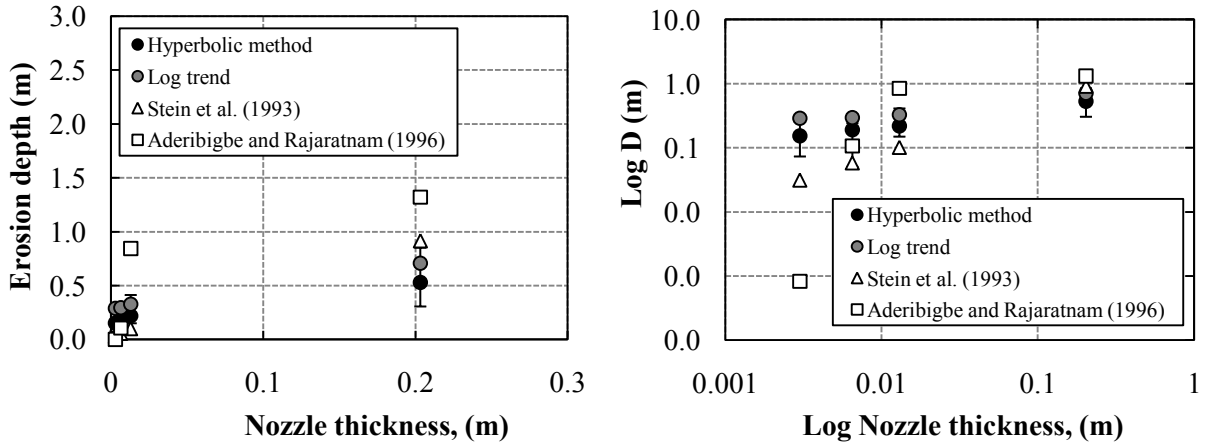

(3) F65S35

Figure 3.9 Comparisons of equilibrium depth

3.10. Conclusion

The equilibrium erosion depths of cohesive soils are evaluated using UMETB. Four different planar nozzle sizes, 0.003 m, 0.065 m, 0.13 m, and 0.2032 m, are used to study the effects of nozzle thickness on the equilibrium depths which are predicted by applying the hyperbolic method and logarithmic trend line. The following conclusions could be drawn.

1. The measured erosion depth increases with the increasing nozzle thickness. However, linear trends between the nozzle thickness and erosion depth are not established.

2. The erosion rate increases with respect to the nozzle thickness. Moreover, the erosion rate is increased with respect to the increasing finer contents and degree of compaction.

3. The hyperbolic methods may be one of the useful techniques to predict the equilibrium erosion depth with smaller nozzle thickness. However, due to the layering compaction and mass erosion,

the hyperbolic methods may have some error ranges.

4. The logarithmic trend lines can be an alternative to predict the equilibrium erosion depth. As predicting the higher equilibrium depth, it may be an appropriate method for the conservative design of hydraulic structures.

5. The computed equilibrium erosion depth based on Stein (1993) and Aderibigbe and Rajaratnam (1996) shows relatively comparable results within the predicted erosion depth using both hyperbolic methods and logarithmic trend lines.

6. To predict the equilibrium erosion depth based on the measured data set during relatively short run time, it may not be reasonable to use both the hyperbolic method and logarithmic trend line.

CHAPTER IV

SELF SEALING BENTONITE APRON TO PREVENT GAP DEVELOPMENT FOR FLOOD WALLS IN NEW ORLEANS

4.1. Abstract

As a result of Hurricane Katrina, many sections of the floodwall protection system in New Orleans, LA were damaged or suffered catastrophic failure. One key aspect of failure reported is the strength reduction of the marsh layer or piping in the sandy soil underneath the levee and is associated with the gap development and water infiltration between the soil and floodwall. This study evaluated the potential to prevent this gap development by introducing a buried layer of bentonite and sand mixture. Bentonite is a highly expansive mineral, which is used in this test to swell and prevent water from infiltrating the gap. Test results confirmed this, and showed that bentonite and sand mixture was very effective in its ability to swell and reduce water flow. Several mixtures of sand and bentonite were tested, however, the mixture of 70% sand and 30% bentonite proved to be the more effective mixture, by swelling fast enough to seal the gap but exerting negligible swelling pressure .

4.2. Introduction

New Orleans, Louisiana suffered many failures as a result of Hurricane Katrina; many of the failures were a result from erosion caused by overtopping water. However, some failures

were reported to occur before overtopping, because of instability in the levee system (IPET 2007). One of the primary reasons for this instability is a development of a gap between the floodwall and the soil, due to an increase in water pressure; this occurrence can be seen in Figure 4.1. The formation of this gap can introduce multiple failure modes to the floodwall including: increased horizontal water pressure on the floodwall, disturbance of subsurface layers, and also increase uplift pressures on the soil and floodwall (Brandon et al. 2008).

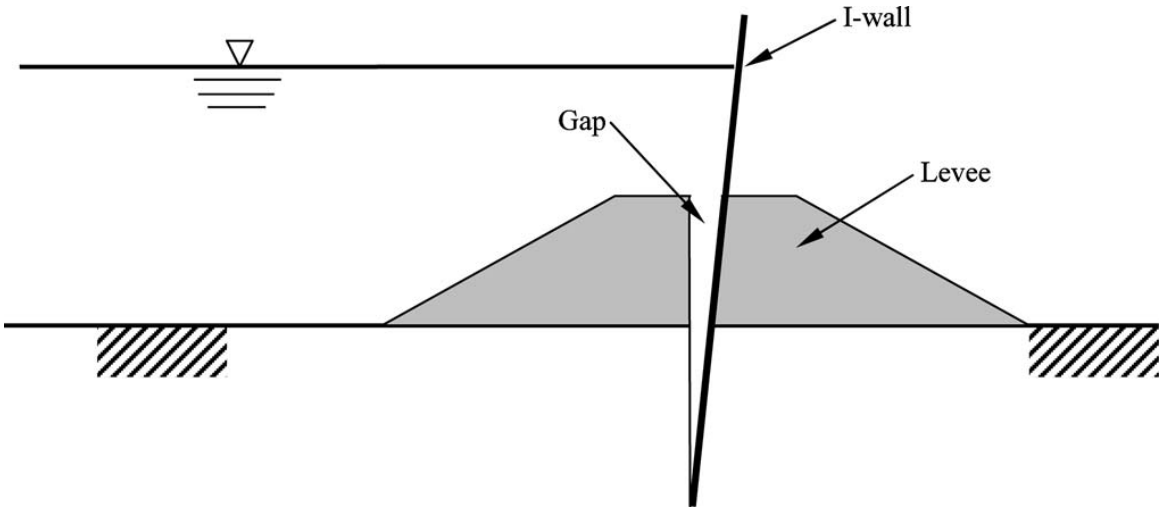

Figure 4.1 Gap formation between flood wall and soil (Brandon et al. 2008)

Figure 4.2 Photograph of Gap Formation (Brandon et al. 2008)

Hurricane Katrina caused significant flooding and damage to New Orleans, Louisiana primarily due to the elevation and location of New Orleans. At its lowest point, New Orleans is roughly seven feet below sea level as illustrated in Figure 4.3.

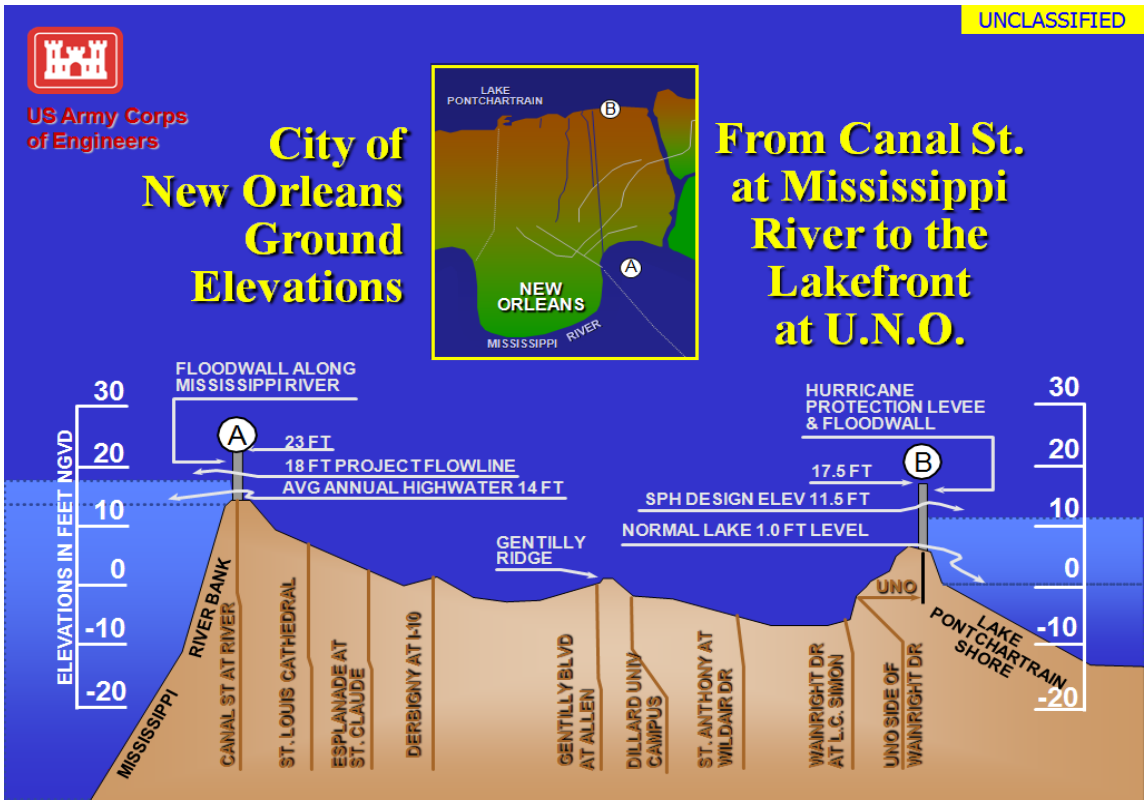

Figure 4.3 Representative Cross Section of New Orleans (IPET 2007)

In order to deal with high levels of water, the city of New Orleans has built a series of elevated floodwalls and levees. Therefore, many areas surrounding New Orleans have raised concrete floodwalls on the top of the levees. The hurricane protection system surrounding New Orleans consists of approximately 56 miles of floodwalls, and 284 miles of other protective structures (IPET 2007).

Hurricane Katrina landed as a category 3 hurricane with wind speed sustaining 125 mph. This was accompanied by widespread storm surge and rainfall. It was estimated that the storm surge was roughly 12-14 feet tall in the IHNC, and that there was 14 inches of rainfall that fell within 24 hours. The hurricane protection system surrounding New Orleans was not designed to handle a storm of this magnitude. New Orleans experienced severe flooding; approximately 80%

of the metropolitan area was flooded. Two-thirds of this flooding can be attributed to water flowing through failed floodwalls or breaches (IPET 2007).

There were approximately 50 breaches that were a result of Hurricane Katrina. The primary failure mechanism was due to erosion caused by overtopping water. However, four breaches were a result of flood wall foundation instability. The main cause of this instability is the formation of a gap forming between the floodwall and soil.

This study primarily focuses on the prevention or reduction of the gap formed between the floodwall and soil. This is performed by creating a mixture of expansive bentonite and sand, which swells in the presence of water to seal the void caused by the gap. This research focuses on finding an optimum mixture of sand and bentonite that has a high swelling strain, low swelling pressure, and also quick swelling. The mixture should have high swelling strain in order to have enough strength to swell to fill the gap. Also, the swelling pressure should be relatively low; this is to prevent adding any additional horizontal pressure to the floodwall. In addition, the mixture should swell quickly, to reduce or prevent water from continually flowing through the gap in a short amount of time.

4.3. Test Samples

The bentonite that was used for testing is QUIK-GEL®, which is a high yielding Wyoming sodium bentonite (www.Baroididp.com). The sand that was used is QUIKRETE® All-Purpose Sand (No. 1152) (www.quickcrete.com). The bentonite was classified as CH, with 99% passing the #200 sieve, and the sand was classified as SW with 1.5% passing the #200 sieve. There were five different mixtures of bentonite and sand that were used for testing: 50/50, 60/40, 70/30, 80/20, and 90/10 (with % sand being the first number and % bentonite being the

second number) by weight. All test samples were compacted at 90% of the maximum dry density (γ_d max) according to USACE standards (Vroman 2008). The basic soil properties for these samples can be seen in Table 1. However, compaction is carried out in three separate 2 inch (5.08 cm) layers in order to obtain uniform compaction. To mimic field compaction techniques, a gasoline powered tamper (Dynapac, LF45) was used. Maximum dry density and optimum water content were measured for each mixture by the Standard Proctor Test (ASTM D698), before any soil samples are made.

Table 4.1. Fundamental Soil Properties

Sample	γ_d max (t/m^3)	Optimum Water content (ω_{opt})
50/50 Sand 50 % Bentonite 50%	1.52	5.71
60/40 Sand 60 % Bentonite 40%	1.65	4.66
70/30 Sand 70 % Bentonite 30%	1.68	3.64
80/20 Sand 80 % Bentonite 20%	1.75	2.59
90/10 Sand 90 % Bentonite 10%	1.71	0.43

The purpose of mixing sandy soil and bentonite is because the permeability of bentonite is very low. With the addition of sandy soil which has a high permeability, the permeability of the sand and bentonite mixture is increased. However, the sand/bentonite mixture must have enough expansive properties to swell and seal the gap formed by the floodwall.

4.4. Test Set Up and Procedure

4.4.1. Test Set Up

The University of Mississippi Swelling Frame (UMSF) is concrete and wood apparatus designed to mimic flood wall leaning in New Orleans as shown in Figure 4.3. The UMSF has a floodwall that can have a controlled lean or deflection. The UMSF is a 2/3 scale model to the actual floodwalls in New Orleans; UMSF floodwall is 4 feet (1.22 m) high, and New Orleans floodwall is 6 feet (1.8 m) high. When the wall is leaned out, a gap is formed between the soil sample and floodwall similar to the field conditions in New Orleans. This test uses a hinge condition at the bottom of the wall, while actual field conditions are more close to a cantilever condition. Therefore, it is noted the actual deformation is horizontal in this study. The dimensions of the apparatus are 4 ft x 4 ft x 8 ft (1.22 m x 1.22 m x 2.44 m); the dimensions of the soil sample are 20.25 inch (51.44 cm) [width] x 93.5 inch (245.11 cm) [length] x 6 inch (15.24 cm) [height]. This can be seen in Figure 4.4.1.

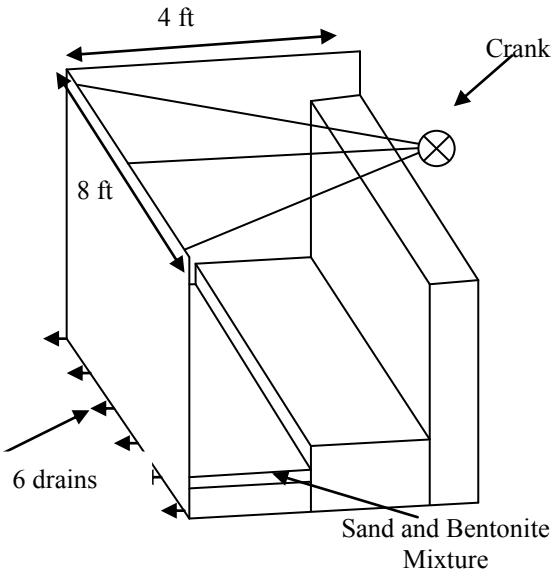

Figure 4.4.1 UMSF

Figure 4.4.2 Schematic of UMSF

The sand and bentonite mixture was submerged for 24 hours in water. This ensures that the bentonite and sand mixture had ample opportunity to become saturated and swell. In addition, saturating the soil sample mimics field conditions during times of excess rainfall and flooding. The water level was kept at a constant .9144 meters, to ensure that all tests were conducted under the same water pressure. The water level was also kept at .9144 meters while testing; the addition of water was required in some cases, because of the water being allowed to leak.

Six ¼ inch (6.35 mm) drains, as seen in Figure 4.4.2, were installed at the bottom of the floodwall. The primary purpose of the drains is to capture water that flows past the sand and bentonite mixture. If water is able to flow through the gap formed, then the bentonite has not swelled and filled the gap. Water volume is measured in time increments in order to obtain a flow rate. The volume is measured every hour and recorded.

The crank winch was placed to control the deflection of the floodwall as shown in Figure 4.4.2. The crank is released every hour, which allows the horizontal pressure of the water to lean the floodwall outward. The wall is deflected ¼ inch (6.35 mm) every hour. This behavior simulates the gap formation continuing to become larger with time, since the wall is continuously being leaned out. The process of leaning the wall and measuring the flow takes nine hours; therefore the duration of the test is nine hours. Nine hours was selected based on field hydrographs and failure time of floodwalls in IPET 2007.

4.4.2. Testing Procedure

The following test procedure is followed in this study.

1. Mix the sand and bentonite samples.
2. Insert screws into the drains to ensure they are not clogged during compaction.
3. Compact sand and bentonite mixture in the UMSM.
4. Fill the UMSM with water.
5. Allow to stay submerged for 24 hours.
6. Remove the screws from the drain, and hook up water collection device.
7. Slowly release the crank allowing the wall to deflect (6.35”/hr).
8. Watch and record any water flow from the drains.
9. Check water level to ensure it is constant, add water if necessary.
10. Repeat steps 7-9 for the total duration of the test.

4.4.3. Laboratory tests to quantify swelling characteristics of soils

A modified version of the Standard Unconsolidated Undrained Triaxial Compression Test (ASTM D-4767) was used to find the volumetric swelling strain of each sample. Instead of applying a load to the sample and measuring the axial strain, the sample was slowly saturated by flushing water from the bottom to the top of the sample and the swelling volume was measured. Sand and bentonite were mixed in the same proportions to one another as in the UMSF test to create cylindrical samples, and then water was supplied into the sample which causes the bentonite to expand. The volume increase from this expanding is then measured. The equipment used was a load frame (Humboldt Master Loader HM-3000) and a triple burette assembly (Humboldt Flex Panel 1). The load frame consisted of a load applying base, cell, pore pressure sensor, load cell, and displacement measuring sensor. The cell is a clear cylindrical shaped apparatus that is sealed and filled with desired amount of water, and connected via tubing to the flex panel. The sample is placed on a base pedestal with the same diameter as of the sample, 7 cm, inside the cell. The three burette assemblies consist of a cell burette, a base burette, and a top burette. The base burette is filled with water and pressure is applied from the top which pushes the water into the sample via tubing connecting the burette and bottom pedestal of the cell. As the sample saturates, it expands which in turn causes the water in the cell to be pushed out and into the cell burette which is connected via tubing. The height of each sample was kept less than 3 cm to minimize the stabilization time. Graphs of the volumetric strain verses log time are graphed and compared to each other.

4.5. Numerical Simulation to Justify Bentonite Apron

Fast Langrangian Analysis of Continua (FLAC^{3d}) was used for the modeling of the bentonite apron. There are two main goals of this modeling. First, determine the effects of the gap formation on the overall structural integrity of the floodwall. Second, determine if the bentonite apron is a practicable solution to seal the gap without applying additional high swelling pressure on the floodwall.

To determine the effects of the gap formation a model was created as seen in Figure 4.5. This is modeled after the London Avenue Canal of New Orleans, which did not fail during Hurricane Katrina; but was the location of a full scale load test that was conducted in 2007. This model has a false cofferdam installed; to prevent the effects of seepage during the analysis. As a result, this allows the model to only show effects from the gap formation.

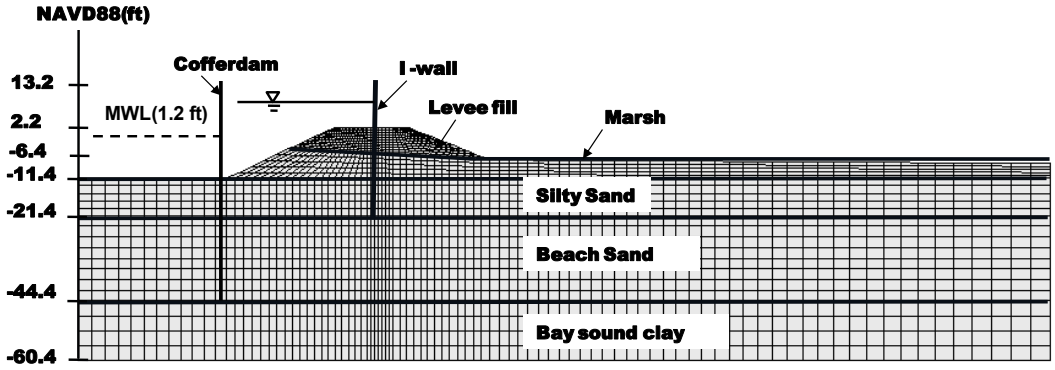

Figure 4.5 Depiction of Model for Effects of Gap Formation (Adhikari et al. 2011)

The same model was used to test the effectiveness of the bentonite apron; however, the cofferdam was removed to reflect realistic loading, and a 1'x1' bentonite and sand mixture was added. FLAC^{3D} is unable to mimic the time dependent swelling behavior of the bentonite apron; therefore, only the swelling pressure for infinite time and the corresponding definite swelling

deformation was used. IN the numerical simulation the swelling pressure deformation for the S50B50 mixture was used since it has the maximum swelling pressure to be in the conservative side. This extreme swelling pressure and deformation relationship was obtained in the laboratory and can be seen in Figure 4.6. As seen in Figure 4.6 the percent swell (ΔV/V) was minimal and less than 1%.

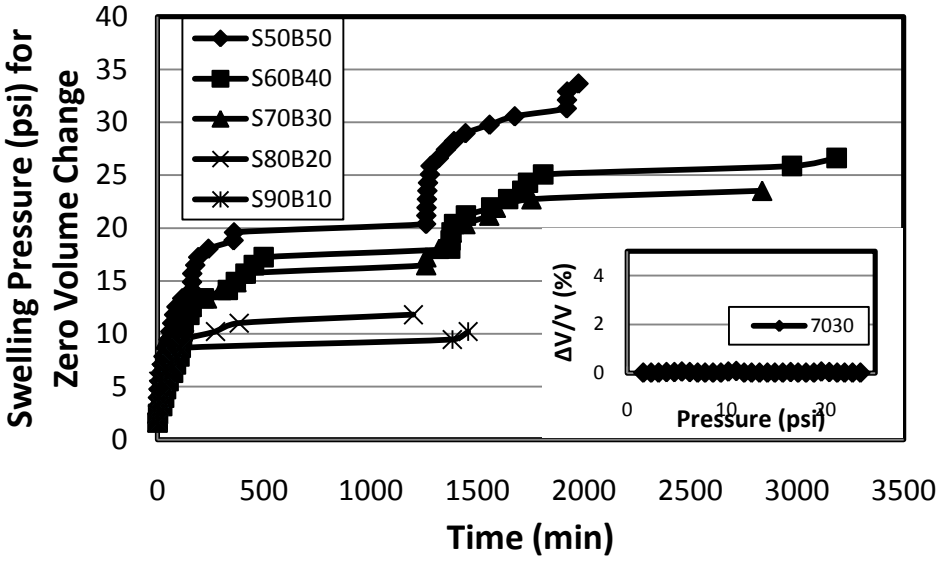

Figure 4.6 Swelling Pressure and Deformation Relationship

4.6. Results

4.6.1. S50B50

This sample was chosen as a starting point to evaluate the potential for a bentonite and sand mixture to swell and seal the gap. It can be seen in Figure 4.7.1 that the mixture swelled and sealed in the gap in the UMSF. However, the gap was not sealed very quickly, and a

substantial amount of water was discharged through the gap. In line with these findings, Figure 4.7.2 shows the mixture took a significant amount of time in order to swell to its full potential. From these results it can be inferred that additional sand needs to be added in order to decrease the amount of time it takes the mixture to swell to its full potential.

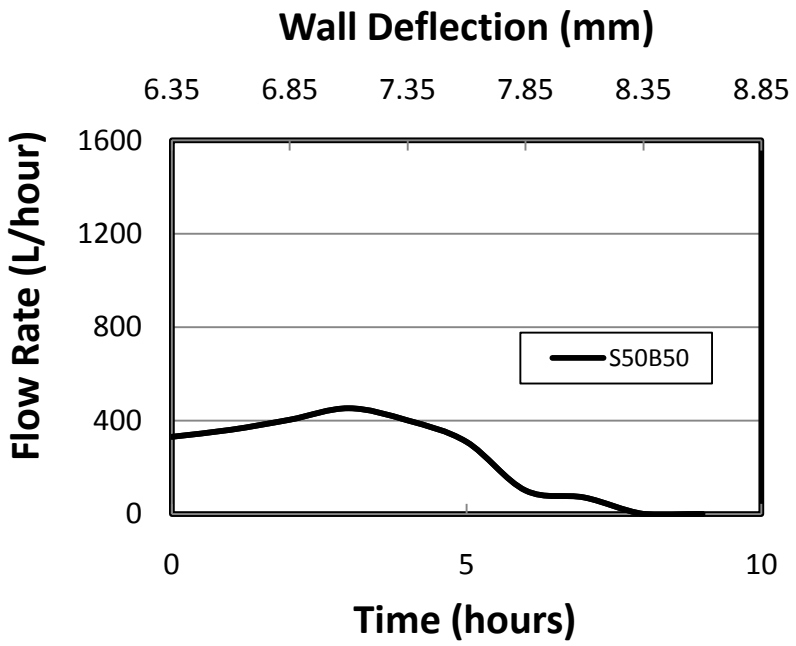

Figure 4.7.1 Flow Rate vs Time for S50B50 (UMSM)

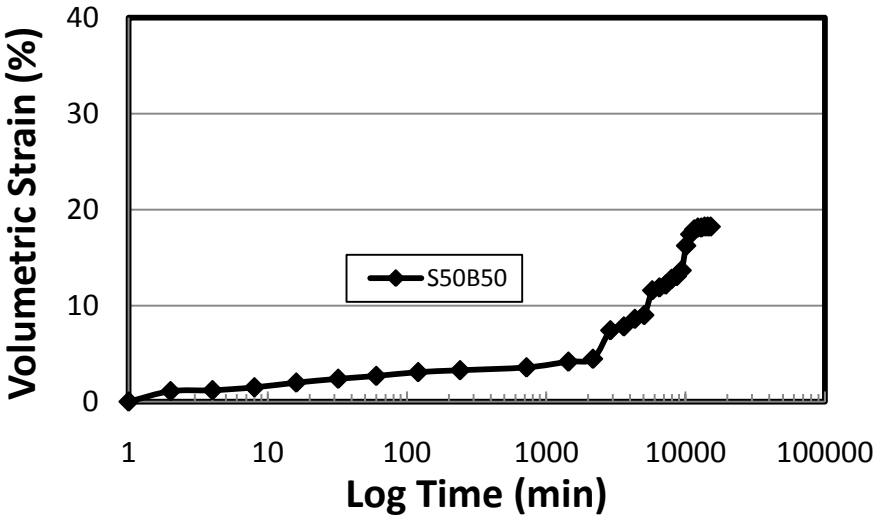

Figure 4.7.2 Volumetric Strain vs Log Time for S50B50

4.6.2. S60B40

In this sample the proportion of sand was increased to allow water to more easily penetrate the mixture so that the bentonite could swell more quickly. From Figure 4.8.1 it can be seen that the flow rate was decreased. The mixture still allowed a large amount of water to penetrate the gap. In addition, from Figure 4.8.2 it can be seen that the ultimate volumetric strain

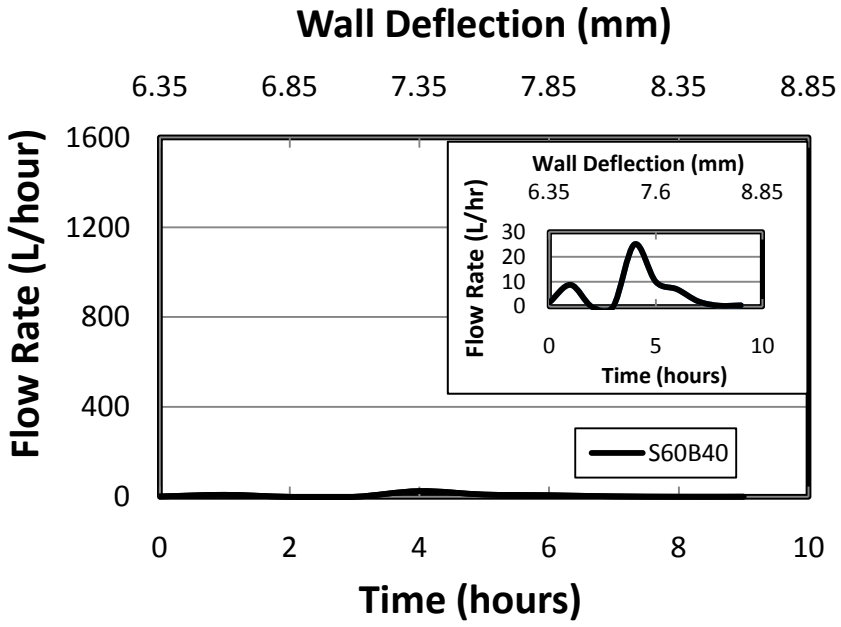

was somewhat reduced; but from comparing Figure 4.7.2 and Figure 4.8.2 it can be seen that the initial slope is increased.

Figure 4.8.1 Flow Rate vs Time for S60B40 (UMSM)

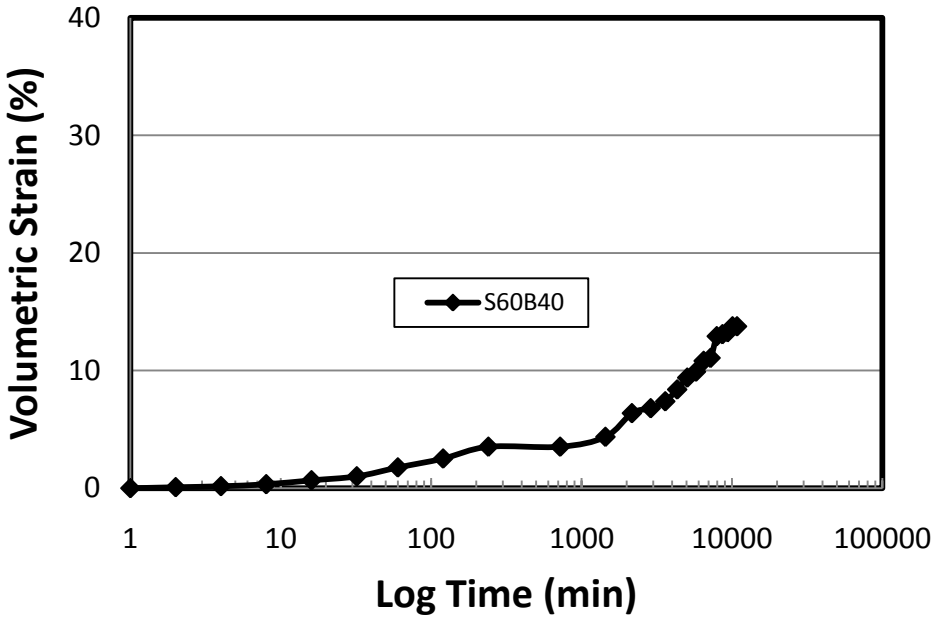

Figure 4.8.2 Volumetric Strain vs Log Time for S60B40

4.6.3. S70B30

After the addition of 10% more sand to the mixture the flow rate was almost completely reduced as seen in Figure 4.9.1. There was a slight increase in the flow in the early stages of the test, but was quickly dissipated to zero. From the graph in Figure 4.9.1, it can be seen that the total flow for the duration of the test was kept under 15 L/hr. The volumetric strain was also increased at a much faster rate than the previous sample, even though the volumetric strain at 10000 minutes is lower as seen in Figure 4.9.2.

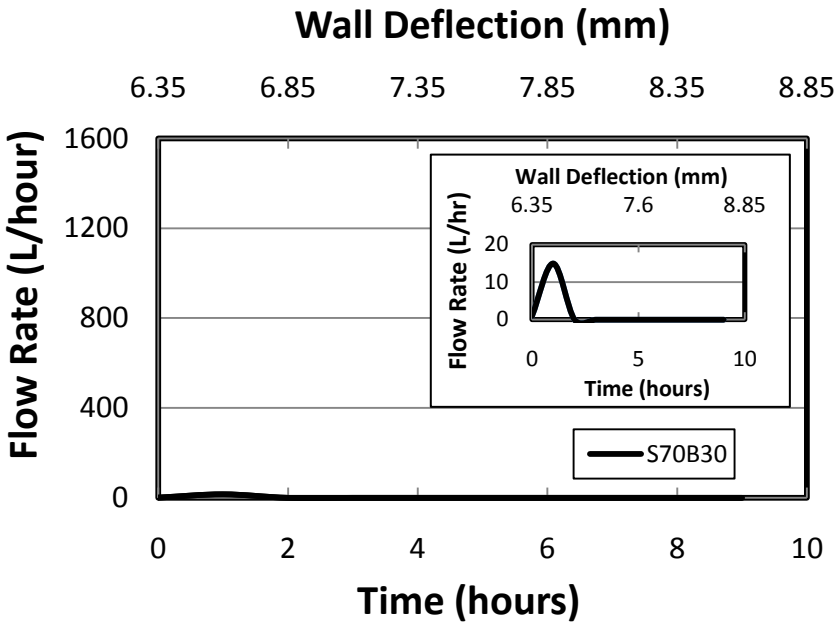

Figure 4.9.1 Flow Rate vs Time for S70B30 (UMSM)

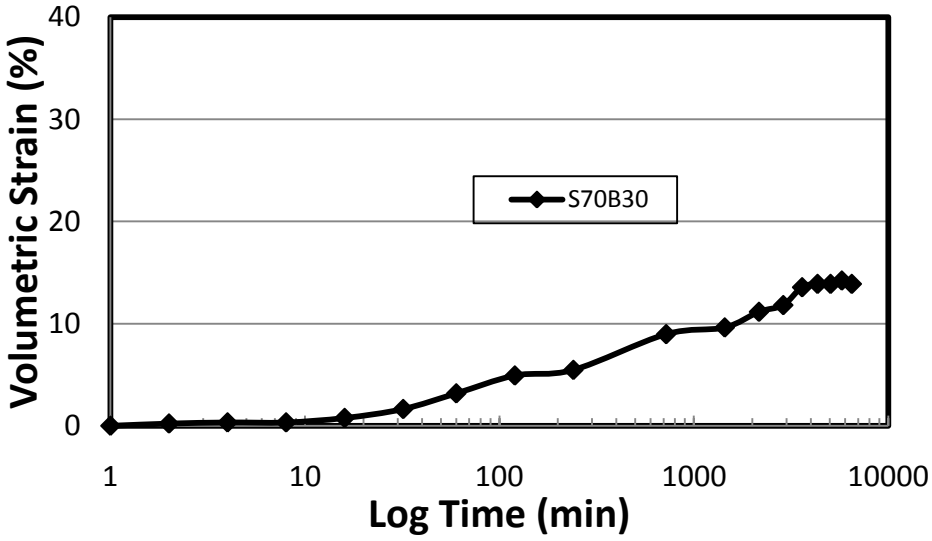

Figure 4.9.2 Volumetric Strain vs Log Time for S70B30

4.6.4. S80B20

In order to further enhance the self-sealing performance of the sand/bentonite mix, an additional 10% of sand was added to this mixture. The amount of water leak increased significantly, as seen in Figure 4.10.1. The primary reason for this is the sand and bentonite mixture had too much sand and therefore the permeability was greatly increased. In addition, the bentonite was at such a low percentage, it didn't have the ability to swell to seal the gap. The volumetric strain never reached 10%, this can be seen in Figure 4.10.2. Also, from Figure 4.10.2 it can be seen that the graph swelled much faster than previous samples, however, the volumetric strain never reached a suitable percentage.

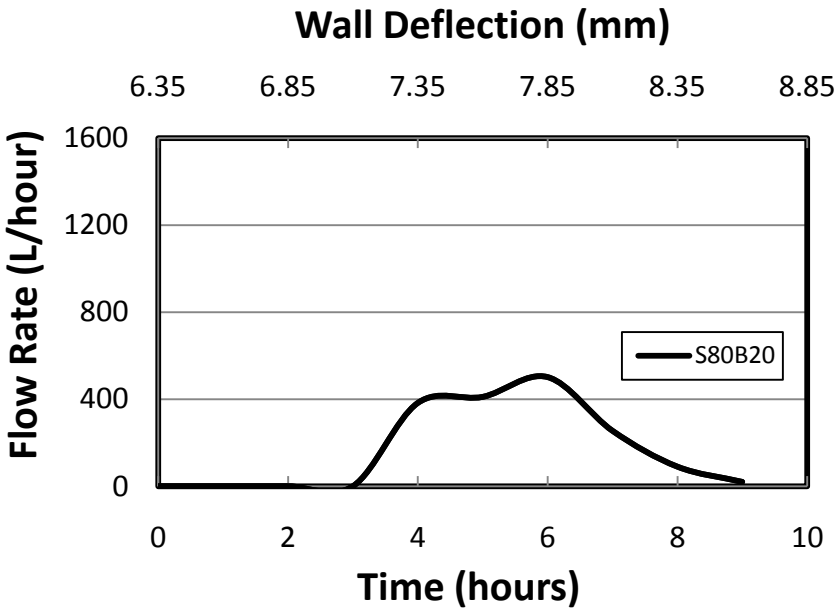

Figure 4.10.1 Flow Rate vs Time for S80B20 (UMSM)

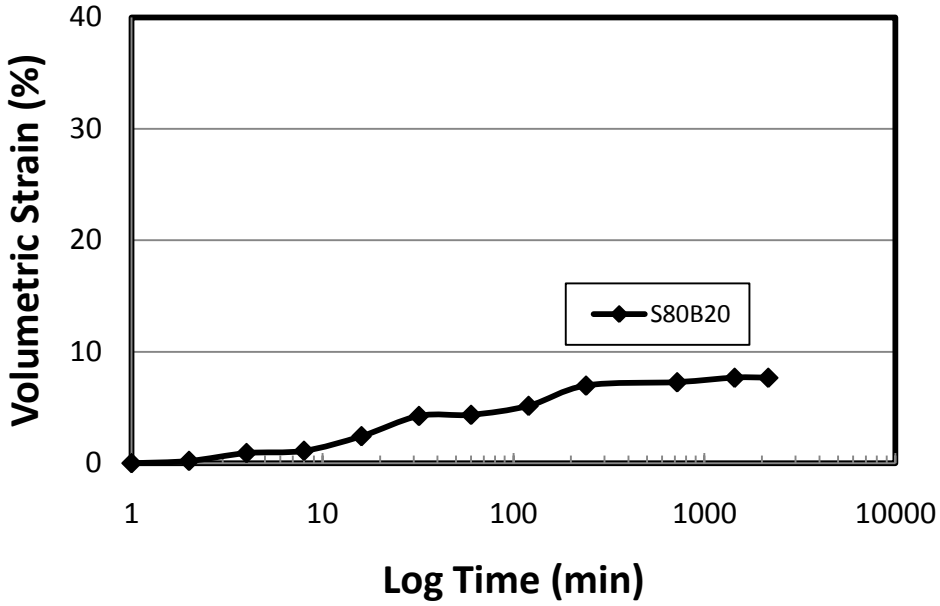

Figure 4.10.2 Volumetric Strain vs Log Time for S80B20

4.6.5. S90B10

In order to validate our previous findings that the sand had increased past the critical percentage of effectiveness, another test was conducted with an increase of 10% sand. The results were validated; the flow rate was the highest recorded, and this can be seen in Figure 4.11.1. Also, the volumetric strain was reduced almost to zero. This sand and bentonite mixture proved quite ineffective for sealing the gap formation because the water flowed freely in the USMS and there was not enough swelling in the triaxial testing.

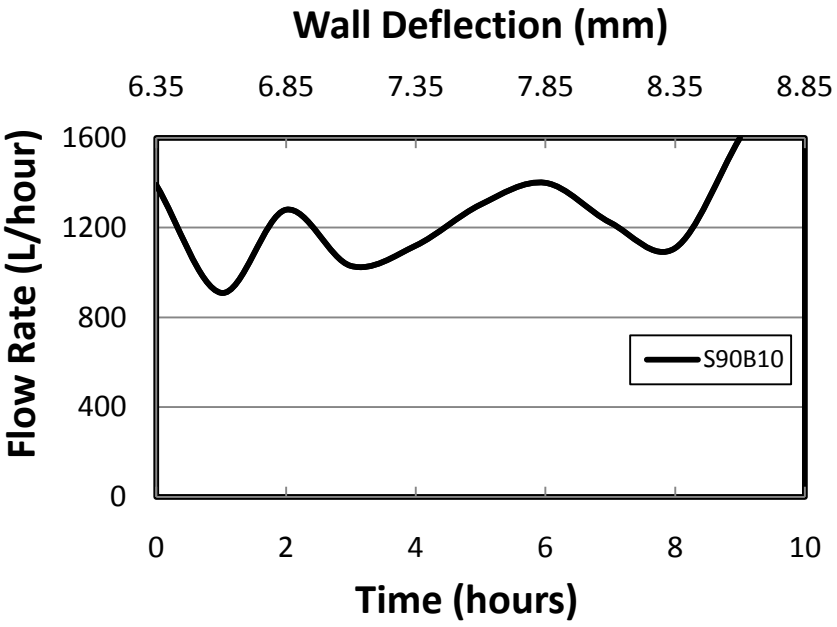

Figure 4.11.1 Flow Rate vs Time for S90B10 (UMSM)

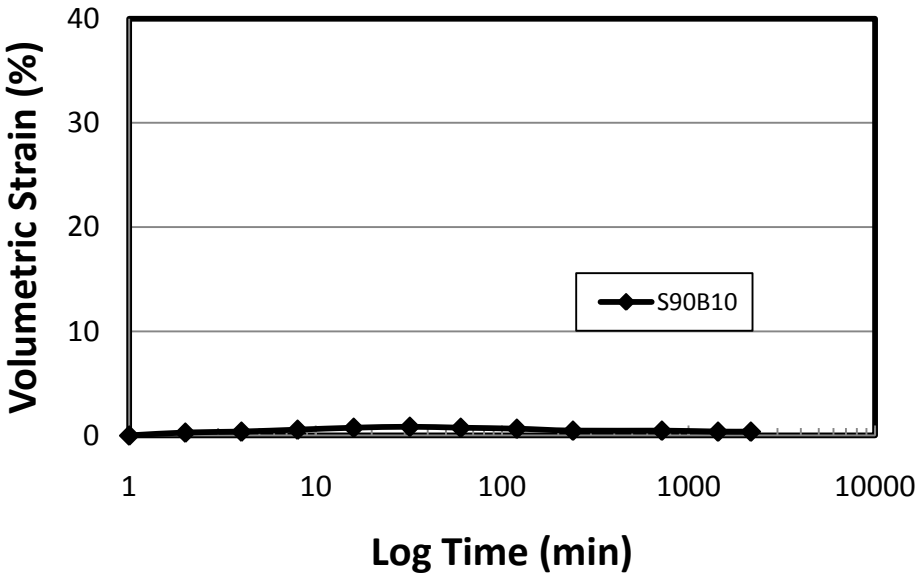

Figure 4.11.2 Volumetric Strain vs Log Time for S90B10

4.6.6. Numerical Simulation

To determine the effects of the gap formation on the floodwall four scenarios were tested: no gap, gap with no pore pressure, gap with pore pressure, and gap with pressure and a permeable sheet pile. The permeable sheet pile mimics a loosened interlocking of the sheet piles after being driven in dense sand (Sills et al. 2008). The load vs displacement curves are shown in Figure 4.11. The displacement represented in Figure 4.12, is the global displacement of the floodwall.

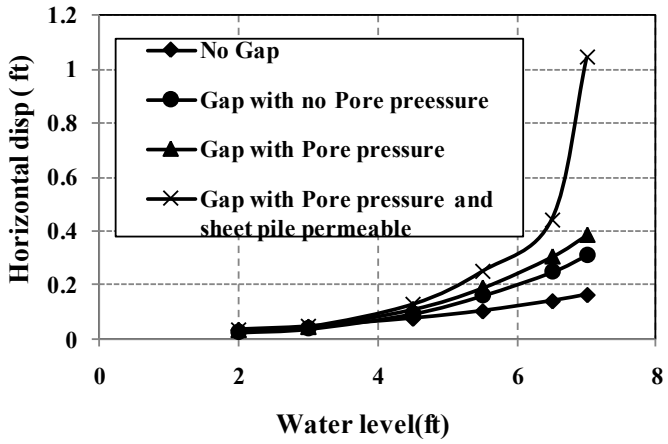

Figure 4.12 Load vs Displacement (Adhikari et al. 2011)

As seen in Figure 4.11, there is a substantial difference between the gap condition and no gap. In addition, it can be concluded that the gap condition is much more critical than the no gap condition. Furthermore, the displacement increases with increasing loads; which causes the gap to expand.

To determine the effectiveness of the bentonite apron four scenarios were created for the model which includes: no gap, gap with impermeable sheet pile, gap with permeable sheet pile,

and bentonite apron. The load deflection curves can be in Figure 4.13.

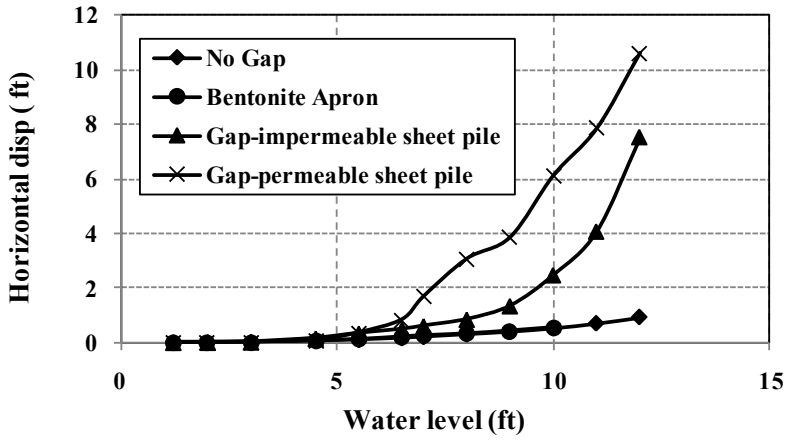

Figure 4.13 Load Deflection Curve at the Top of the Floodwall

From Figure 4.13, it can be seen that the bentonite apron follows the same trend as the no gap condition. The bentonite apron successfully swelled to fill the gap. Furthermore, the bentonite apron did not cause additional displacement of the floodwall, from exerting additional swelling pressure. Also, the bentonite significantly reduced the horizontal displacement of the floodwall, as compared to both of the gap conditions.

4.7. Conclusions

The goal of this research was to determine if a sand and bentonite mixture could swell quick enough to seal the gap formed between the soil and floodwall. The bentonite apron proved to be effective at swelling to seal the gap formed by the deflection of floodwalls. A critical bentonite and sand mixture was found using both full scale swelling and also triaxial swelling test. The bentonite and sand mixture was able to swell relatively quickly while also having enough strength to seal the gap.

1. S70B30 was found to be the most effective at sealing the gap quickly, because of the high

swelling speed and pressure.

2. Water was unable to penetrate the full 6 inches of sand and bentonite mixture. Water only penetrated two inches of the sample. This allows the bentonite apron to be used to reseal gaps more than once.
3. According to the numerical simulation the gap formation causes additional horizontal displacement of the floodwall. Furthermore the gap formation is more critical to the overall integrity of the floodwall.
4. The bentonite apron does not exert any additional pressure onto the floodwall. This condition mimics the same deflection of the floodwall, as no gap forming.

CHAPTER V

CONCLUSIONS

The limitation of the current hurricane protection system for protecting the city of New Orleans was the basis of this research. There was a need for a new alternative method of protecting against floodwall failures during times of excess water, besides simply raising the height of the floodwall. This research focused on testing new methods to address the failure mechanisms of floodwalls during Hurricane Katrina. In addition, this research resolved problems surrounding past failures, and aimed to develop a new retrofitting strategy to ensure the likelihood of another major catastrophic failure of floodwalls is reduced. This retrofitting strategy is to provide a reasonable, cost effective, and applicable to current floodwall conditions.

5.1. Erosion Resistant Reinforcement

Reinforcement of soils, using ground modification proved to be a reliable solution for erosion induced failures. Both ground modifiers used in this research reduced the erosion. However, both modifiers are substantially different in applicability and effectiveness.

POSS is applied by spraying the liquid onto the surface of the ground; therefore, POSS is applicable to almost any situation. POSS decreased erosion by 99%, but it was only decreased to a depth of approximately 9-12 cm. The increase in erosion resistance comes from an increase in shear strength, and also a decrease in the water content of the soil; the POSS molecules bond

to the soil grains which not only strengthen the soil, but acts as a barrier against the infiltration of water. It should also be noted there is a curing time associated with POSS. POSS needs to be cured or dried for a minimum of two weeks, before it is effective.

The Vetiver is a plant, and would be applied by planting seeds in the area of concern. The Vetiver was very effective at preventing erosion; no recordable erosion occurred. There was no erosion for the stem and root system and also the root system only. The Vetiver that was tested was a twelve year old plant, with a very dense root and stem system. Therefore, to mimic the conditions that were tested, a twelve year old Vetiver system would need to be planted. It should be also noted that Vetiver is only applicable to warm/humid climates, with moderate amounts of rainfall.

5.2. Full Scale Testing for Erosion Behavior

The equilibrium erosion depths were the main focus of the full scale tests; this is the depth at which erosion will be the greatest and also erosion will no long occur. Three different soil samples were tested for 4 different nozzle thicknesses (.003 m, .0065 m, .013 m, and .2032 m). The variable nozzle thickness is the main parameter that fluctuates between laboratory testing and real world scenarios. This is because all parameters such as: velocity of plunging water, density, Reynolds number, and flow rate are kept constant to mimic field conditions. However, the limitations of the UMETB do not allow for increasing the thickness of water past .013 m. The equilibrium erosion depth is crucial in the design and implication of any new protection system for New Orleans.

From the tests, it was determined that increasing the nozzle thickness also increases

erosion. Although the tests did not show a linear trend of equilibrium erosion depth vs. nozzle thickness, the results obtained are still applicable. The gathered data proved very beneficial in predicting the equilibrium depth for a changing nozzle thickness. It should be noted that some methods used for this prediction may not be reliable. Therefore, the results at this time, only give a range or an estimate of predicated equilibrium erosion depth.

5.3. Application of Bentonite Apron

A bentonite and sand mixture were used in this study to mitigate problems with floodwall instability and loss of strength. The problem, which eventually led to failure, was the introduction of a gap forming between the floodwall and soil. The gap formation is caused from the leaning of the floodwall under high water pressure. The development of the gap allowed for the infiltration of water which eventually led to piping and internal erosion of the levee, causing instability and loss of strength in the floodwall.

Every mixture that was tested reduced the amount of water infiltration. Eventually, an optimum mixture was found in 70% sand and 30% bentonite. This optimum mixture allowed the least amount of water to infiltrate the gap, as compared to the other mixtures; which proves the mixture was able to expand quick enough to seal the gap. Furthermore, this mixture showed high swelling strain. According to the numerical analysis, the swelling pressure was not significant enough to cause any additional deformation to the floodwall.

5.4. Recommendations

5.4.1. POSS

POSS proved effective at strengthening soil against erosion but the limitations were: effective depth 9-12, less effective for higher degrees of compaction, less effect for higher percentages of clay content. Recommendations: try to increase the rate of infiltration for POSS. One solution is the addition of water to POSS while spraying, it would dilute the chemical, but may increase the infiltration to the soil sample. Another recommendation is spraying POSS when the sample is being compacted; spray POSS in several layers at different depths. In addition, the half-life or length of time POSS is effective would be essential in long term disaster mitigation.

5.4.2. Vetiver Plant

Vetiver was most effective at reducing erosion (no recordable erosion). However, the current limitations of the Vetiver plant include: 12 year growth period and not applicable to cold regions. Recommendation: testing of the Vetiver plant at different ages, which would require planting and growing Vetiver. This would give data for the Vetiver's erosion protection throughout the plants life cycle. In addition, erosion testing for different species of plants that are more abundantly grown in colder regions should be conducted.

5.4.3. Field Erosion Depth

Although the current technique is effective at estimating the equilibrium erosion depth, it is only an estimate. Additional tests for different soils samples and different nozzle thicknesses need to be conducted. If this data is gathered, there will be a lot less interpretation on the graphs,

and therefore much more accurate prediction of field erosion depth.

5.4.4. Bentonite and Sand Mixture

The bentonite and sand mixture was successful at sealing the gap formed between the floodwall and soil. Additional tests to determine the applicability and long term uses of the design should be conducted. The determination of the actual dispersive behavior of the mixture, and if the mixture can be applied to the surface, as compared to buried. If the mixture doesn't show high dispersive behavior, the application of the mixture would be much easier and cost effective. In addition, multiple tests on the mixture to determine how long the mixture will be effective at sealing the gap should be conducted

5.4.5. Application of Retrofitting System to Mitigate Floodwall Failures

All tests in this research were conducted separately and independently. It is recommended to conduct full scale tests that involve the application of multiple facets of this research. This would involve the application of the Vetiver plant and POSS; while simultaneously testing the sand and bentonite mixture. This full scale test would give an opportunity to apply each method, and determine the applicability and also the time required to install each modification. In addition, the tests would assess the effectiveness of the whole unit, instead each part individually. After the full scale tests have been conducted a conclusion can be made on the direction of the modifications.

LIST OF REFERENCES

REFRENCES

Aderibigbe, O., and Rajaratnam, N. (1996). "Erosion of loose beds by submerged circular impinging vertical turbulent jets." *J. Hydraulic Research,* IAHR, 34(1), 19-33.

Alonso, E. E., E. Romero, et al. (2005). "Expansive bentonite-sand mixtures in cyclic controlled-suction drying and wetting." Engineering Geology **81**(3): 213-226.

ASTM D5311 - 92(2004)e1 Standard Test Method for Load Controlled Cyclic Triaxial Strength of Soil

Bonetto, F., and Lahey Jr., R. T. (1993). "An experimental study on air carryunder due to a plunging liquid jet." *Int. J. Multiphase Flow*., 19(2), 281-294

Briaud, J. L., Ting, F. C. K., Chen, H. C., Cao, Y., Han, S. W., (2001b). "Erosion Function Apparatus for Scour Rate Predictions." *J. of Geotech. and Geoenvir. Eng.*, ASCE, Vol. 127(2), 105-113.

Briaud, J.-L., Ting, F. C. K., Chen, H. C., Gudavalli, R., Perugu, S., Wei, G., 1999 (a), "SRICOS: Prediction of Scour Rate in Cohesive Soils at Bridge Piers," Journal of Geotechnical Engineering, Vol. 125, No. 4, April 1999, pp. 237-246, American Society of Civil Engineers, Reston, Virginia, US

Briaud, J.-L., Ting, F. C. K., Chen, H.C., Cao, Y., Han, S. W., Kwak, K.W., 2001(a), "Erosion Function Apparatus for Scour Rate Predictions," Journal of Geotechnical Engineering,Vol. 127, No. 2, February 2001, pp. 105-113,American Society of Civil Engineers, Reston, Virginia, US

Chanson, H., Aoki, S., and Hoque, A. (2002). "Similitude of air bubble entrainment and dispersion in vertical circular plunging jet flows. An experimental study with fresh water, salty freshwater & sea water." *Coastal/Ocean Engineering Report*, No. COE00-1, Dept. of Architecture and Civil Eng., Toyohashi University of Technology, Japan.

Clark, L. A. and Wynn, T. M. (2007). "Methods for determining streambank critical shear stress and soil erodibility: Implications for erosion rate predictions." *Transactions of the ASABE,* 50(1), 95-106.

Cummings, R. D., and Chanson, H. (1997a). "Air entrainment in the developing flow region of plunging jets-Part 1:Theoretical development." *J. of Fuids Eng*., Trans. ASME, 119(3), 597-608.

Flory, P. J. (1946). "Effects of Molecular Structure on Physical Properties of Butyl Rubber." Industrial & Engineering Chemistry 38(4): 417-436.

Hanson G. J. and Hunt, S. L., (2006b), "Lessons learned using laboratory jet test method to measure soil erodibility of compacted soils." For Presentation at The 2006 ASABE Annual International Meeting, Paper No 062054.

Hanson G. J. and Sherry. L. Hunt, (2006a), "Determining the erodibility of compacted soils for embankment dams," *Proceedings of USSD Conference*. San Antonio, TX April 30-May 3

Hanson G. J., K. R. Cook, S. L. Hunt, (2005), "Physical modeling of overtopping erosion and breach formation of cohesive embankments," ASABE, 2003 ASAE Annual Meeting as Paper No. 032066 and 032067.

Hanson, G. J, K. M. Robinson, K. R. Cook, (2002), "Scour Below an Overfall: Part II. Prediction" ASAE Vol. 45(4), 957-964. .

Hengchaovanich, D. and Nilaweera, N. S. (1996). An assessment of strength properties of vetiver grass roots in relation to slope stabilization. Proc. First Int. Vetiver Conf. Thailand pp. 153-8.

IPET (Interagency Performance Evaluation Taskforce), (2007). "Performance evaluation of the New Orleans and Southeast Louisiana Hurricane Protection System." *U.S. Army Corps of Engineers, https://IPET.wes.army.mil*.

J. Graham, F. Saadat, M. N. Gray, D. A. Dixon, and Q.-Y. Zhang, "Strength and volume change behavior of a sand–bentonite mixture" Can. Geotech. J. 26(2): 292–305 (1989)

Jang, W. (2010), *Erosion Study of New Orleans Levee Soils Subjected to Plunging Water*, Ph. D. Dissertation, University of Mississippi, 295p.

Jang, W., Song, C. R., Kim, J., Cheng, A. H.-D., and Al-Ostaz, A. (2010). "Erosion study of New Orleans levee material subjected to plunging water." *J. of Geotech. and Geoenvir. Eng.*, 10.1061/(ASCE)GT.1943-5606.0000439 (Sep. 17, 2010)

Julian, J. P., and Torres, R. (2006). "Hydraulic erosion of cohesive riverbanks." G*eomorphology,* 76(1-2), 196-206.

Kim. J., Song, C. R., Wang, G., and A. H.-D. (2011). "Reducing erosion of earthen levees using engineered flood wall surface" J. of Geotech. and Geoenvir. Eng., 10.1061/(ASCE)GT.1943-5606.0000500 (Jan 8, 2011)

Komine, H. and N. Ogata (2004). "Predicting Swelling Characteristics of Bentonites." J. Geotech. and Geoenvir. Engrg. 130(8): 818-829.

Mitchell J.K. (1993) Fundamentals of soil behavior. Third edition. John Wiley and Sons, Inc., New York. 437 pp, see Chapter 3, Soil Mineralogy, p. 61-62. ISBN 978-0471463023

Moore, W. L., and Masch, F. D. Jr. (1962). "Experiments on the scour resistance of cohesive sediments." *J. Geophys. Res*., 67(4), 1437-1449.

P. V. Sivapullaiah, A. Sridharan, and V. K. Stalin (1996). "Swelling behavior of soil–bentonite mixtures" Can. Geotech. J. 33(5): 808–814

Paper, No. 91-2086.

Rajartnam, N. (1976). "Turbulent Jets." Elsevier Science Publishing Company, New York, 304.

Smerdon, E.T,, and Beasley, R. T. (1961). "Critical tractive forces in cohesive soils." *Agricultural Eng.,* **42**(1), 26–29.

Song, C.R., Kim, Jinwon, Wang G. and Cheng, A.H-D. (2009). "Reducing erodibility of earthen levee using engineered floodwall sections," *Journal of Geotechnical Engineering Division, ASCE, submitted for publication*

Stein, O. R, Julien, P. Y, (1991). "Measurement of Rill Erosion Sediment Detachment." *ASAE*

Stein, O. R, Julien, P. Y., and Alonso, C. V, (1993). "Mechanics of jet scour downstream of a headcut." *Journal of Hydraulic Research of IAHR,* 31(6), 732-738.

Stein, O. R, Nett, D. D, (1997). "Impinging jet calibration of excess shear sediment detachment parameters." *Transactions of the ASAE,* 40(6), 1573-1580.

Stein, O.R. and Julien, P.Y. (1991), "Measurement of Rill Erosion Sediment Detachment" ASAE Paper No. 91-2086.

Tan, T. S., T. Inoue, and S. L. Lee (1991) "Hyperbolic method for consolidation analysis, *J. Geotech. Eng.*, ASCE, 117(11), 1723–1737.

Tran Tan Van, Paul Truong, and Elise Pinners. Disaster Management, *Vetiver System for Natural Disaster Mitagation in Vietnam.,5-13*

Vroman, Noah, D. (2008). "Embankment Spec." Personal Communication.

Wan, C. F. and Fell, R. (2004). "Investigation of rate of erosion of soils in embankment dams." *J. of Geotech. and Geoenvir. Eng.*,ASCE, 130(4), 373-380.

Xie, M., S. S. Agus, et al. (2004). "An upscaling method and a numerical analysis of swelling/shrinking processes in a compacted bentonite/sand mixture." International Journal for Numerical and Analytical Methods in Geomechanics 28(15): 1479-1502.

APPENDICES

APPENDIX A: POSS

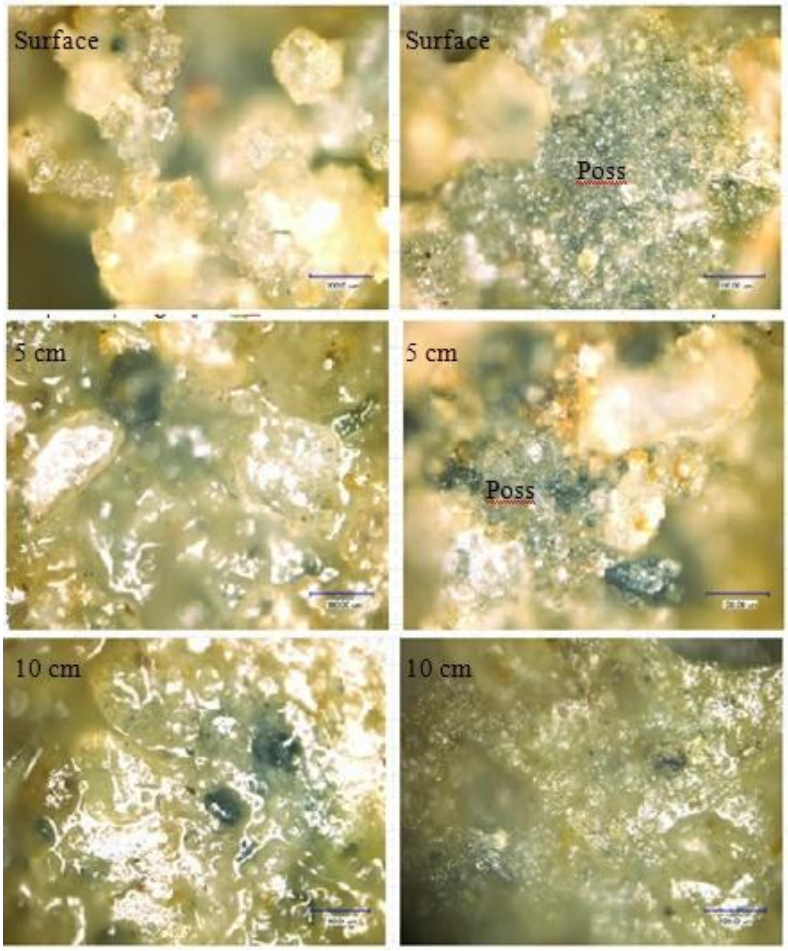

Figure A1. Microscopic Images of Bare Soil (left) and POSS (right)

Figure A2. Application of POSS

APPENDIX B: BENTONITE SWELLING PRESSURE

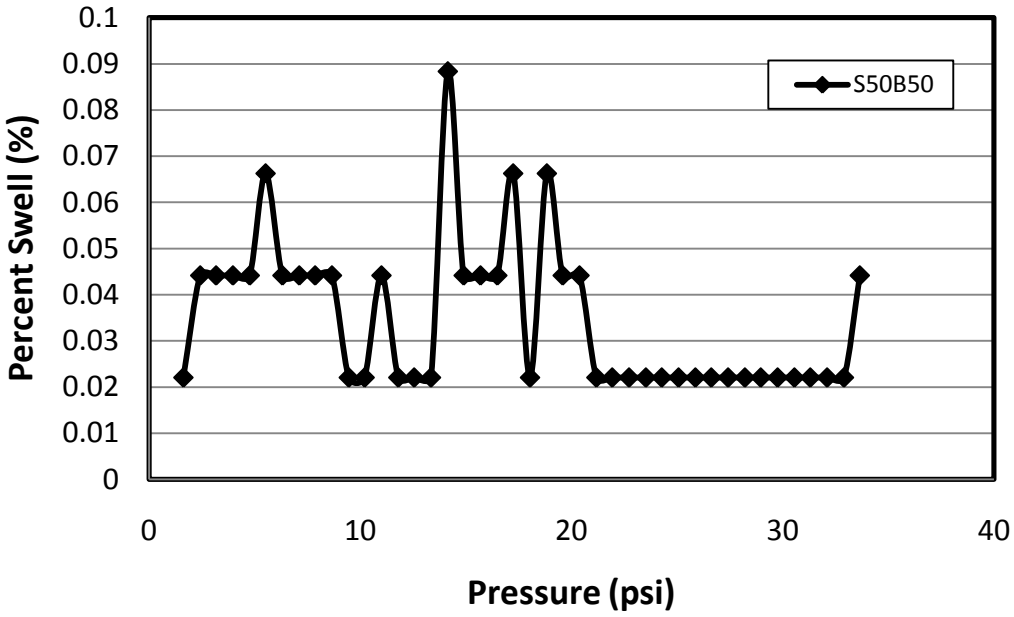

Figure B1. S50B50 Swelling Pressure: 2-Day Swell Pressure=33.66 psi

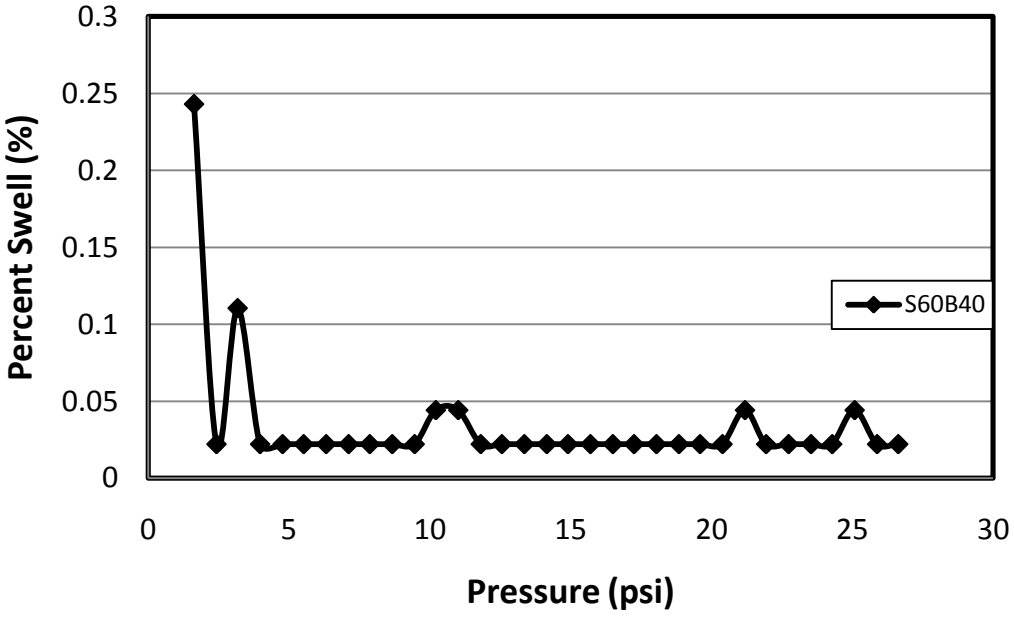

Figure B2. S60B40 Swelling Pressure: 2-Day Swell Pressure=25.08 psi

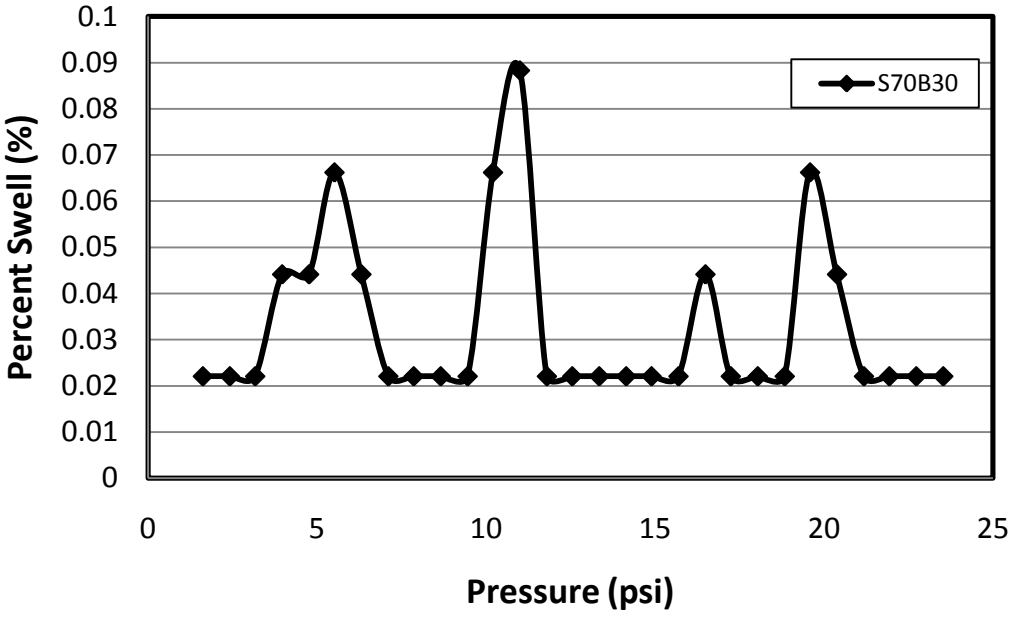

Figure B3. S70B30 Swelling Pressure: 2-Day Swell Pressure=23.53 psi

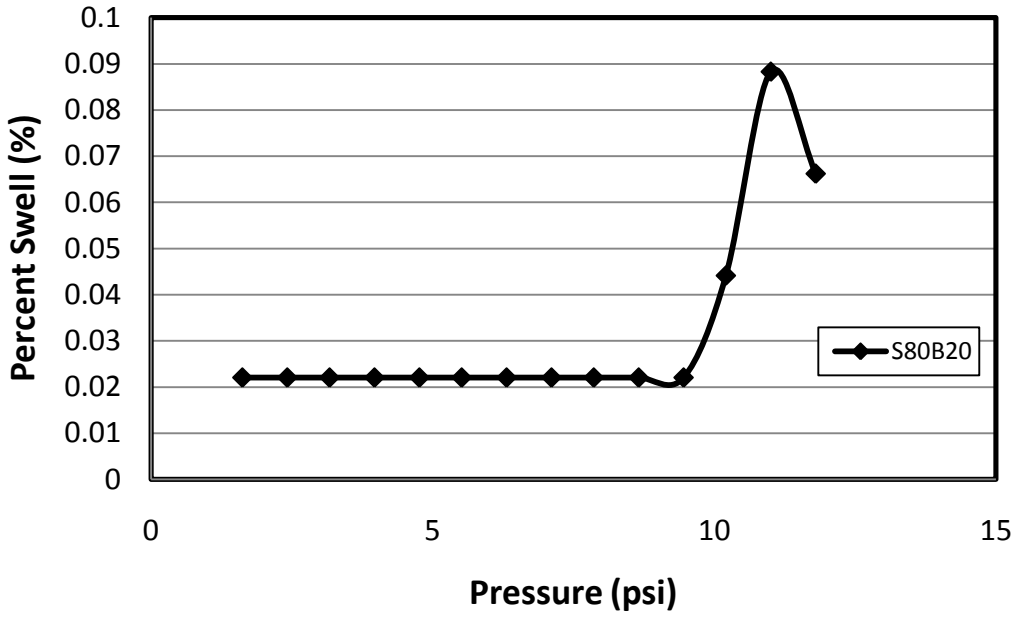

Figure B4. S80B20 Swelling Pressure: 2-Day Swell Pressure=11.8psi

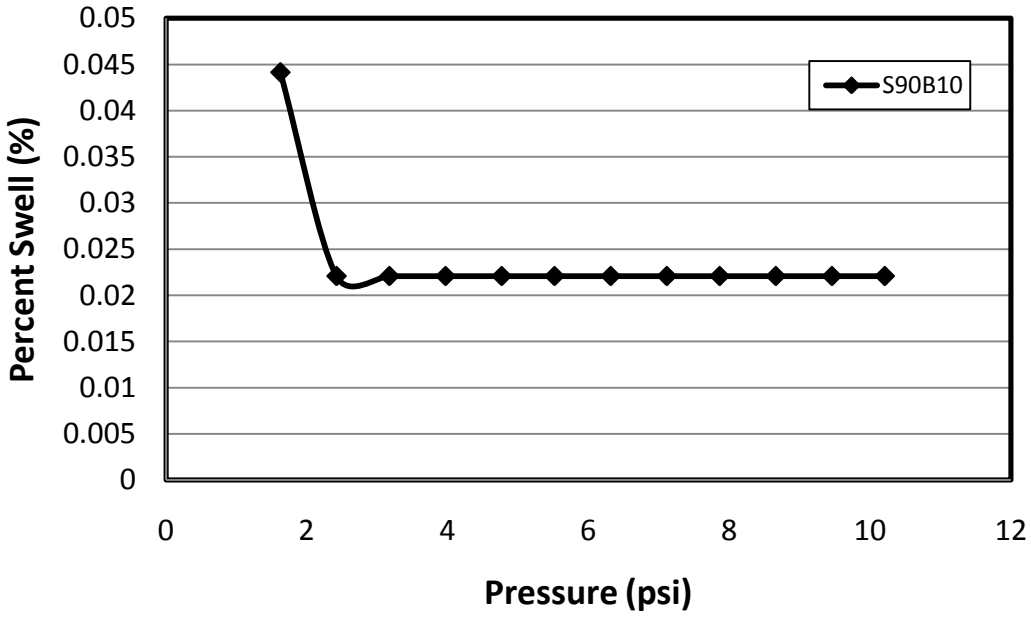

Figure B5. S90B10 Swelling Pressure: 2-Day Swell Pressure=10.21 psi

APPENDIX C: FULL SCALE BENTONITE SWELLING

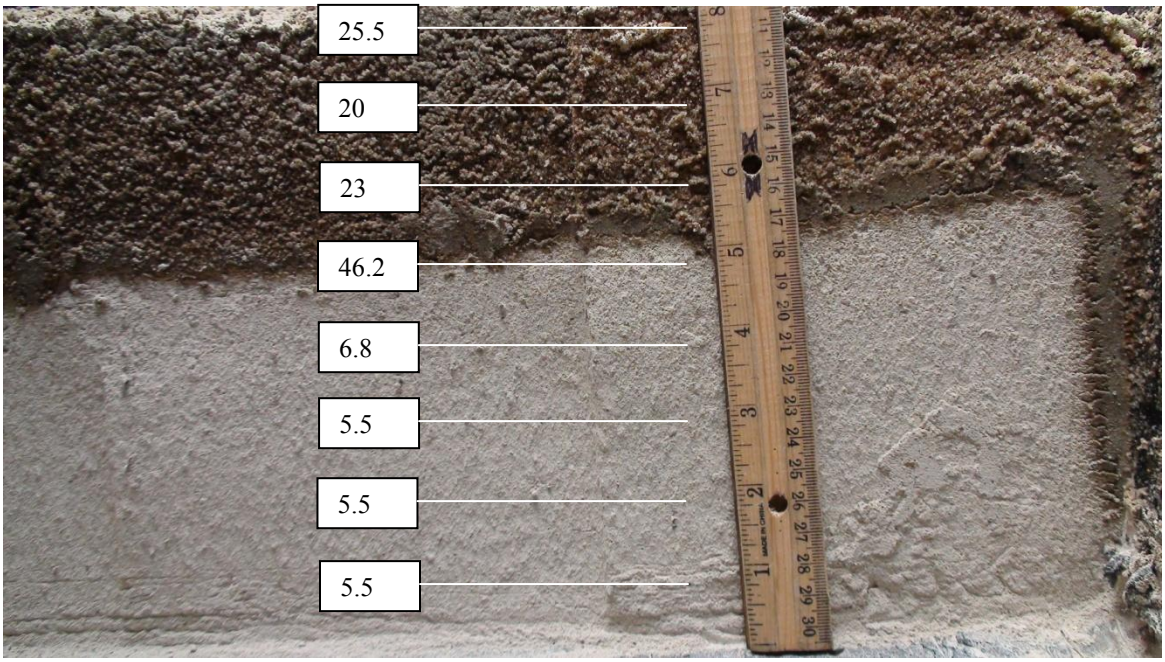

Figure C1. S50B50 Water Content Shown with Depth

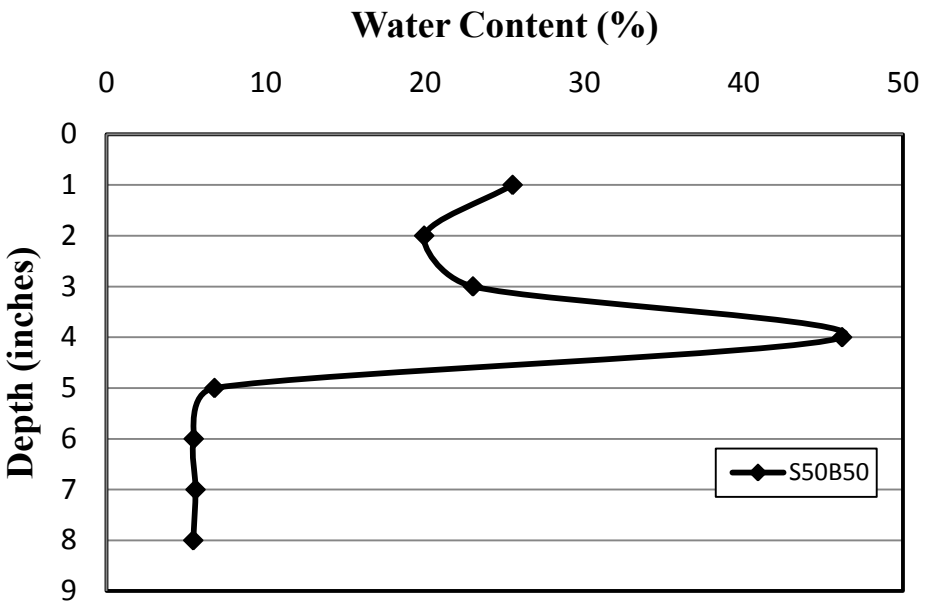

Figure C2. S50B50 Water Content vs. Depth

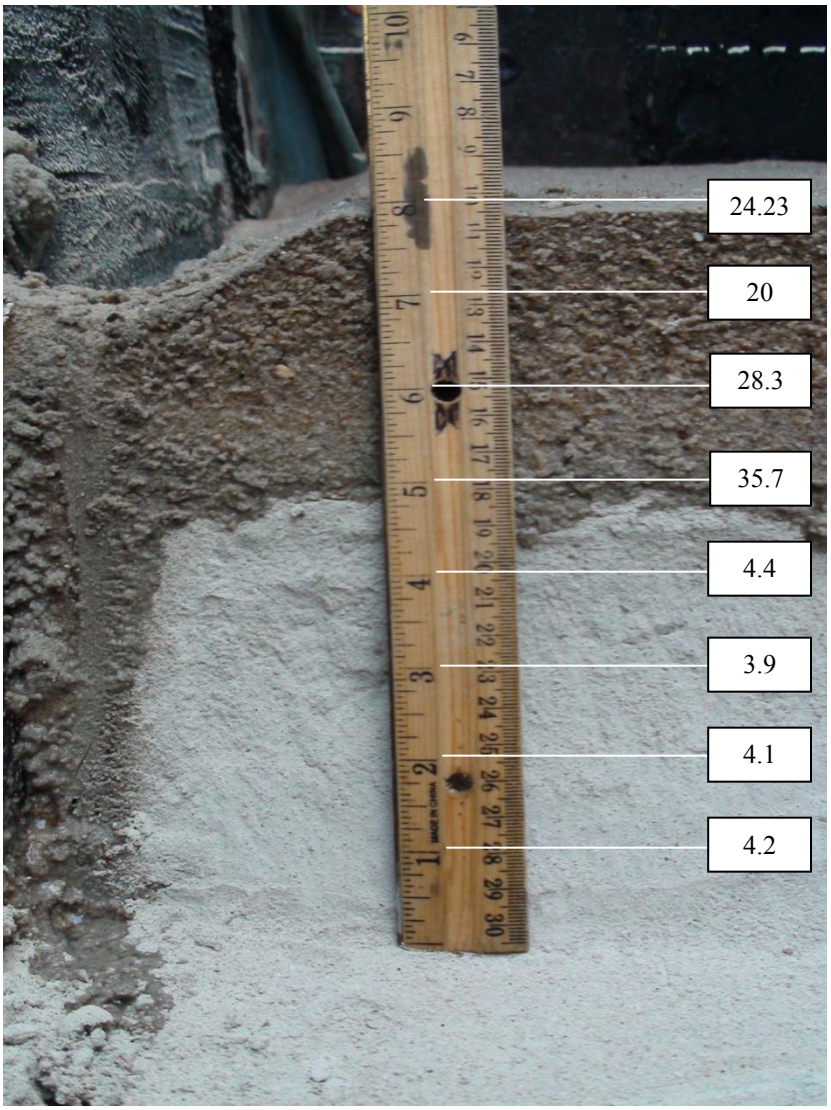

Figure C3. S60B40 Water Content Shown with Depth

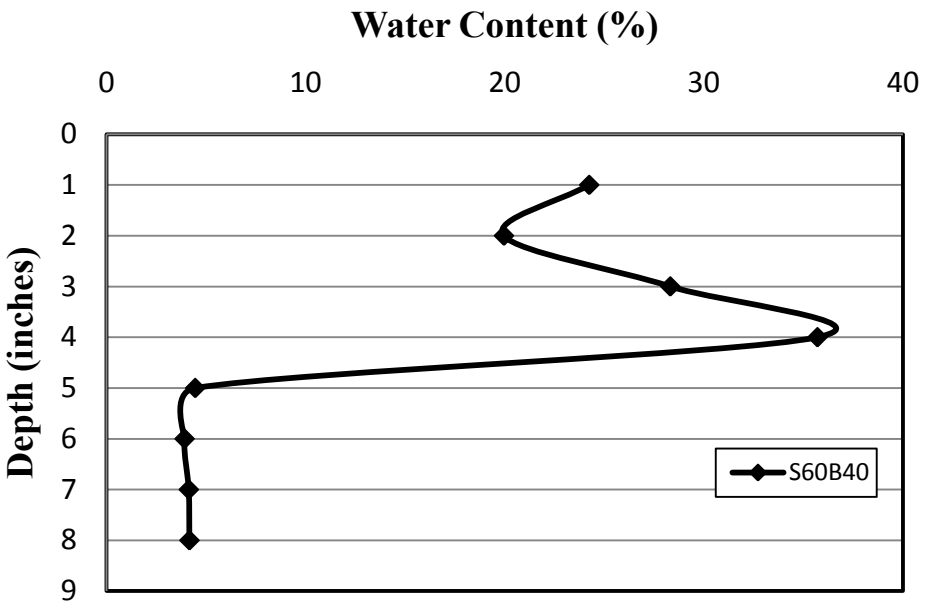

Figure C4. S60B40 Water Content vs. Depth

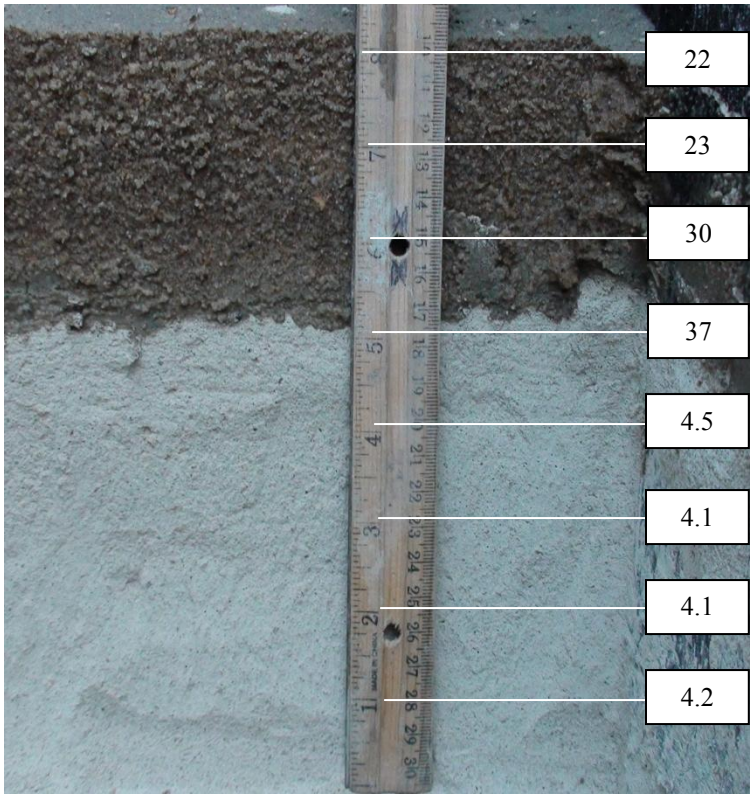

Figure C5. S70B30 Water Content Shown with Depth

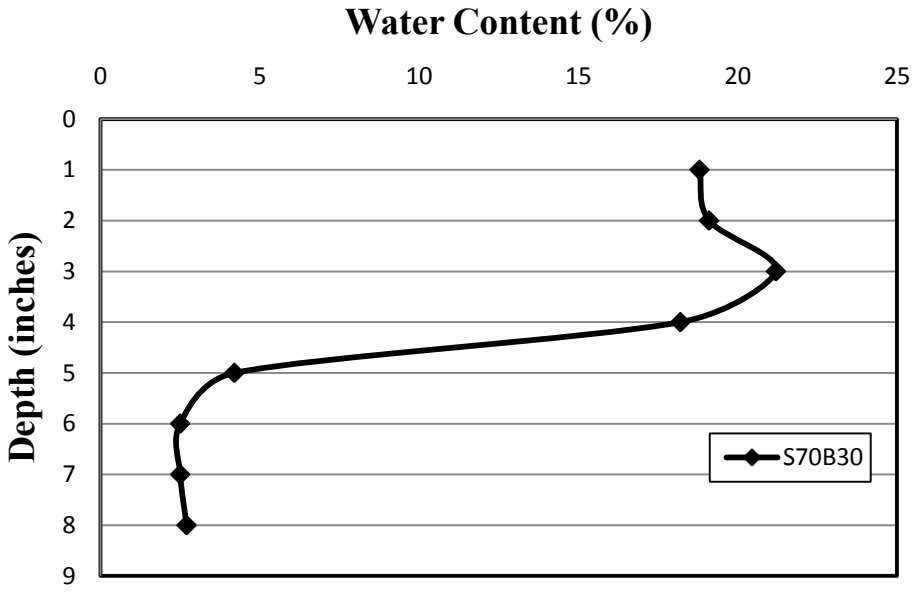

Figure C6. S70B30 Water Content vs. Depth

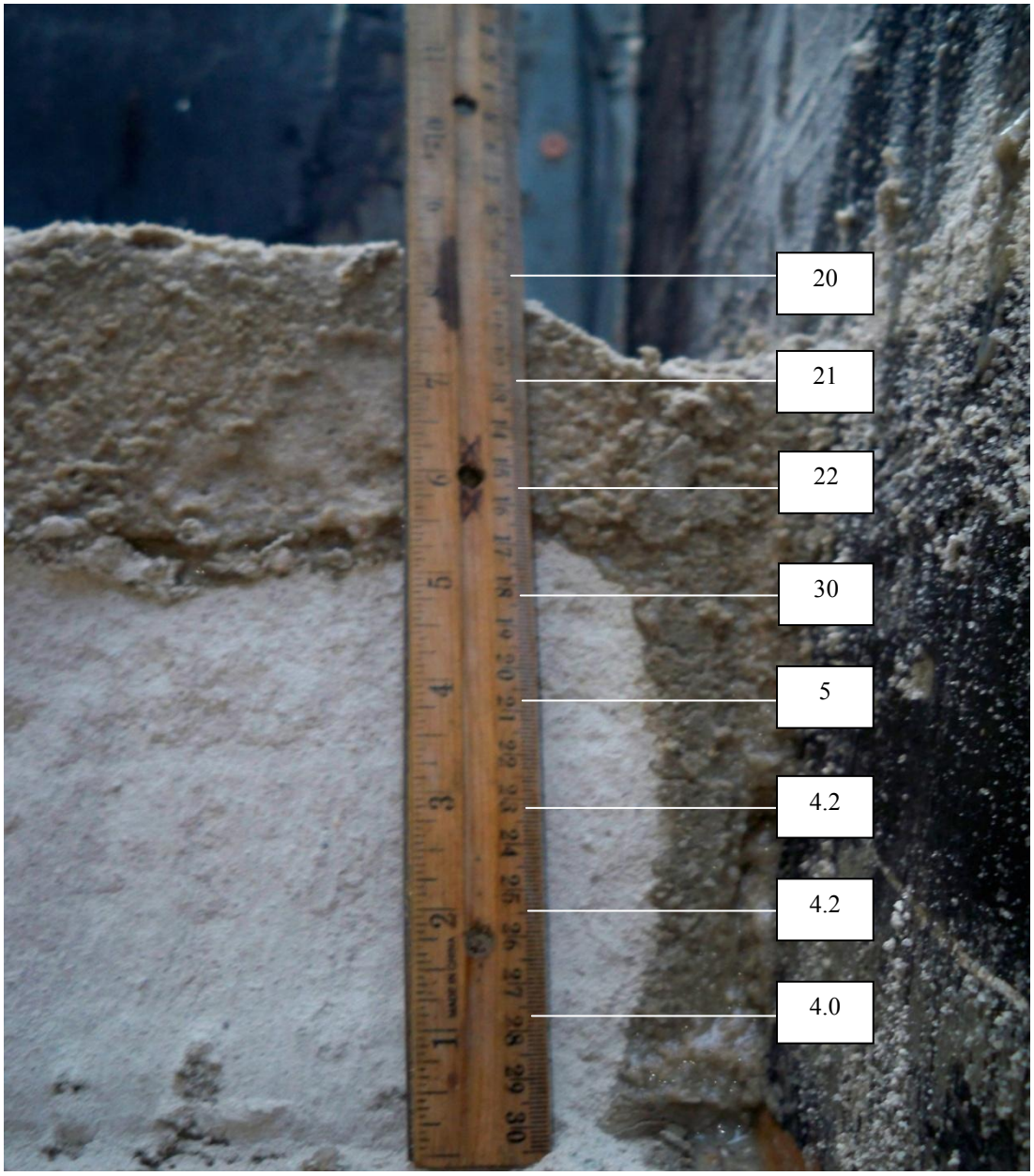

Figure C7. S80B20 Water Content Shown with Depth

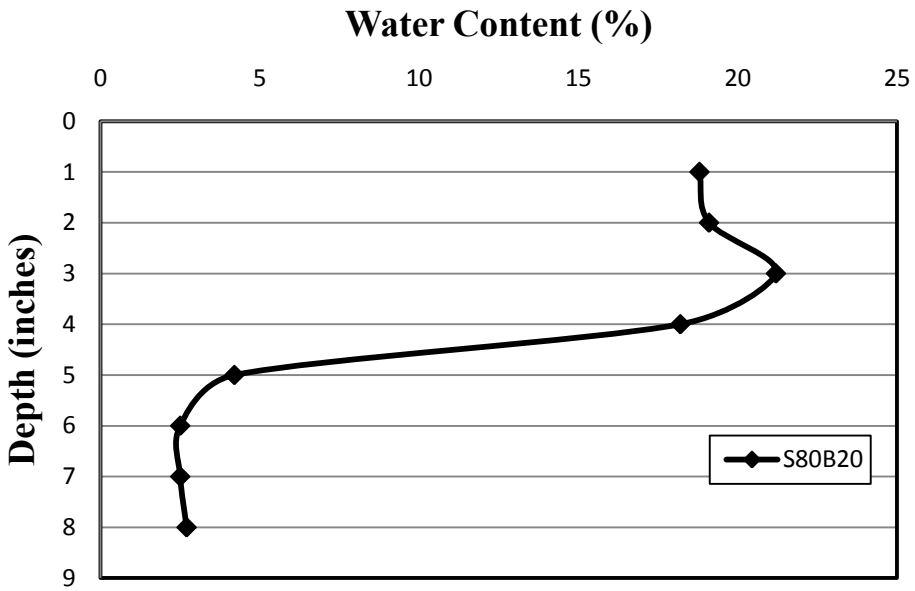

Figure C8. S80B20 Water Content vs. Depth

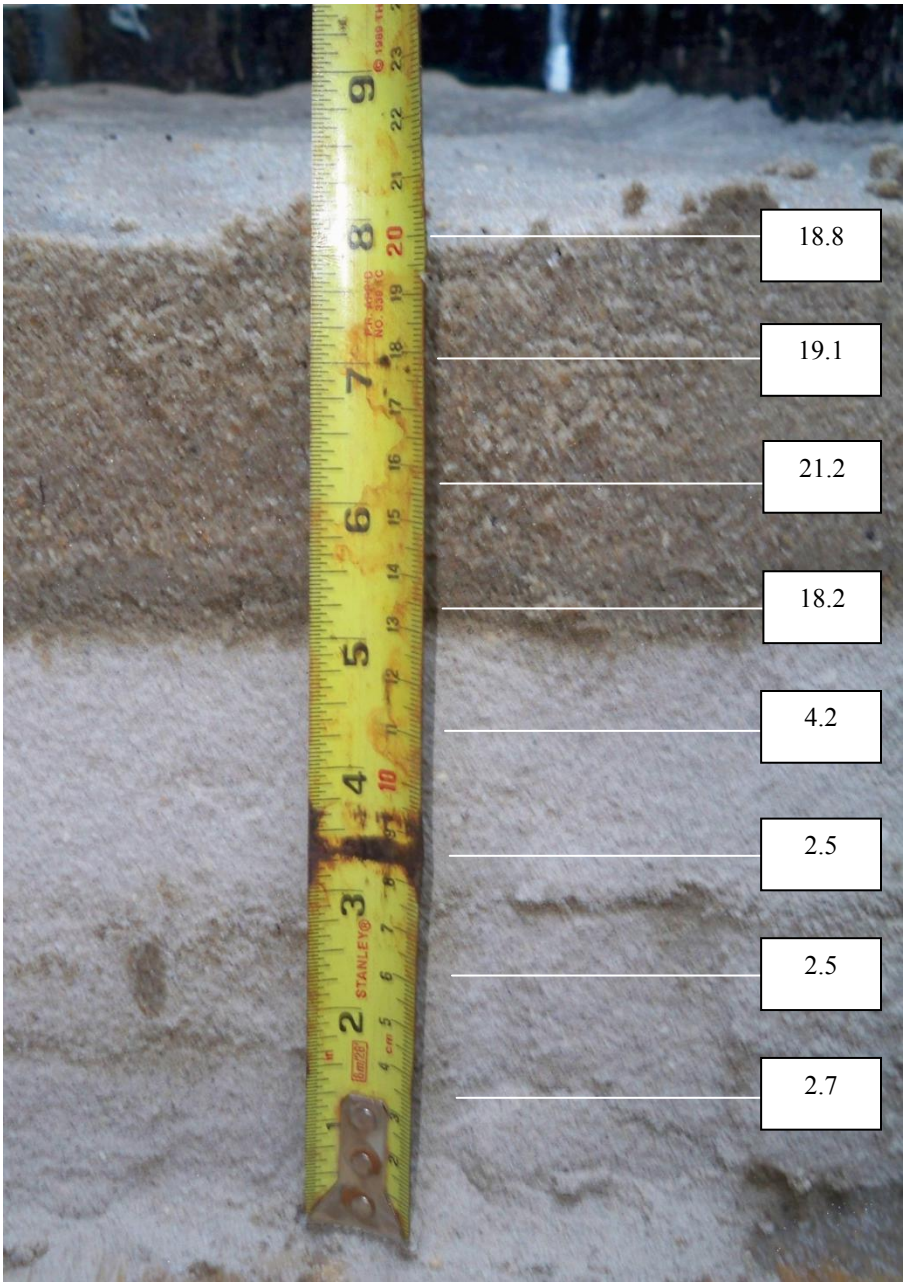

Figure C9. S90B10 Water Content Shown with Depth

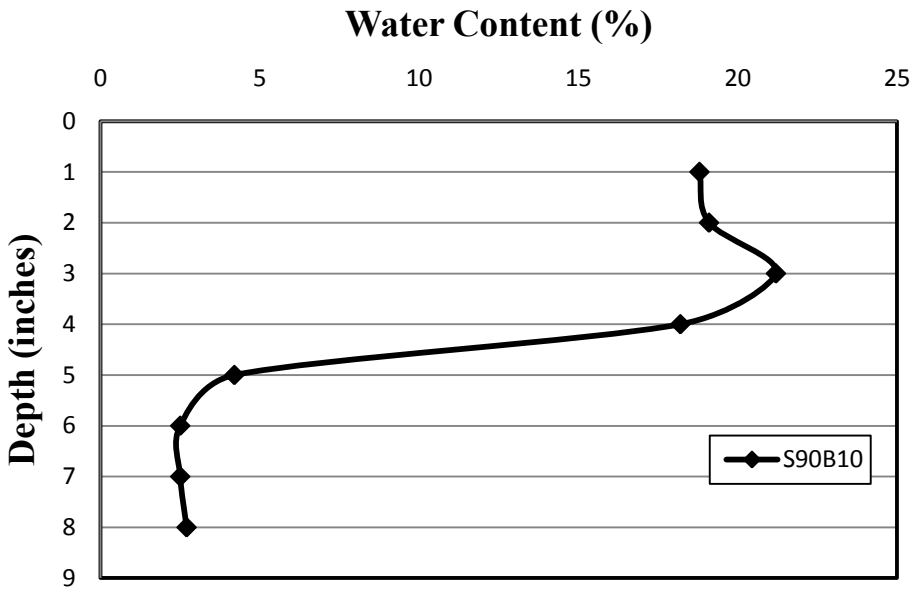

Figure C10. S90B10 Water Content vs. Depth

APPENDIX D: EROSION RATE VARRYING NOZZLE THICKNESS

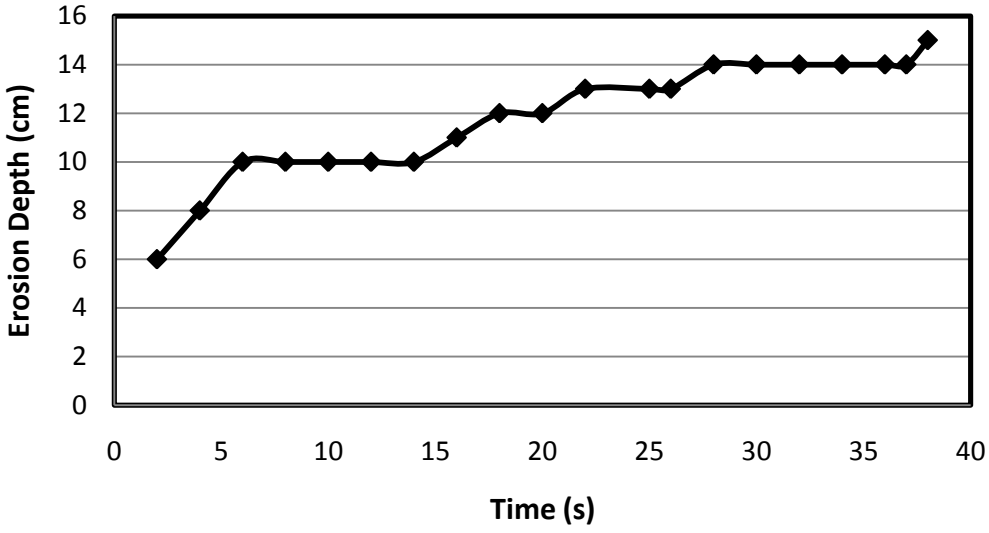

Figure D1. F50S50 DOC 83%: Nozzle Thickness=.003 m

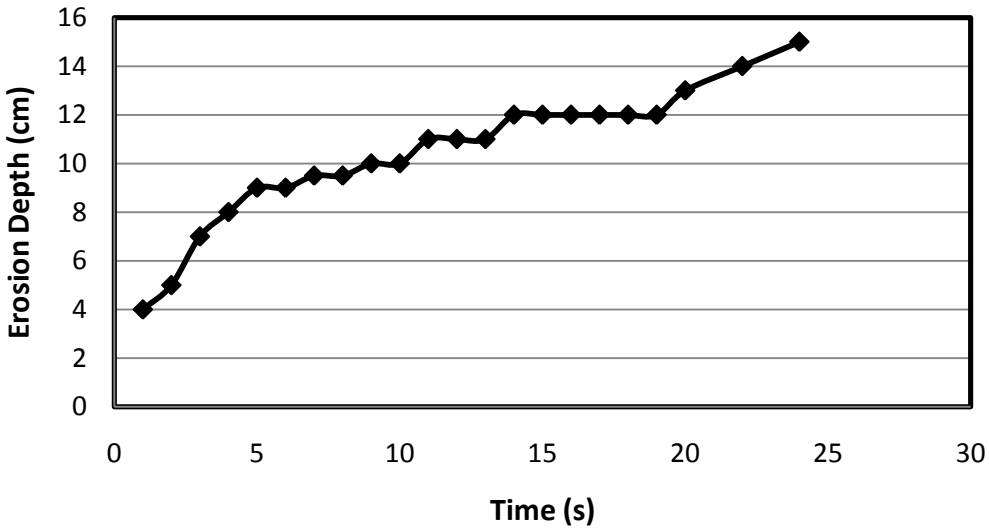

Figure D2. F50S50 DOC 83%: Nozzle Thickness=.0065 m

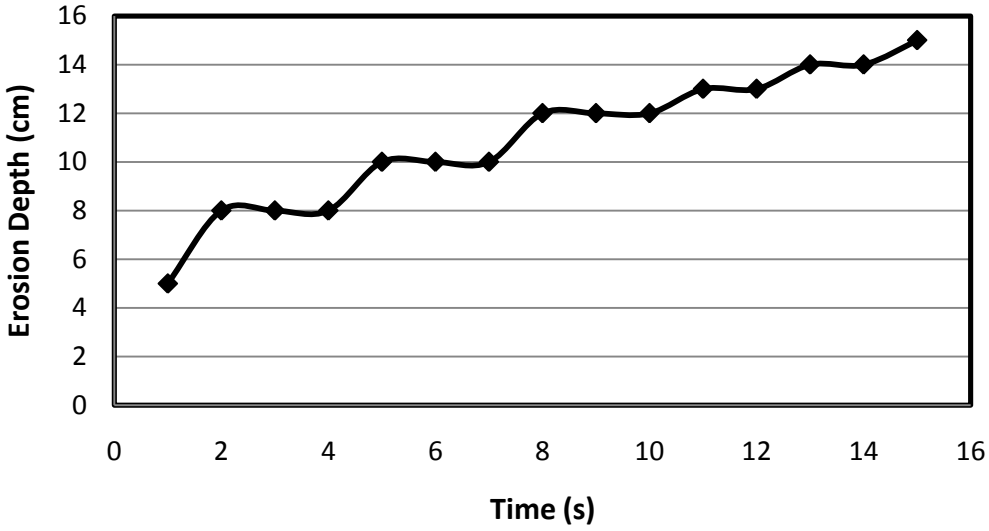

Figure D3. F50S50 DOC 83%: Nozzle Thickness=.013 m

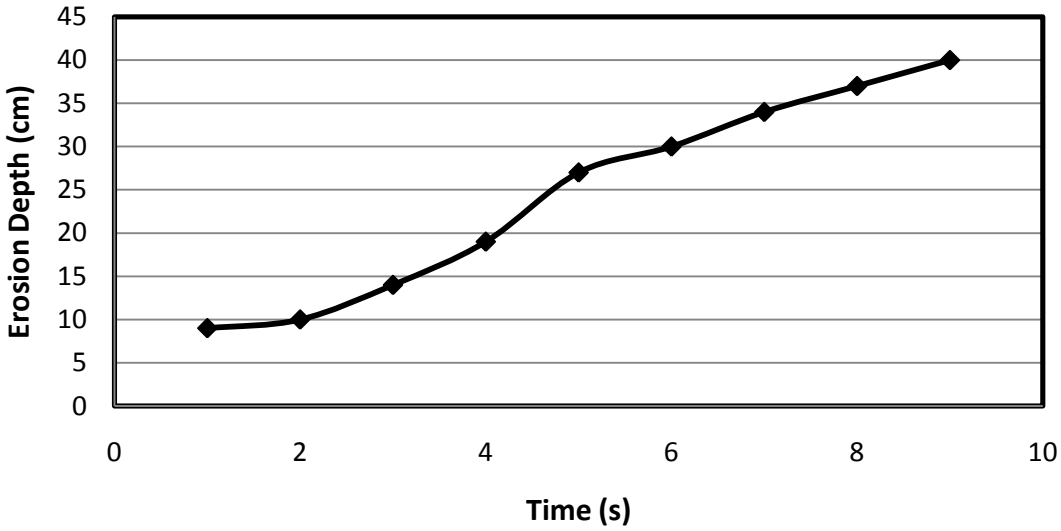

Figure D4. F50S50 DOC 83%: Nozzle Thickness=..2032 m

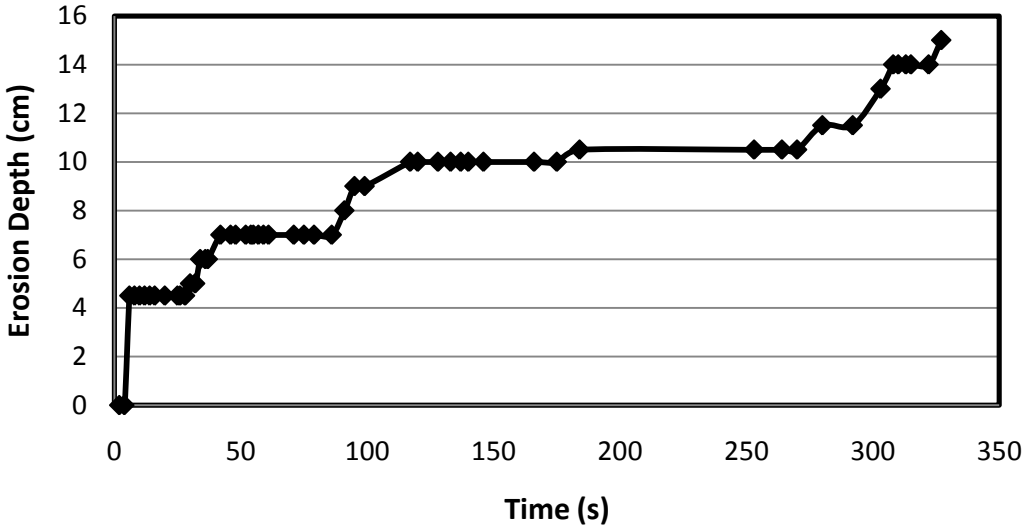

Figure D5. F57S43 DOC 88%: Nozzle Thickness=.003 m

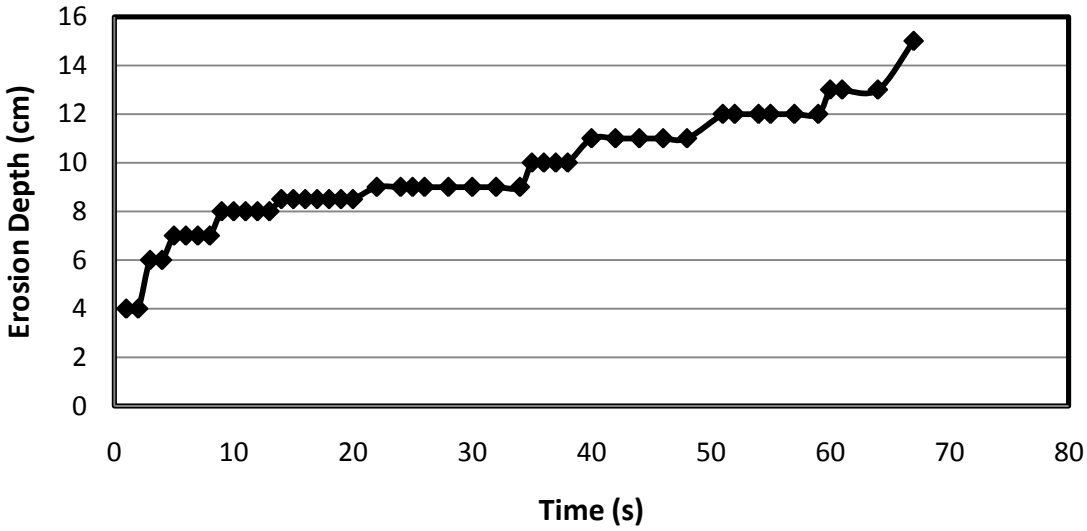

Figure D6. F57S43 DOC 88%: Nozzle Thickness=.0065 m

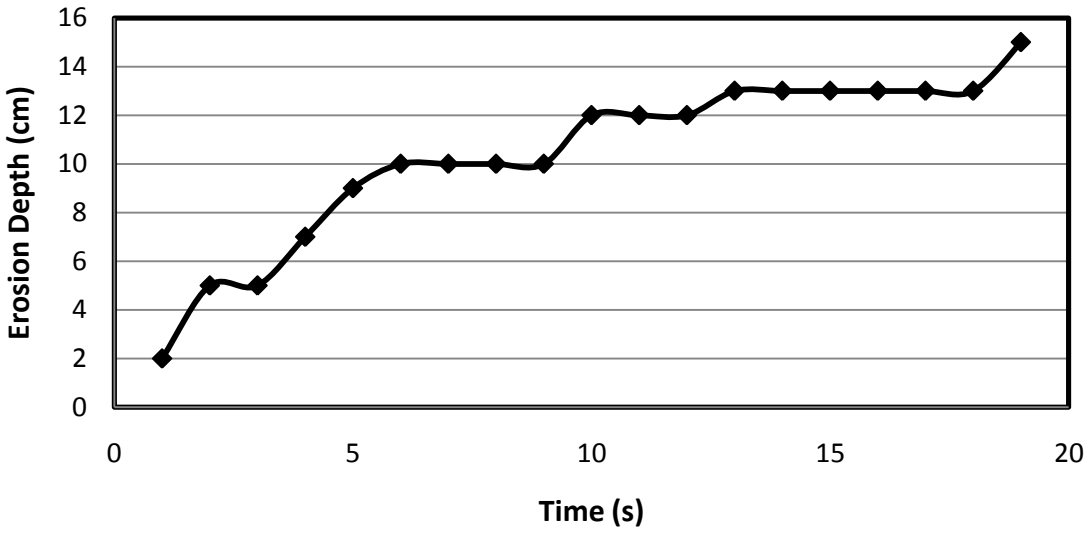

Figure D7. F57S43 DOC 88%: Nozzle Thickness=.013 m

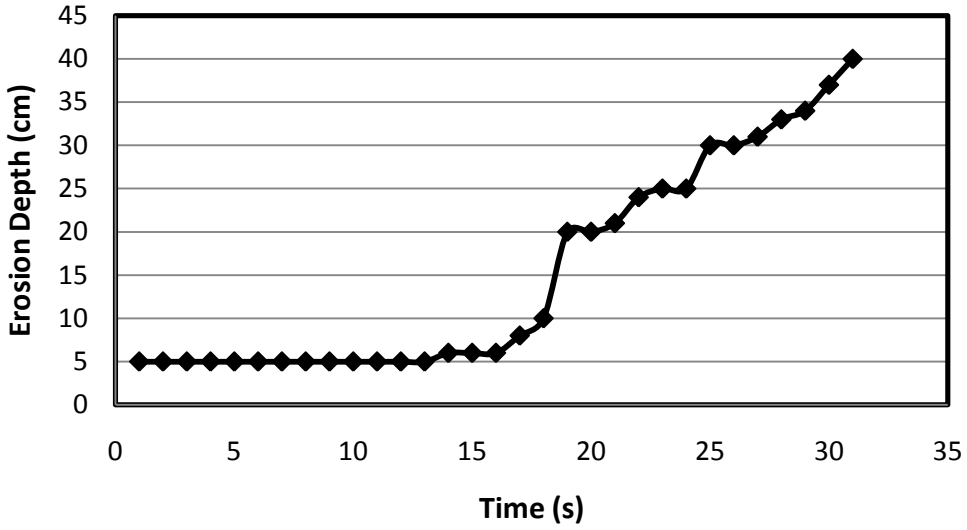

Figure D8. F57S43 DOC 88%: Nozzle Thickness=.2032 m

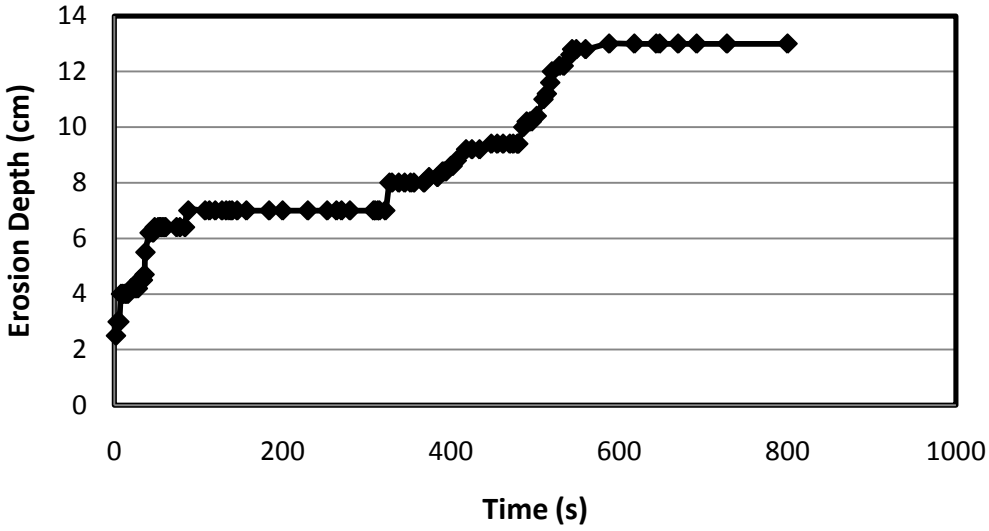

Figure D9. F65S35 DOC 91%: Nozzle Thickness=.003 m

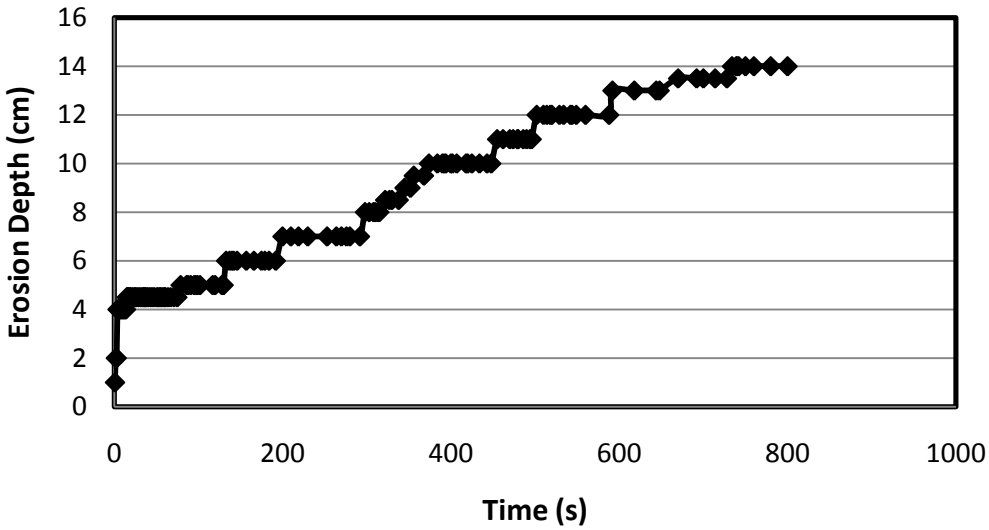

Figure D10. F65S35 DOC 91%: Nozzle Thickness=.0065 m

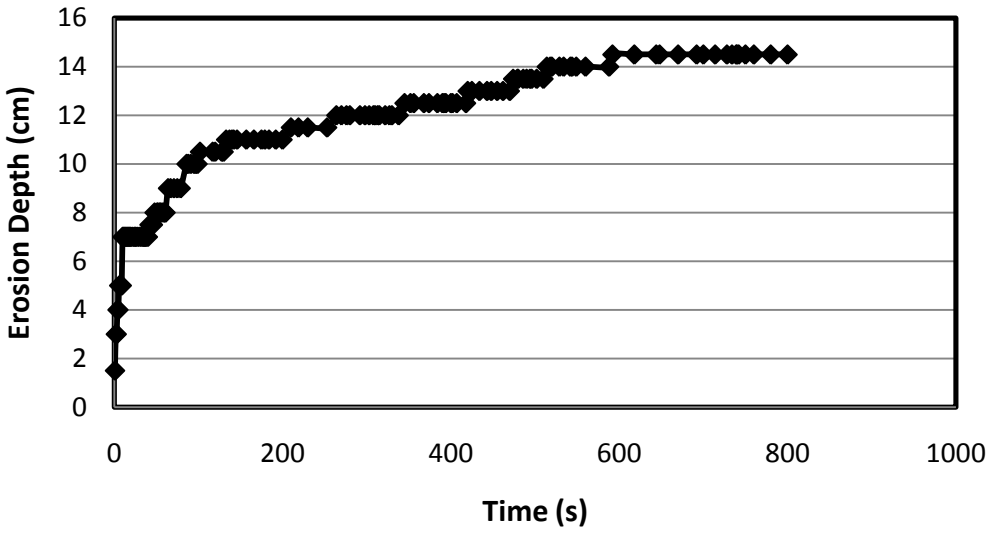

Figure D11. F65S35 DOC 91%: Nozzle Thickness=.013 m

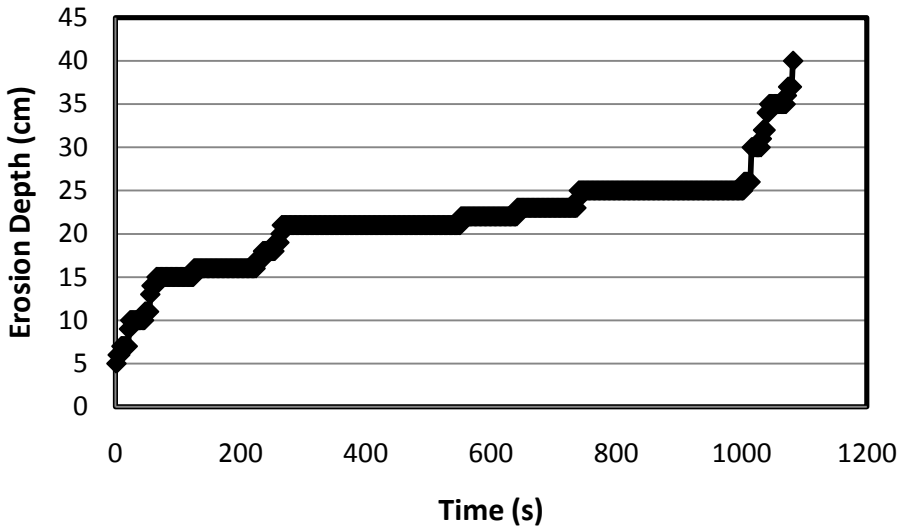

Figure D12. F65S35 DOC 91%: Nozzle Thickness=.2032 m

VITA

James Tyler Kidd was born on November 10, 1986, in New Albany Mississippi, to Billy and Melanie Kidd. He finished high school from South Pontotoc Attendance Center in May 2005. He received his Bachelor of Science in Civil Engineering from the University of Mississippi in May 2009.